

The LHeC Project

Max Klein
University of Liverpool

Overview
Physics
Accelerator
Detector

Seminar at UCL, London, 11.5.2012

<http://cern.ch/lhec>

Legend:

- CERN existing LHC
 - CLIC 500 GeV
 - CLIC 3 TeV
 - ILC 500 GeV
 - LHeC
- Potential underground railway

Jura Mountains

IP

The LHeC Project

Max Klein

University of Liverpool

Geneva

Lake Geneva

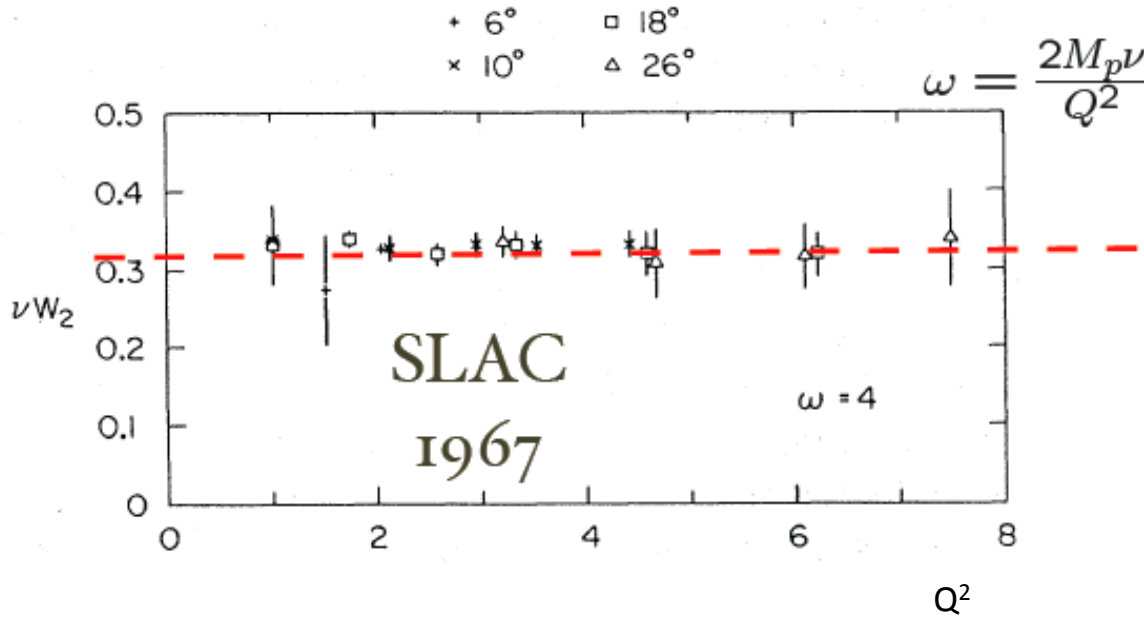
©2010 Google

Schematic layouts for several potential future projects are shown on this Google Earth view of the Geneva region around CERN:

- CLIC (Compact Linear Collider) at collision energies of 500GeV and 3 TeV.
- ILC (International Linear Collider) at 500GeV energy
- The Linac-Ring Solution of LHeC (A new electron beam supplied via a 60 GeV

Seminar at UCL, 11.5.2012

Foundation of DIS



Bjorken scaling \rightarrow Partons \rightarrow Quark-Parton Model \rightarrow QCD

SLAC 1967 $s = 2M_p E_e \approx 20 \text{ GeV}^2$

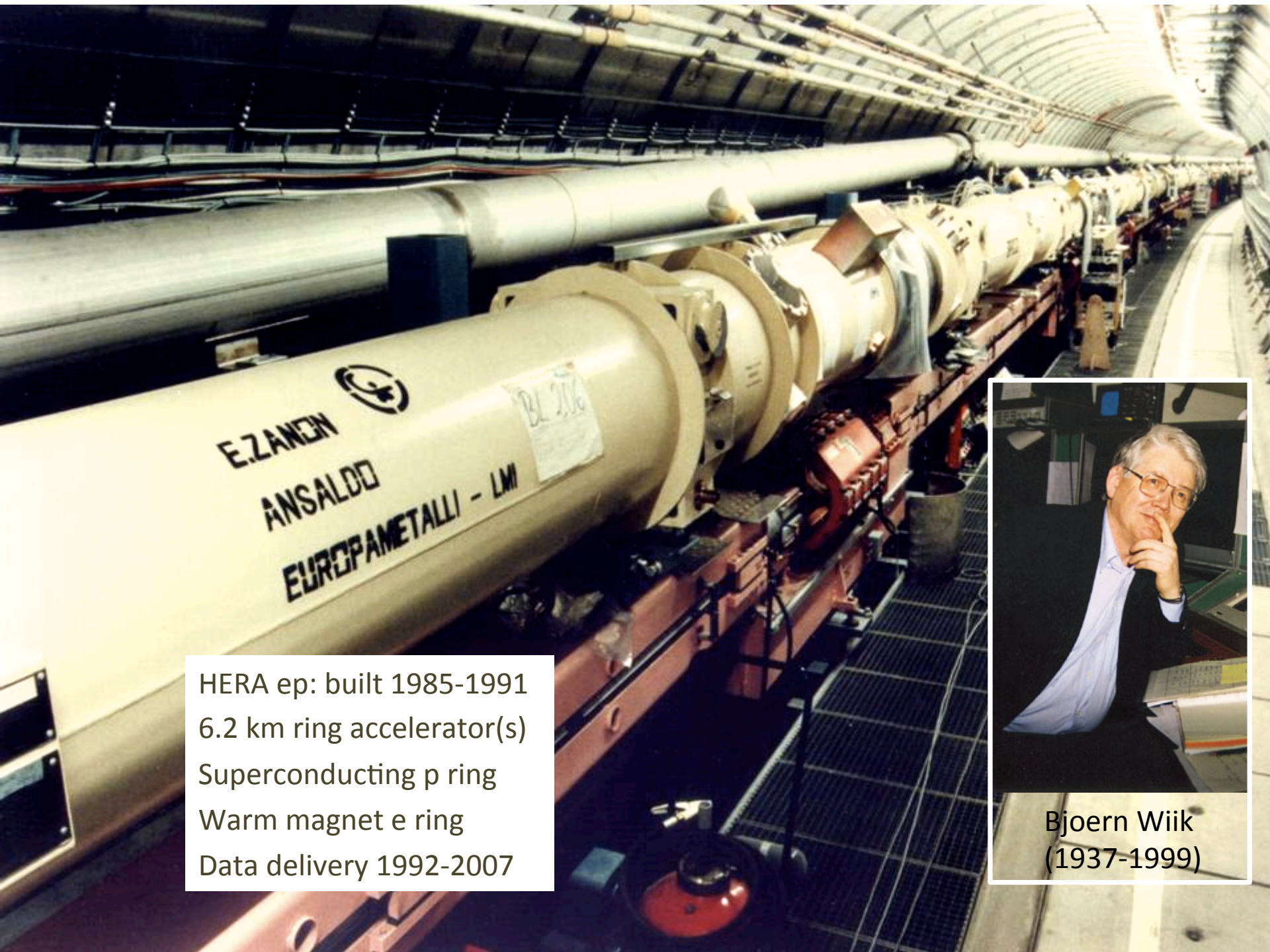
LHeC 2024 $s = 4E_p E_e \approx 2 \cdot 10^6 \text{ GeV}^2$

With 2m (2*1km) linac, but off p at rest or the LHC

2 mile electron linac



"Pief" Panowsky (1919-2007)

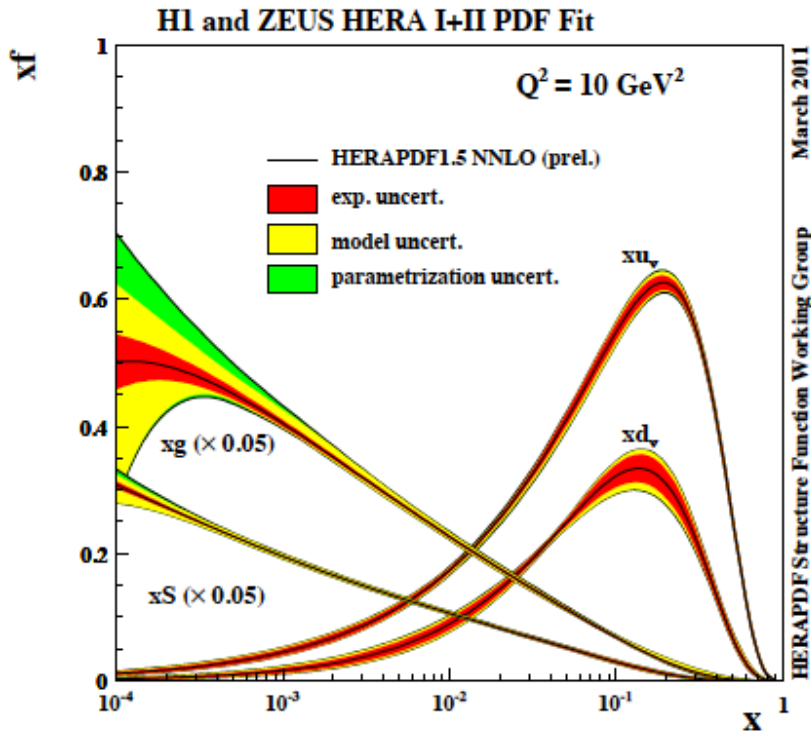


HERA ep: built 1985-1991
6.2 km ring accelerator(s)
Superconducting p ring
Warm magnet e ring
Data delivery 1992-2007

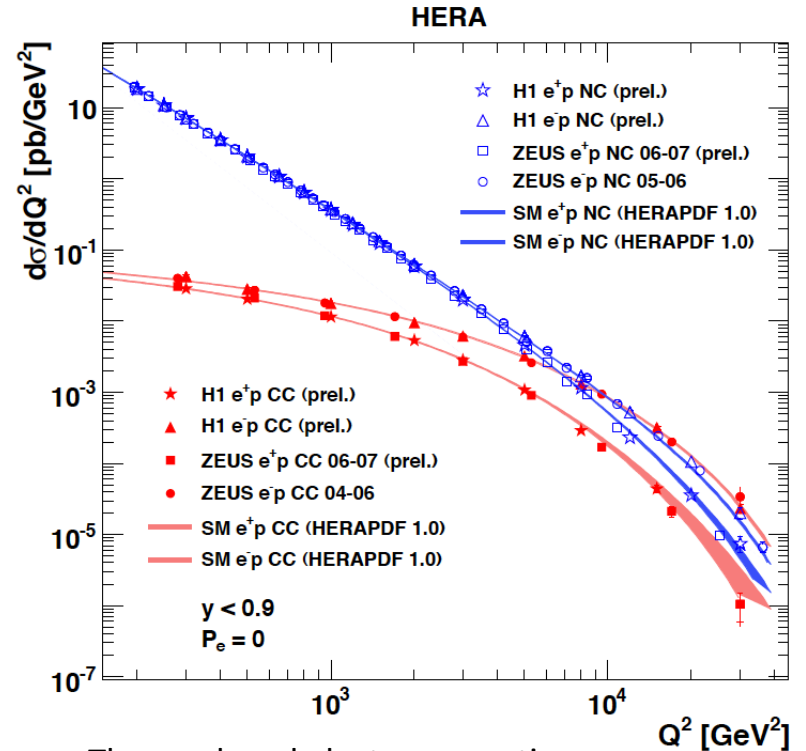


Bjoern Wiik
(1937-1999)

Results from HERA



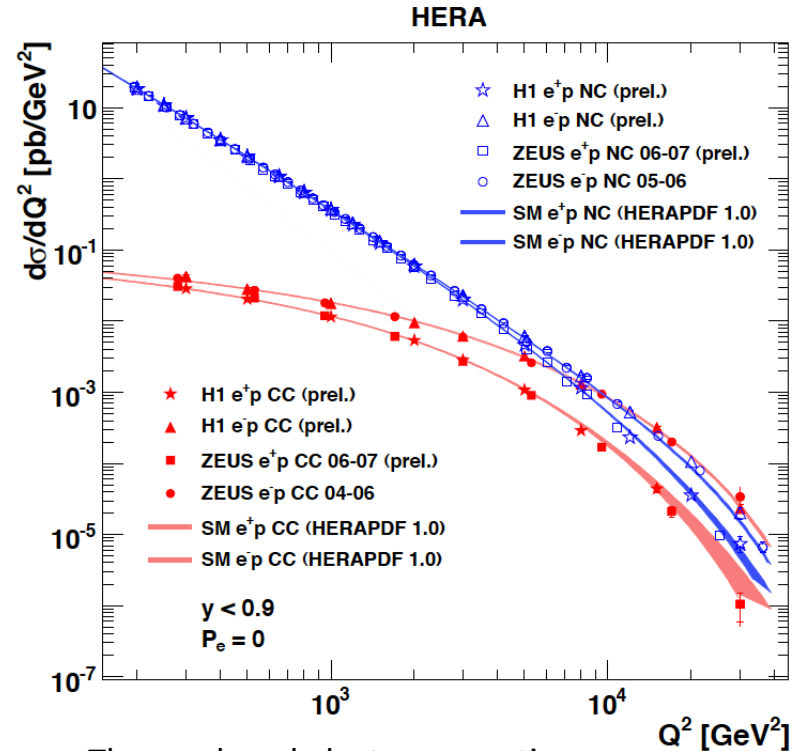
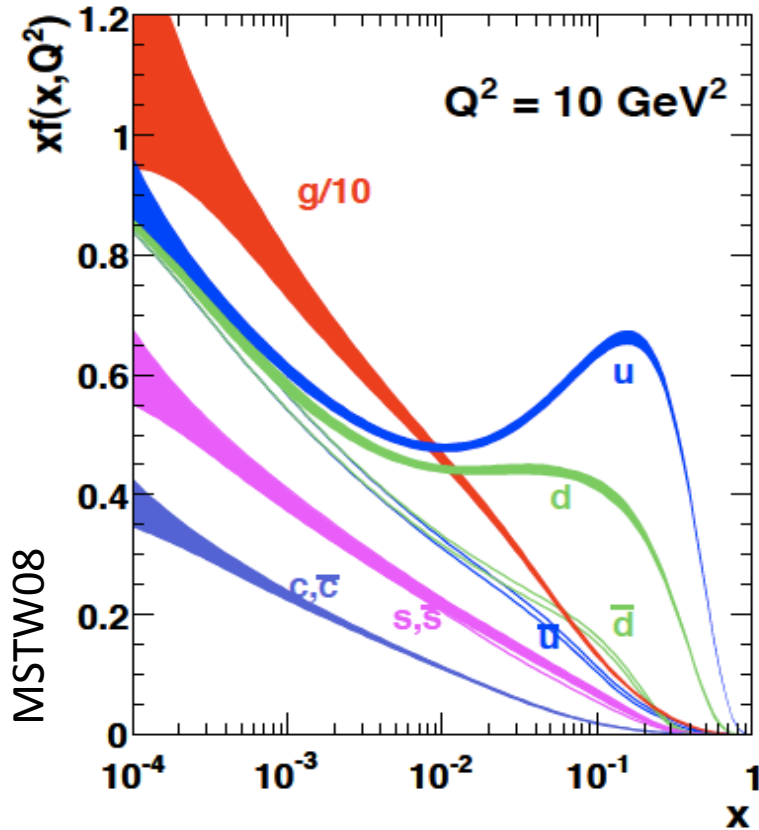
F_2 rises towards low x , and xg too.
Parton evolution - QCD to NNLO



The weak and electromagnetic interactions reach similar strength when $Q^2 \geq M_{W,Z}^2$

Measurements on α_s , Basic tests of QCD: longitudinal structure function, jet production, γ structure
Some 10% of the cross section is diffractive ($ep \rightarrow eXp$): diffractive partons; c,b quark distributions
 New concepts: unintegrated parton distributions (k_T), generalised parton distributions (DVCS)
 New limits for leptoquarks, excited electrons and neutrinos, quark substructure, RPV SUSY
 Interpretation of the Tevatron measurements (high E_t jet excess, M_W , searches..)

Results from HERA

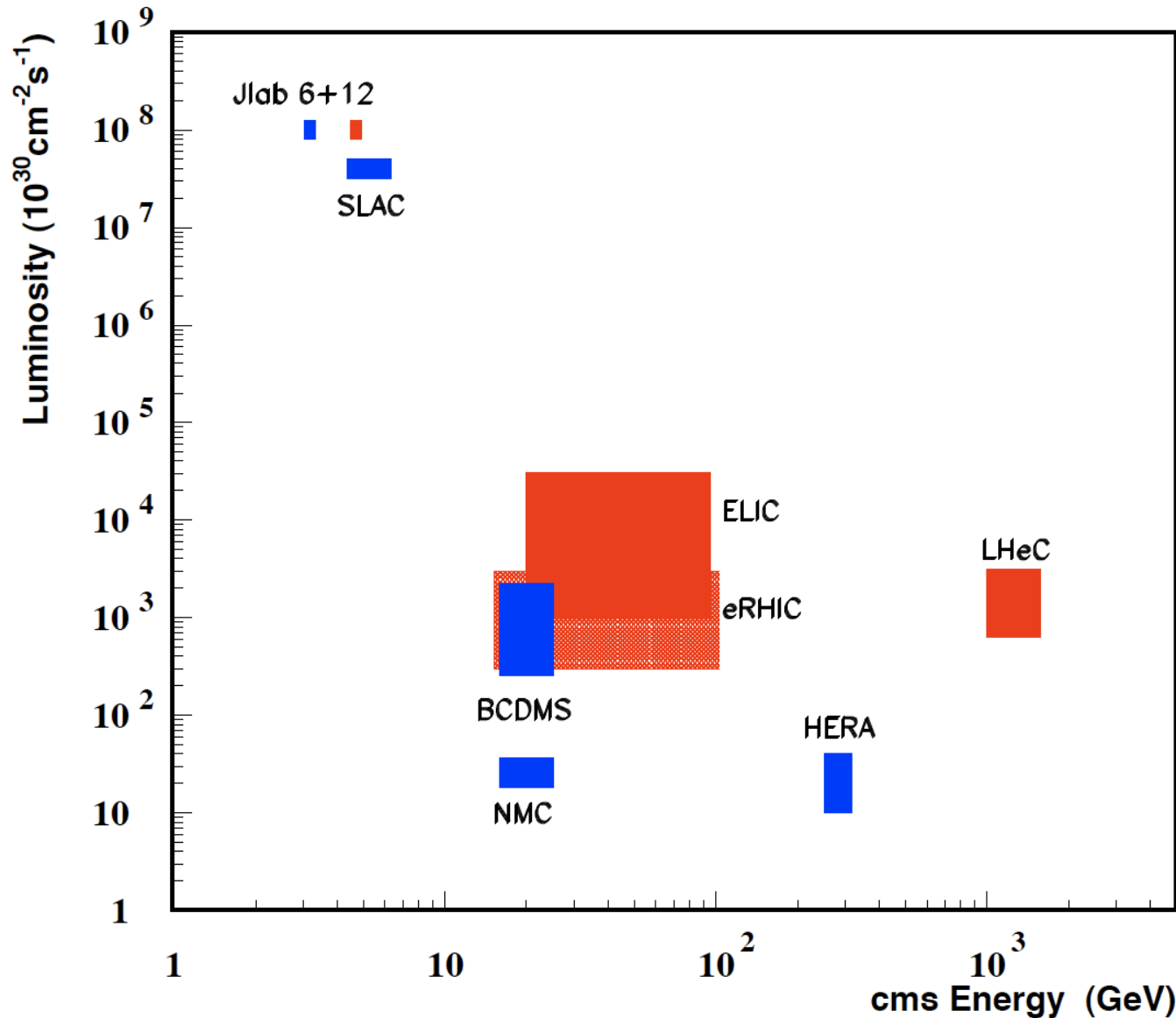


The weak and electromagnetic interactions reach similar strength when $Q^2 \geq M_{W,Z}^2$

Measurements on α_s , Basic tests of QCD: longitudinal structure function, jet production, γ structure
Some 10% of the cross section is diffractive ($ep \rightarrow eXp$): diffractive partons; c,b quark distributions
 New concepts: unintegrated parton distributions (k_T), generalised parton distributions (DVCS)
 New limits for leptoquarks, excited electrons and neutrinos, quark substructure, RPV SUSY
 Interpretation of the Tevatron measurements (high E_t jet excess, M_{W} , searches..)

DIS beyond HERA

Lepton-Proton Scattering Facilities



Built

Proposed

The LHeC is the only proposal and possibility to exceed HERA energy (and luminosity).

cc MK

Storage Ring

$$L = \frac{N_p \gamma}{4\pi \epsilon_p \rho_n} \cdot \frac{I_e}{\sqrt{\beta_{px} \beta_{py}}}$$

$$N_p = 1.7 \cdot 10^{11}, \epsilon_p = 3.8 \mu\text{m}, \beta_{px(y)} = 1.8(0.5)m, \gamma = \frac{E_p}{M_p}$$

$$L = 8.2 \cdot 10^{32} \text{cm}^{-2} \text{s}^{-1} \cdot \frac{N_p 10^{-11}}{1.7} \cdot \frac{m}{\sqrt{\beta_{px} \beta_{py}}} \cdot \frac{I_e}{50 \text{mA}}$$

$$I_e = 0.35 \text{mA} \cdot P[\text{MW}] \cdot (100/E_e[\text{GeV}])^4$$

L VS E_e

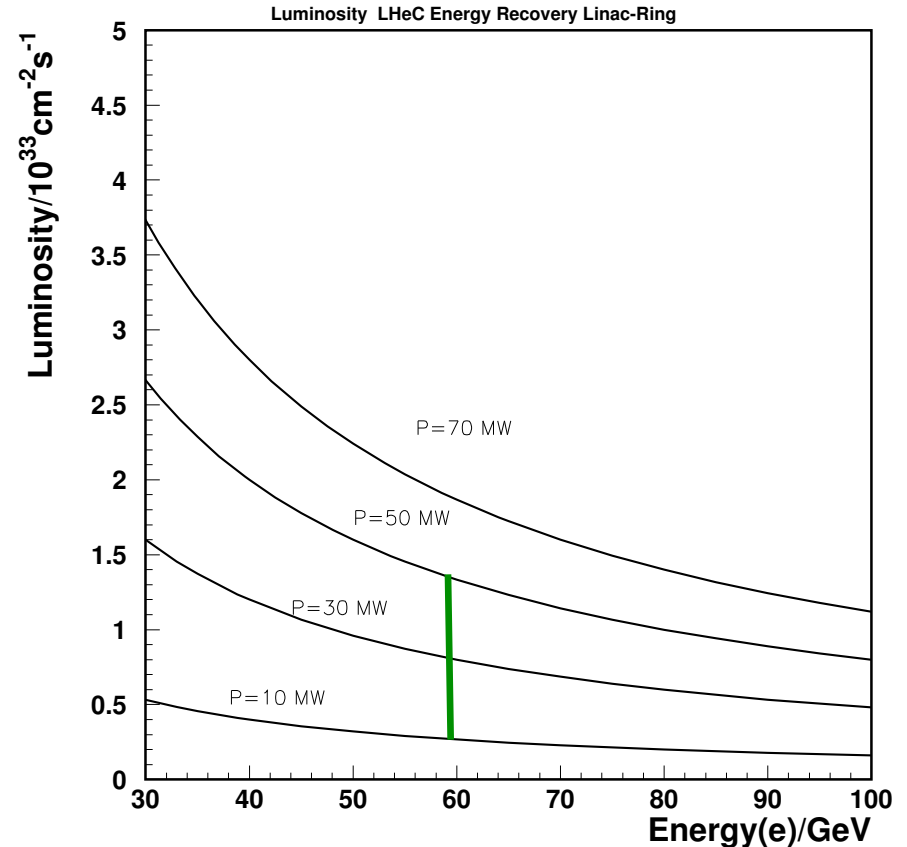
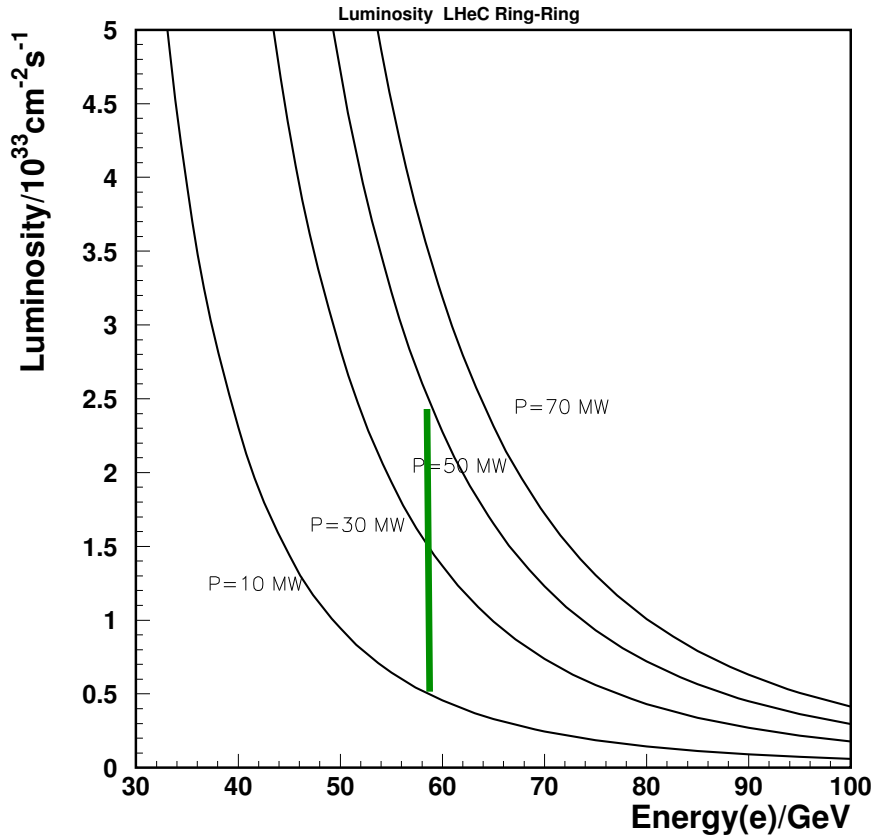
Energy Recovery Linac

$$L = \frac{1}{4\pi} \cdot \frac{N_p}{\epsilon_p} \cdot \frac{1}{\beta^*} \cdot \gamma \cdot \frac{I_e}{e}$$

$$N_p = 1.7 \cdot 10^{11}, \epsilon_p = 3.8 \mu\text{m}, \beta^* = 0.2 \text{m}, \gamma = 7000 / 0.94$$

$$L = 8 \cdot 10^{31} \text{cm}^{-2} \text{s}^{-1} \cdot \frac{N_p 10^{-11}}{1.7} \cdot \frac{0.2}{\beta^* / \text{m}} \cdot \frac{I_e / \text{mA}}{1}$$

$$I_e = \text{mA} \frac{P_E / \text{MW}}{E_e / \text{GeV}}, P_E = P / (1 - \eta), \eta \approx 0.95$$



Project Milestones

2007: Invitation by SPC to ECFA and by (r)ECFA to work out a design concept

2008: First CERN-ECFA Workshop in Divonne (1.-3.9.08)

2009: 2nd CERN-ECFA-NuPECC Workshop at Divonne (1.-3.9.09)

2010: Report to CERN SPC (June)

3rd CERN-ECFA-NuPECC Workshop at Chavannes-de-Bogis (12.-13.11.10)

NuPECC puts LHeC to its Long Range Plan for Nuclear Physics (12/10)

2011: Draft CDR (530 pages on Physics, Detector and Accelerator) (5.8.11)
being refereed and updated

2012: Publication of CDR – European Strategy

New workshop (Chavannes, June 14-15, 2012)



Goal: TDR by 2015

Perspective: Operation by 2023 (synchronous with pp)

Organisation for CDR

Scientific Advisory Committee

Guido Altarelli (Roma)
Sergio Bertolucci (CERN)
Stan Brodsky (SLAC)
Allen Caldwell (MPI Muenchen) - Chair
Swapan Chattopadhyay (Cockcroft Institute)
John Dainton (Liverpool)
John Ellis (CERN)
Jos Engelen (NWO)
Joel Feltesse (Saclay)
Roland Garoby (CERN)
Rolf Heuer (CERN)
Roland Horisberger (PSI)
Young-Kee Kim (Fermilab)
Aharon Levy (Tel Aviv)
Lev Lipatov (St. Petersburg)
Karlheinz Meier (Heidelberg)
Richard Milner (MIT)
Joachim Mnich (DESY)
Steve Myers (CERN)
Guenther Rosner (Glasgow)
Alexander N. Skrinsky (INP Novosibirsk)
Anthony Thomas (JLab)
Steve Vigdor (Brookhaven)
Ferdinand Willeke (Brookhaven)
Frank Wilczek (MIT)



Steering Committee

Oliver Bruening (CERN)
John Dainton (Liverpool)
Albert De Roeck (CERN)
Stefano Forte (Milano)
Max Klein (Liverpool) - Chair
Paul Laycock (Liverpool)
Paul Newman (Birmingham)
Emmanuelle Perez (CERN)
Wesley Smith (Wisconsin)
Bernd Surrow (MIT)
Katsuo Tokushuku (KEK)
Urs Wiedemann (CERN)
Frank Zimmermann (CERN)

Working Group Convenors

Accelerator Design

Oliver Bruening (CERN)
John Dainton (Liverpool)

Interaction Region

Bernhard Holzer (CERN)
Uwe Schneekloth (DESY)
Pierre van Mechelen (Antwerpen)

Detector Design

Peter Kostka (DESY)
Alessandro Polini (Bologna)
Rainer Wallny (Zurich)

New Physics at Large Scales

Georges Azuelos (Montreal)
Emmanuelle Perez (CERN)
Georg Weiglein (Hamburg)

Precision QCD and Electroweak

Olaf Behnke (DESY)
Paolo Gambino (Torino)
Thomas Gehrmann (Zurich)
Claire Gwenlan (Oxford)

Physics at High Parton Densities

Néstor Armesto (Santiago de Compostela)
Brian A. Cole (Columbia)
Paul R. Newman (Birmingham)
Anna M. Stasto (PennState)

CERN Referees

Ring Ring Design

Kurt Huebner (CERN)
Alexander N. Skrinsky (INP Novosibirsk)
Ferdinand Willeke (BNL)

Linac Ring Design

Reinhard Brinkmann (DESY)
Andy Wolski (Cockcroft)
Kaoru Yokoya (KEK)

Energy Recovery

Georg Hoffstaetter (Cornell)
Ilan Ben Zvi (BNL)

Magnets

Neil Marks (Cockcroft)
Martin Wilson (CERN)

Interaction Region

Daniel Pitzl (DESY)
Mike Sullivan (SLAC)

Detector Design

Philippe Bloch (CERN)
Roland Horisberger (PSI)

Installation and Infrastructure

Sylvain Weisz (CERN)

New Physics at Large Scales

Cristinel Diaconu (IN2P3 Marseille)
Gian Giudice (CERN)
Michelangelo Mangano (CERN)

Precision QCD and Electroweak

Guido Altarelli (Roma)
Vladimir Chekelian (MPI Munich)
Alan Martin (Durham)

Physics at High Parton Densities

Alfred Mueller (Columbia)
Raju Venugopalan (BNL)
Michele Arneodo (INFN Torino)

- DRAFT 1.0
- Geneva, August 5, 2011
- CERN report
- ECEA report
- NuPECC report
- LHeC-Note-2011-001 GEN

A. Klein

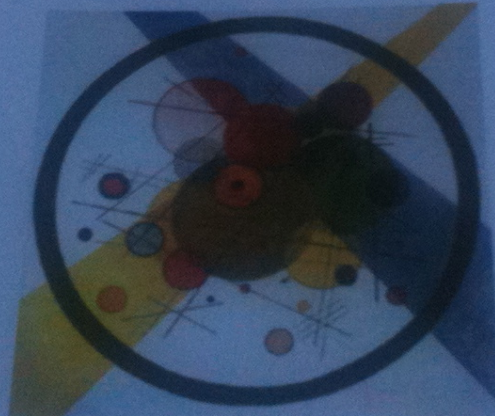


A Large Hadron Electron Collider at CERN

Report on the Physics and Design
Concepts for Machine and Detector

LHeC Study Group

THIS IS THE VERSION FOR REFEREEING, NOT FOR DISTRIBUTION



LHeC-Note-2011-003 GEN

To be submitted for publication

Draft LHeC Design Report
530 pages refereed →
Publication end of May 12

Most of plots from CDR.

LHeC Study Group

J.L. Abelleira Fernandez^{10,15}, C.Adolphsen³⁹, S.Alekhin^{40,11}, A.N.Akai⁰¹, H.Aksakal³⁰, P.Allport¹⁷, J.L.Albacete³⁷, V.Andreev²⁵, R.B.Appleby²³, E.Arikan³⁰, N.Armesto³⁸, G.Azuelos²⁶, M.Bai⁴⁷, D.Barber^{11,17,23}, J.Bartels¹², J.Behr¹¹, O.Behnke¹¹, S.Belyaev¹⁰, I.BenZvi⁴⁷, N.Bernard¹⁶, S.Bertolucci¹⁰, S.Bettoni¹⁰, S.Biswal³², J.Blumlein¹¹, H.Boettcher¹¹, H.Braun⁴⁸, S.Brodsky³⁹, A.Bogacz²⁸, C.Bracco¹⁰, O.Bruening¹⁰, E.Bulyak⁰⁸, A.Bunyatian¹¹, H.Burkhardt¹⁰, I.T.Cakir⁵⁴, O.Cakir⁵³, R.Calaga⁴⁷, E.Ciapala¹⁰, R.Ciftci⁰¹, A.K.Ciftci⁰¹, B.A.Cole²⁹, J.C.Collins⁴⁶, J.Dainton¹⁷, A.De.Roeck¹⁰, D.d'Enterria¹⁰, A.Dudarev¹⁰, A.Eide⁴³, R.Enberg⁵⁸, E.Eroglu⁴⁵, K.J.Eskola¹⁴, L.Favart⁰⁶, M.Fitterer¹⁰, S.Forte²⁴, P.Gambino⁴², H. García Morales¹⁰, T.Gehrmann⁵⁰, C.Glasman²², R.Godbole²⁷, B.Goddard¹⁰, T.Greenshaw¹⁷, A.Guffanti⁰⁹, V.Guzey²⁸, C.Gwenlan³⁴, T.Han³⁶, Y.Hao⁴⁷, F.Haug¹⁰, W.Herr¹⁰, B.Holzer¹⁰, M.Ishitsuka⁴¹, M.Jacquet³³, B.Jeaneret¹⁰, J.M.Jimenez¹⁰, H.Jung¹¹, J.M.Jowett¹⁰, H.Karadeniz⁵⁴, D.Kayran⁴⁷, F.Kocac⁴⁵, A.Kilic⁴⁵, K.Kimura⁴¹, M.Klein¹⁷, U.Klein¹⁷, T.Kluge¹⁷, G.Kramer¹², M.Korostelev²³, A.Kosmicki¹⁰, P.Kostka¹¹, H.Kowalski¹¹, D.Kuchler¹⁰, M.Kuze⁴¹, T.Lappi¹⁴, P.Laycock¹⁷, E.Levichev³¹, S.Levonian¹¹, V.N.Litvinenko⁴⁷, A.Lombardi¹⁰, C.Marquet¹⁰, B.Mellado⁰⁷, K.H.Mess¹⁰, A.Milanese¹⁰, S.Moch¹¹, I.I.Morozov³¹, Y.Muttoni¹⁰, S.Myers¹⁰, S.Nandi²⁶, P.R.Newman⁰³, T.Omori⁴⁴, J.Osborne¹⁰, Y.Papaphilippou¹⁰, E.Paoloni³⁵, C.Pascaud³³, H.Paukkunen³⁸, E.Perez¹⁰, T.Pieloni¹⁵, E.Pilicer⁴⁵, B.Pire⁵⁵, A.Polini⁰⁴, V.Ptitsyn⁴⁷, Y.Pupkov³¹, V.Radescu¹³, S.Raychaudhuri²⁷, L.Rinolfi¹⁰, R.Rohini²⁷, J.Rojo²⁴, S.Russenschuck¹⁰, C.A.Salgado³⁸, K.Sampe⁴¹, R.Sassot⁵⁷, E.Sauvan¹⁹, M.Sahin⁰¹, U.Schneekloth¹¹, T.Schoerner Sadenius¹¹, D.Schulte¹⁰, A.N.Skrinsky³¹, W.Smith²⁰, H.Spiesberger²¹, A.M.Stasto⁴⁶, M.Strikman⁴⁶, M.Sullivan³⁹, B.Surrow⁰⁵, S.Sultansoy⁰¹, Y.P.Sun³⁹, L.Szymanowski⁵⁶, I.Tapan⁴⁵, P.Taels⁰², E.Tassi⁵², H.Ten.Kate¹⁰, J.Terron²², H.Thiesen¹⁰, L.Thompson²³, K.Tokushuku⁴⁴, R.Tomás García¹⁰, D.Tommasini¹⁰, D.Trbojevic⁴⁷, N.Tsoupas⁴⁷, J.Tuckmantel¹⁰, S.Turkoz⁵³, K.Tywoniuk¹⁸, G.Unel¹⁰, J.Urakawa⁴⁴, P.VanMechelen⁰², A.Variola³⁷, R.Veness¹⁰, A.Vivoli¹⁰, P.Vobly³¹, R.Wallny⁵¹, S.Wallon⁵⁹, G.Watt¹⁰, G.Weiglein¹², C.Weiss²⁸, U.A.Wiedemann¹⁰, U.Wienands³⁹, F.Willeke⁴⁷, B.-W.Xiao⁴⁶, V.Yakimenko⁴⁷, A.F.Zarnecki⁴⁹, F.Zimmermann¹⁰, R.Zlebcik⁶⁰, F.Zomer³³

Why an ep/A Experiment at TeV Energies?

1. For resolving the quark structure of the nucleon with p, d and ion beams

QPM symmetries, quark distributions (complete set from data!), GPDs, nuclear PDFs ..

2. For the development of perturbative QCD

N^k LO ($k \geq 2$) and h.o. eweak, HQs, jets, resummation, factorisation, diffraction

3. For mapping the gluon field

Gluon for $\sim 10^{-5} < x < 1$, is unitarity violated? J/ψ , F_2^c , ... unintegrated gluon

4. For searches and the understanding of new physics

GUT (α_s to 0.1%), LQs RPV, Higgs (bb, HWW) ... PDFs4LHC... instanton, odderon,..?

5. For investigating the physics of parton saturation

Non-pQCD (chiral symm breaking, strings), black disc limit, saturation border..

..For providing data which could be of use for future experiments [Proposal for SLAC ep 1967]

Candidates for Surprises and Discoveries

PDFs ($t, s, q-\bar{q}, \text{val}, xg$)
Odderon
Instanton
(no) saturation, QCD
QGP initial state

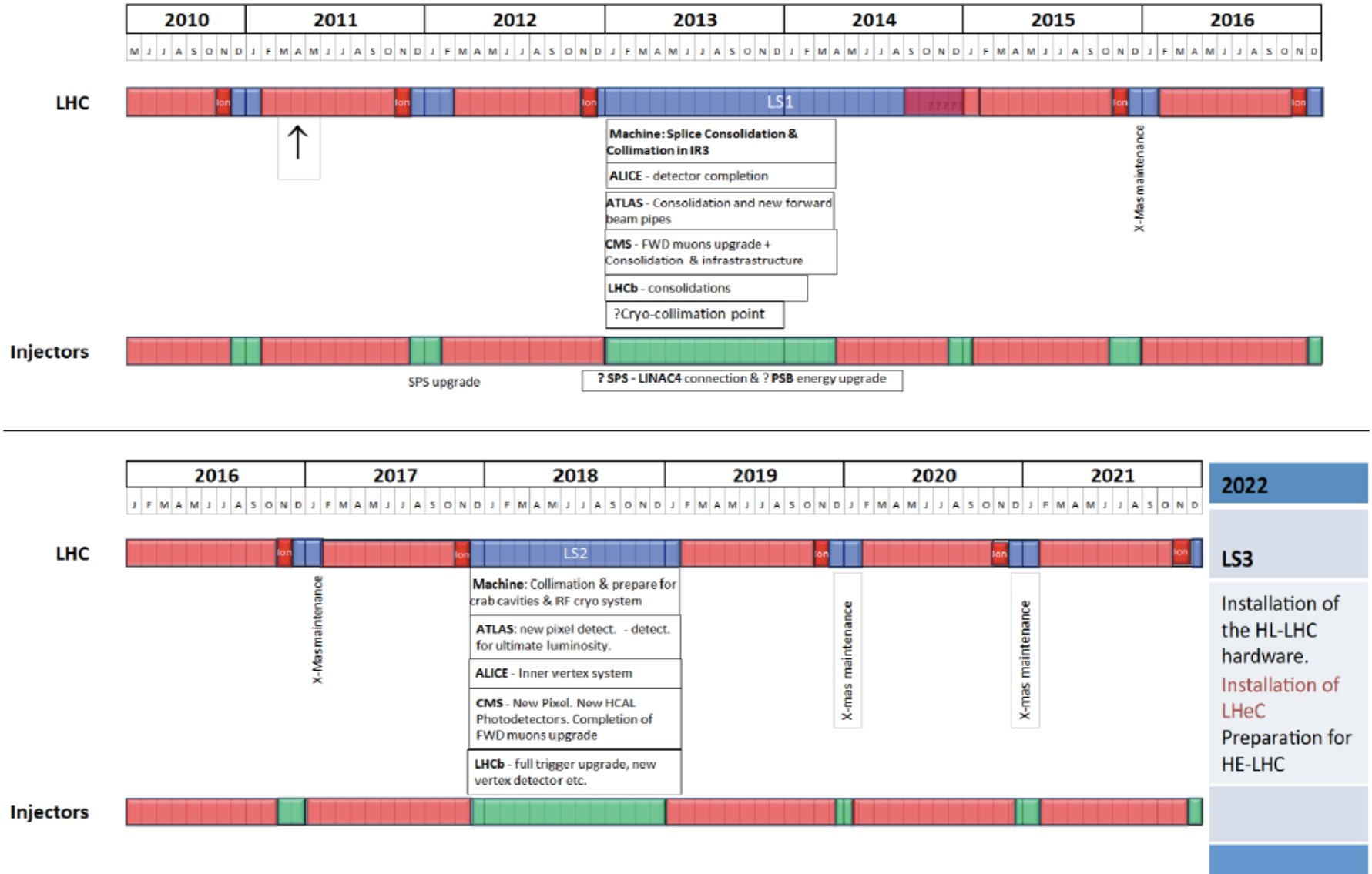
The study of deep inelastic ep scattering is important for the investigation of the nature of the Pomeron and Odderon, which are Regge singularities of the t -channel partial waves $f_j(t)$ in the complex plane of the angular momentum j . The Pomeron is responsible for a growth of total cross sections with energy. The Odderon describes the behaviour of the difference of the cross sections for particle-particle and particle-antiparticle scattering which obey the Pomeronchuk theorem. In perturbative QCD, the Pomeron and Odderon are the simplest colorless reggeons (families of glueballs) constructed from two and three reggeized gluons, respectively. Their wave functions satisfy the generalized BFKL equation. In the next-to-leading approximation the solution of the BFKL equation contains an infinite number of Pomerons and to verify this prediction of QCD one needs to increase the energy of colliding particles. In the $N=4$ supersymmetric generalization of QCD, in the t'Hooft limit of large N_c , the BFKL Pomeron is equivalent to the reggeized graviton living in the 10-dimensional anti-de-Sitter space. Therefore, the Pomeron interaction describing the screening corrections to the BFKL predictions, at least in this model, should be based on a general covariant effective theory being a generalization of the Einstein-Hilbert action for general relativity. Thus, the investigation of high energy ep scattering could be interesting for the construction of a non-perturbative approach to QCD based on an effective string model in high dimensional spaces.

Lev Lipatov in the CDR...

Ultra high precision (detector, e-h redundancy) - new insight
Maximum luminosity and much extended range - rare, new effects
Deep relation to (HL-) LHC (precision+range) - complementarity
→ **LHeC brings a substantial enrichment of LHC physics**

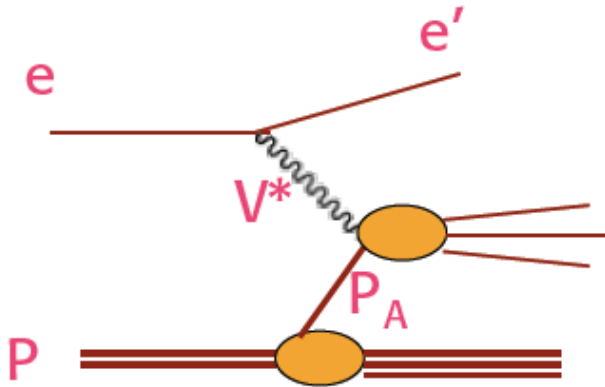
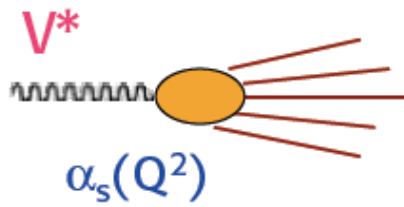
Factorization pp-ep
LQs, RPV SUSY
 e^*
Higgs CP
 α_s indeed small (GUT)

Draft LHC Schedule for the coming decade

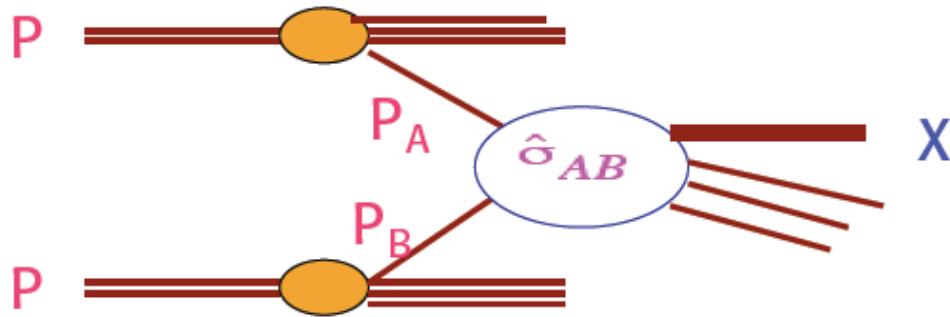


as shown by S. Myers at EPS 2011 Grenoble

Physics with the LHeC



$\alpha_s(Q^2)$ & $q(x, Q^2), g(x, Q^2)$



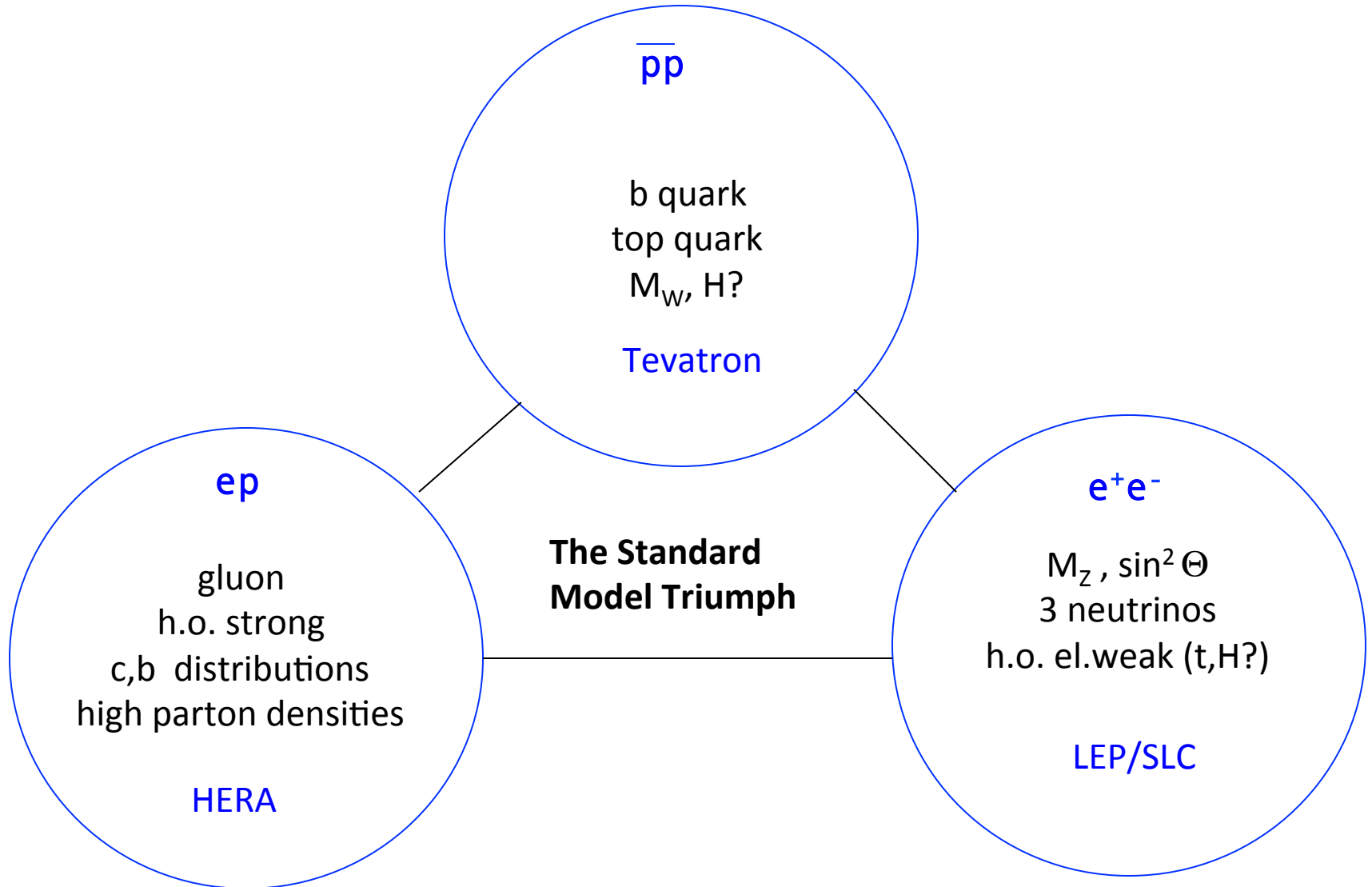
The basic experimental set ups:

- no initial hadron (...LEP, ILC, CLIC)
- 1 hadron (...HERA, LHeC)
- 2 hadrons (...SppS, Tevatron, LHC)

Progress in particle physics needs their continuous interplay to take full advantage of their complementarity



The Fermi Scale [1985-2012]



4 Precision QCD and Electroweak Physics

4.1 Inclusive Deep Inelastic Scattering

4.1.1 Cross Sections and Structure Functions

4.1.2 Neutral Current

4.1.3 Charged Current

4.1.4 Cross Section Simulation and Uncertainties

4.1.5 Longitudinal Structure Function F_L

4.2 Determination of Parton Distributions

4.2.1 QCD Fit Ansatz

4.2.2 Valence Quarks

4.2.3 Strange Quarks

4.2.4 Top Quarks

4.3 Gluon Distribution

4.4 Prospects to Measure the Strong Coupling Constant

4.4.1 Status of the DIS Measurements of α_s

4.4.2 Simulation of α_s Determination

4.5 Electron-Deuteron Scattering

4.6 Charm and Beauty production

4.6.1 Introduction and overview of expected highlights

4.6.2 Total production cross sections for charm, beauty and top quarks

4.6.3 Charm and Beauty production in DIS

4.6.4 Intrinsic Heavy Flavour

4.6.5 D^* meson photoproduction study

4.7 High p_t jets

4.7.1 Jets in ep

4.7.2 Jets in γA

4.8 Total photoproduction cross section

4.9 Electroweak physics

4.9.1 The context

4.9.2 Light Quark Weak Neutral Current Couplings

4.9.3 Determination of the Weak Mixing Angle

153 pages

now

then

5 New Physics at Large Scales

5.1 New Physics in inclusive DIS at high Q^2

5.1.1 Quark substructure

5.1.2 Contact Interactions

5.1.3 Kaluza-Klein gravitons in extra-dimensions

5.2 Leptoquarks and leptogluons

5.2.1 Phenomenology of leptoquarks in ep collisions

5.2.2 The Buchmüller-Rückl-Wyler Model

5.2.3 Phenomenology of leptoquarks in pp collisions

5.2.4 Current status of leptoquark searches

5.2.5 Sensitivity on leptoquarks at LHC and at LHeC

5.2.6 Determination of LQ properties

5.2.7 Leptogluons

5.3 Excited leptons and other new heavy leptons

5.3.1 Excited Fermion Models

5.3.2 Simulation and Results

5.3.3 New leptons from a fourth generation

5.4 New physics in boson-quark interactions

5.4.1 An LHeC-based $\gamma\gamma$ collider

5.4.2 Anomalous Single Top Production at the LHeC Based $\gamma\gamma$ Collider

5.4.3 Excited quarks in $\gamma\gamma$ collisions at LHeC

5.4.4 Quarks from a fourth generation at LHeC

5.4.5 Diquarks at LHeC

5.4.6 Quarks from a fourth generation in Wq interactions

5.5 Sensitivity to a Higgs boson

5.5.1 Higgs production at LHeC

5.5.2 Observability of the signal

5.5.3 Probing Anomalous HWW Couplings at the LHeC

6 Physics at High Parton Densities

6.1 Physics at small x

6.1.1 Unitarity and QCD

6.1.2 Status following HERA data

6.1.3 Low- x physics perspectives at the LHC

6.1.4 Nuclear targets

6.2 Prospects at the LHeC

6.2.1 Strategy: decreasing x and increasing A

6.2.2 Inclusive measurements

6.2.3 Exclusive Production

6.2.4 Inclusive diffraction

6.2.5 Jet and multi-jet observables, parton dynamics and fragmentation

6.2.6 Implications for ultra-high energy neutrino interactions and detection

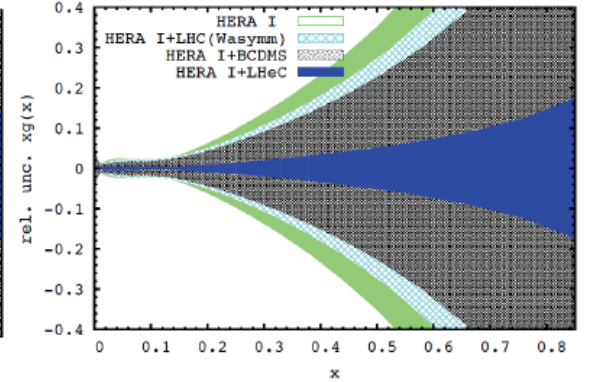
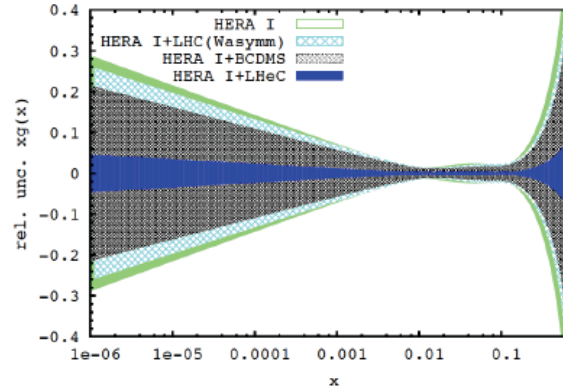
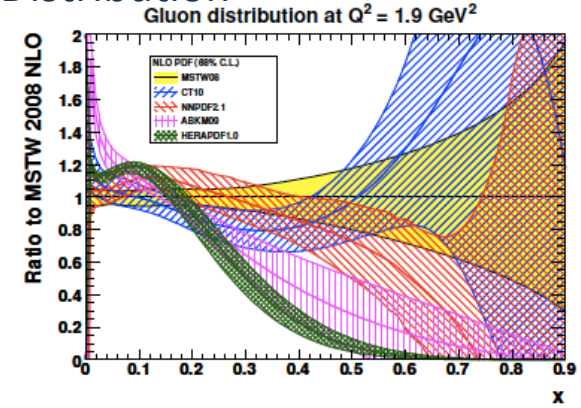
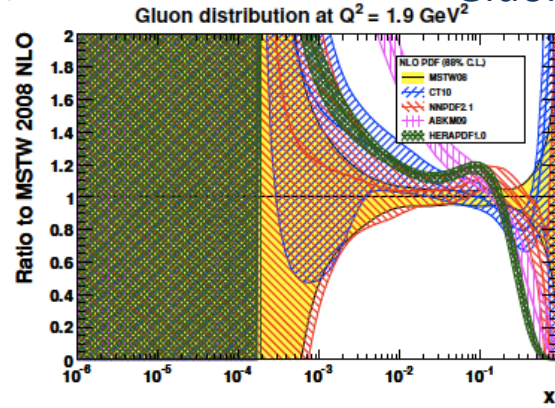


Figure 4.17: Relative uncertainty of the gluon distribution at $Q^2 = 1.9 \text{ GeV}^2$, as resulting from an NLO QCD fit to HERA (I) alone (green, outer), HERA and BCDMS (crossed), HERA and LHC (light blue, crossed) and the LHeC added (blue, dark). Left: logarithmic x , right: linear x .

Precision measurement of gluon density to extreme $x \rightarrow \alpha_s$
 Low x : saturation in ep ? Crucial for QCD, LHC, UHE neutrinos!
 High x : xg and valence quarks: resolving new high mass states!
 Gluon in Pomeron, odderon, photon, nuclei.. Local spots in p ?
 Heavy quarks intrinsic or only gluonic?

Strong Coupling Constant

α_s least known of coupling constants

Grand Unification predictions suffer from $\delta\alpha_s$

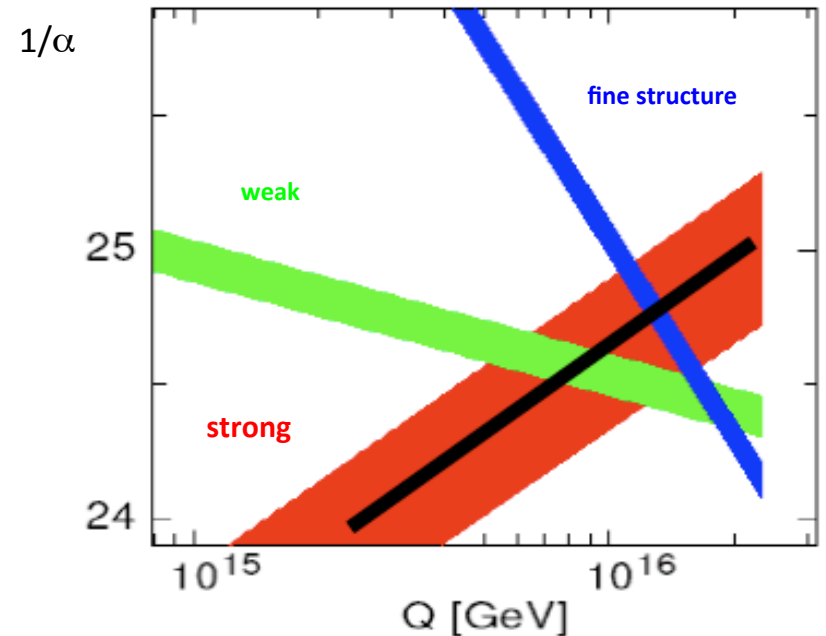
DIS tends to be lower than world average

Recently challenged by MSTW and NNPDF – jets??

LHeC: per mille - independent of BCDMS.

Challenge to experiment and to h.o. QCD →

A genuine DIS research programme rather than one outstanding measurement only.



case	cut [Q^2 in GeV^2]	relative precision in %
HERA only (14p)	$Q^2 > 3.5$	1.94
HERA+jets (14p)	$Q^2 > 3.5$	0.82
LHeC only (14p)	$Q^2 > 3.5$	0.15
LHeC only (10p)	$Q^2 > 3.5$	0.17
LHeC only (14p)	$Q^2 > 20.$	0.25
LHeC+HERA (10p)	$Q^2 > 3.5$	0.11
LHeC+HERA (10p)	$Q^2 > 7.0$	0.20
LHeC+HERA (10p)	$Q^2 > 10.$	0.26

Two independent QCD analyses using LHeC+HERA/BCDMS
Full experimental uncertainties (unc+corr systematics)

DATA

NC e^+ only

exp. error on α_s

0.48%

NC

0.41%

NC & CC

0.23% :=⁽¹⁾

⁽¹⁾ $\gamma_h > 5^\circ$

0.36% :=⁽²⁾

⁽¹⁾ +BCDMS

0.22%

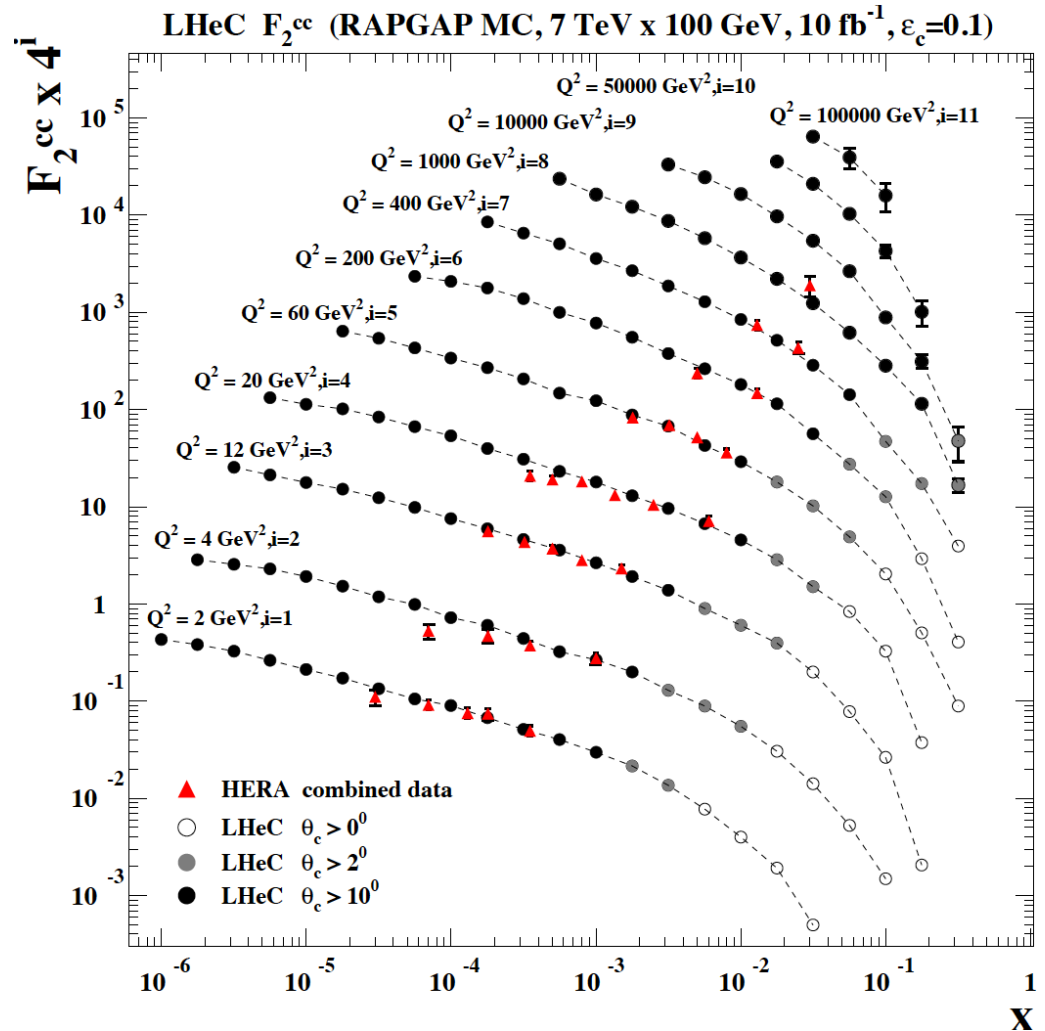
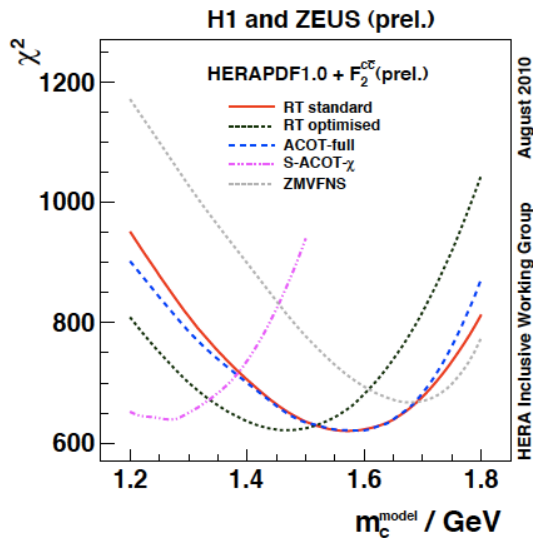
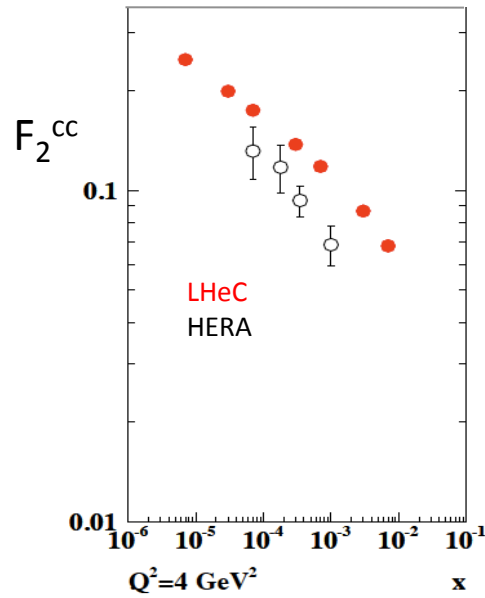
⁽²⁾ +BCDMS

0.22%

⁽¹⁾ stat. *= 2

0.35%

Treatment of charm influences α_s



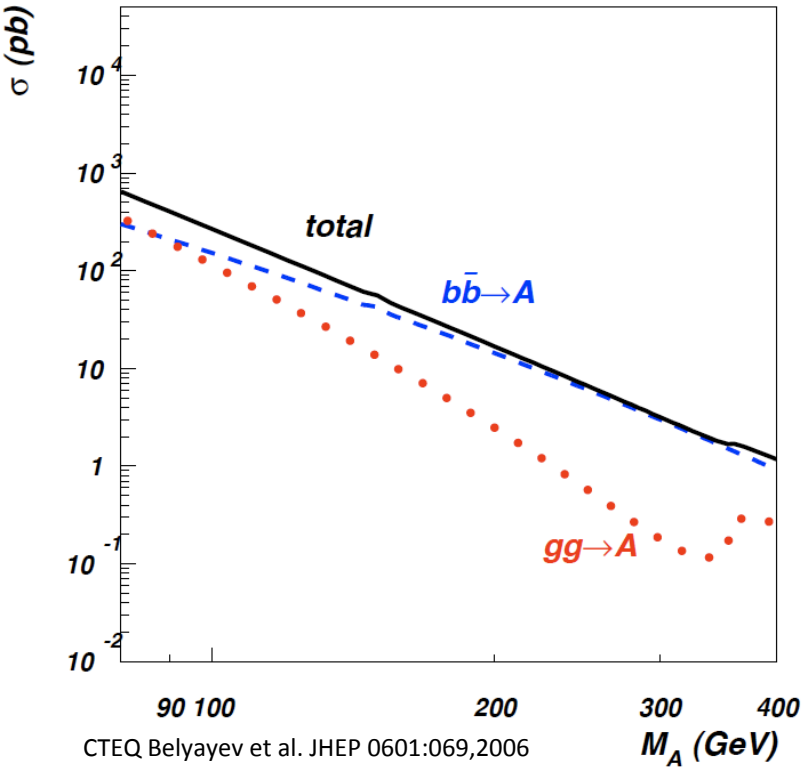
LHeC vs HERA: higher fraction of c, larger range, smaller beam spot, better Silicon detectors

note: 100 MeV of m_c is about 1% on α_s

Intrinsic charm at large x?

Beauty - MSSM Higgs

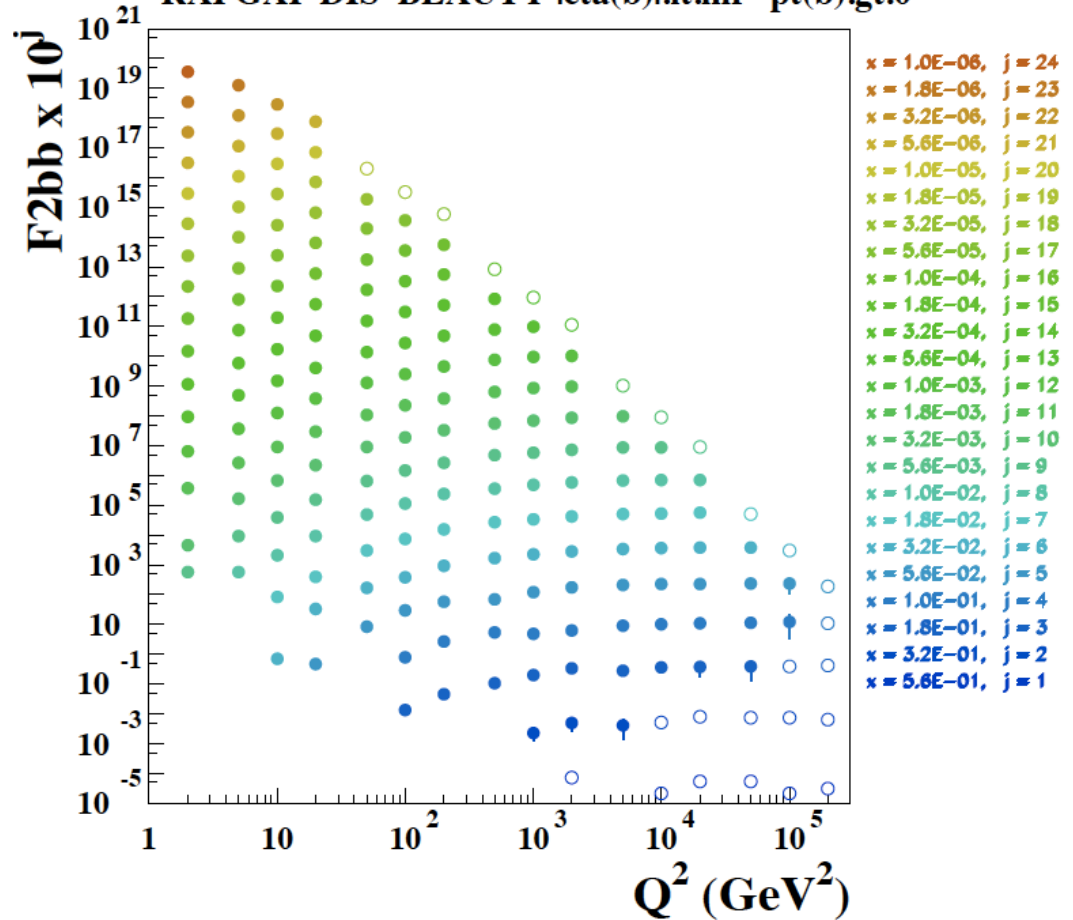
(b) LHC, $\sqrt{s} = 14$ TeV, MSSM, $\tan\beta=10$



In MSSM Higgs production is b dominated

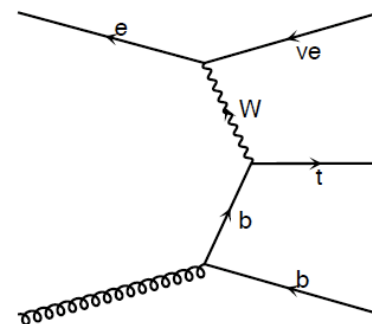
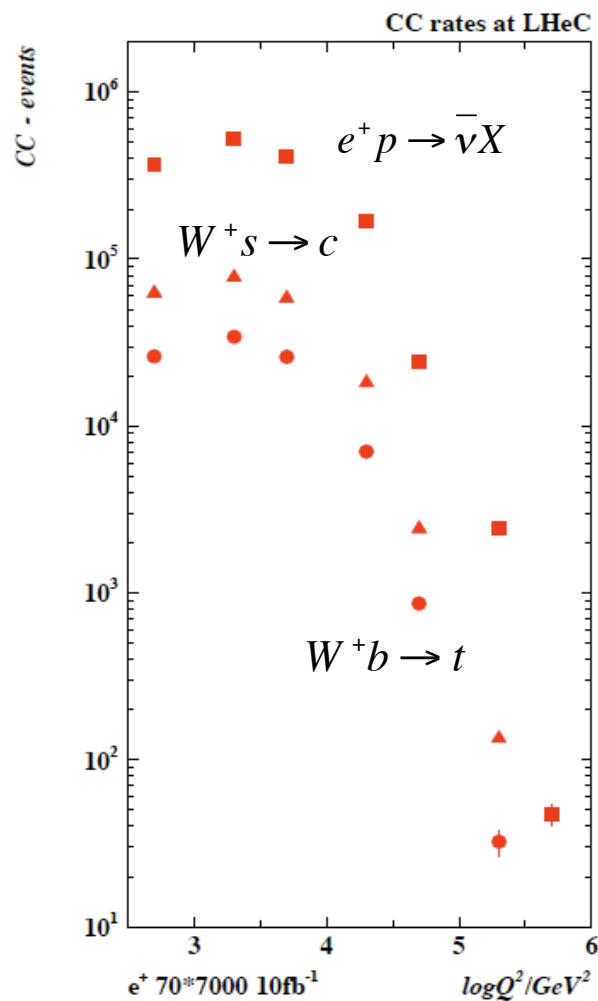
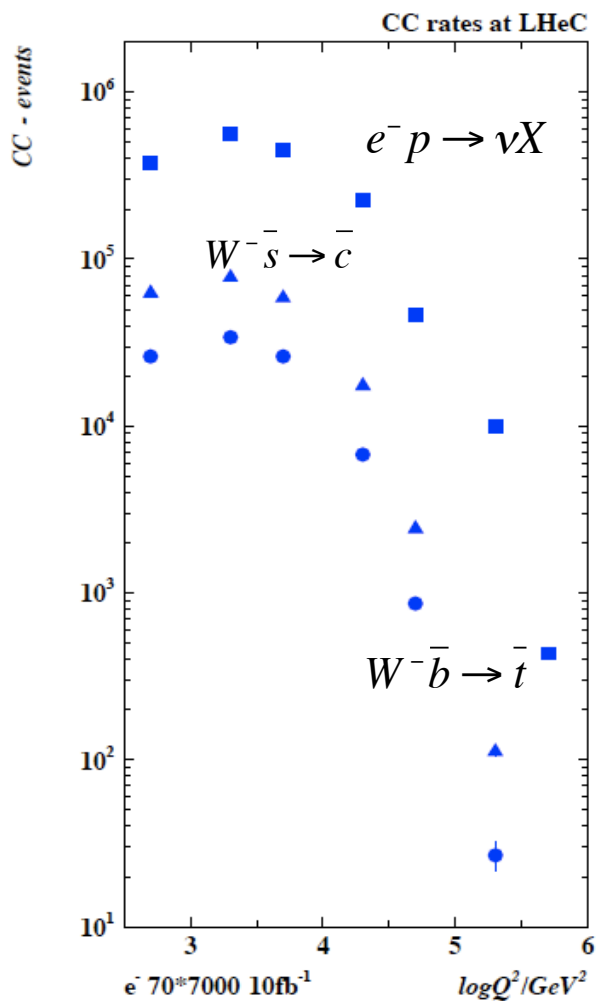
HERA: First measurements of b to ~20%
LHeC: precision measurement of b-df

LHeC 7000x100, 10 fb^{-1} , $b\text{-tag eff. } 0.1$
 RAPGAP DIS BEAUTY $\text{leta}(b) \text{!lt.inf pt}(b) \text{.gt.0}$



LHeC: higher fraction of b, larger range,
 smaller beam spot, better Si detectors

Top and Top Production in Charged Currents



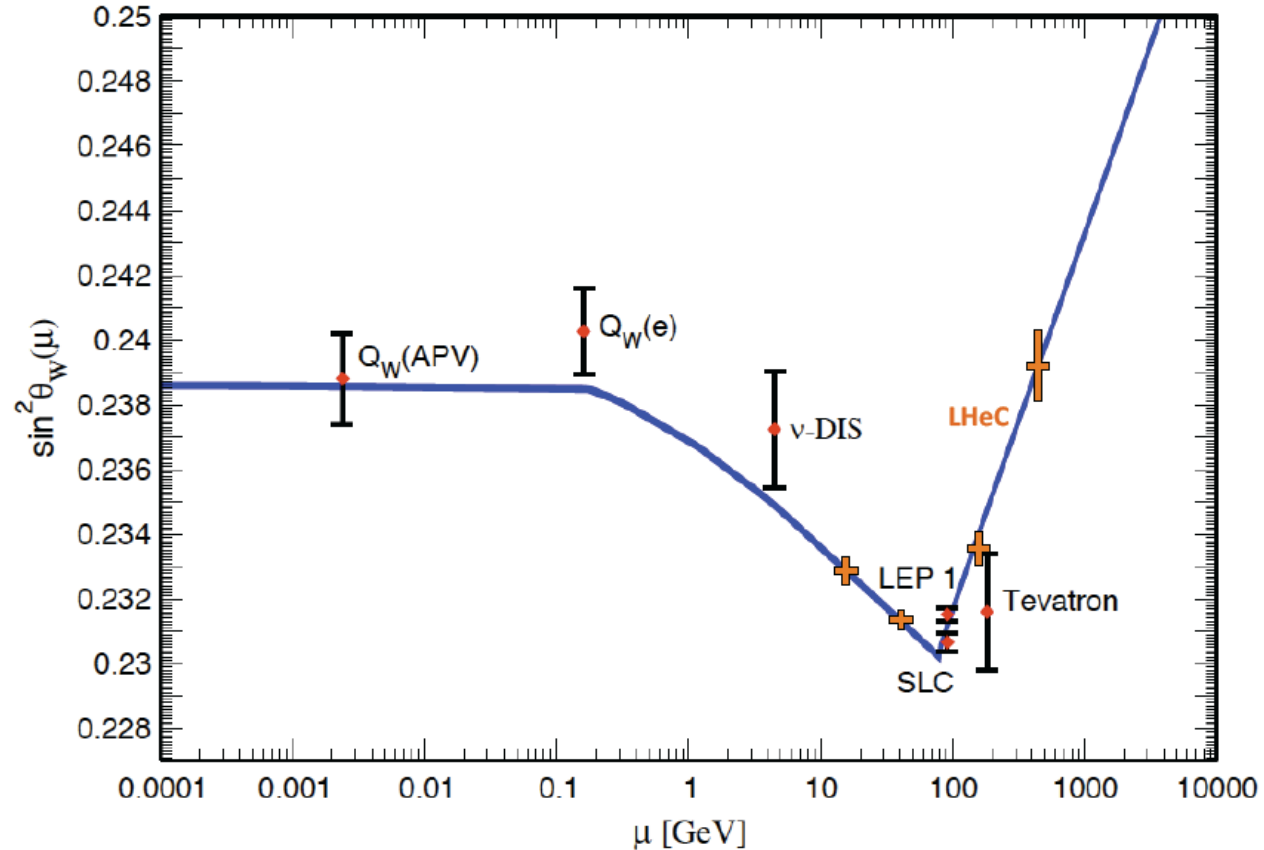
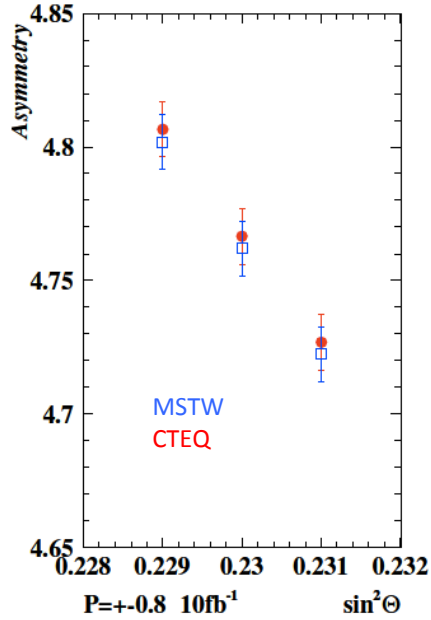
**LHeC copious
single top and anti-top
quark production**

with a CC cross section
of O(10) pb

Study Q^2 evolution of
top quark onset –
6 quark CFNS
(Pascaud at DIS11)

m_{top}
Not yet simulated..

Weak Neutral Currents – Polarisation Asymmetry

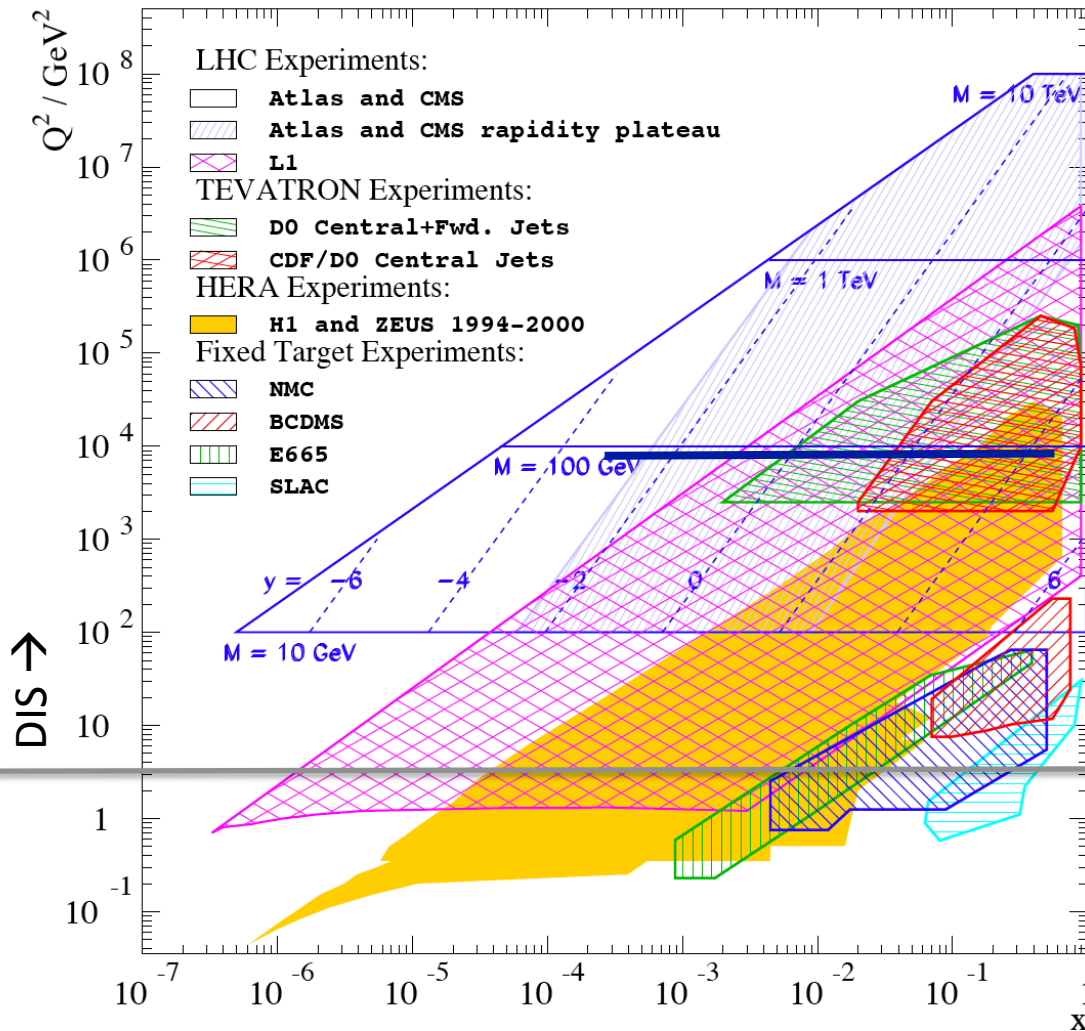


$$A^{\pm} = \frac{\sigma_{NC}^{\pm}(P_R) - \sigma_{NC}^{\pm}(P_L)}{\sigma_{NC}^{\pm}(P_R) + \sigma_{NC}^{\pm}(P_L)}$$

$$A^{\pm} \simeq \mp \kappa_Z a_e \frac{F_2^{\gamma Z}}{(F_2 + \kappa_Z a_e Y_- x F_3^{\gamma Z} / Y_+)} \simeq \mp \kappa_Z a_e \frac{F_2^{\gamma Z}}{F_2}$$

Measure running of the weak mixing angle to high precision with polarised e^- .
[stat. errors, much of syst. cancels, pdfs from LHeC itself]

Complementing the LHC with ep/A



In Drell-Yan kinematics: mass and rapidity relate to Q^2 and x

LHC partons: W,Z +c,b new constraints but severely limited in x, Q^2 range

Discoveries at the LHC will be at high masses: large x and very high Q^2 which require high s , lumi of LHeC for precision PDFs (u,d,xg mainly)

If the Higgs exists, its study will become a major field of research: ep: $WW \rightarrow H \rightarrow b\bar{b}$ (CP odd/even?)

top distribution in the proton TDF

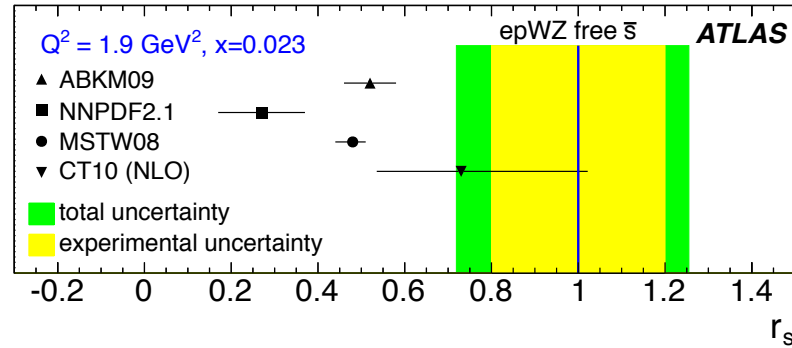
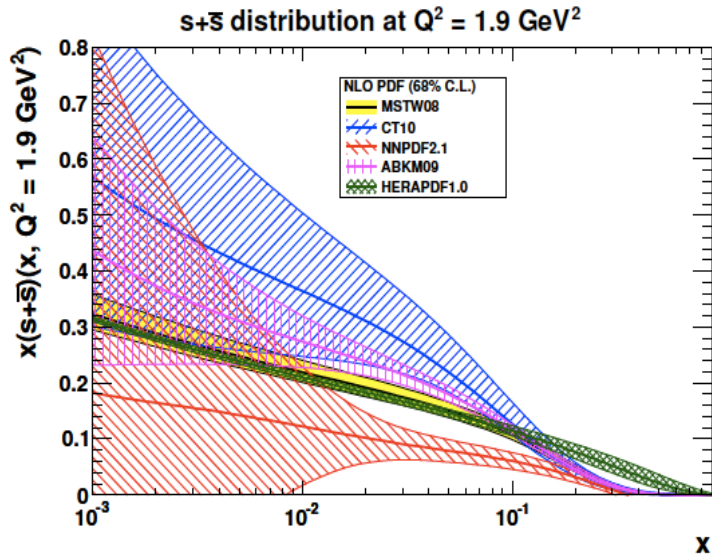
IF RP is violated and LQ or RPV SUSY discovered: LHeC is uniquely suited

AA: QGP: study initial state in eA
Resolve parton distributions in nuclei

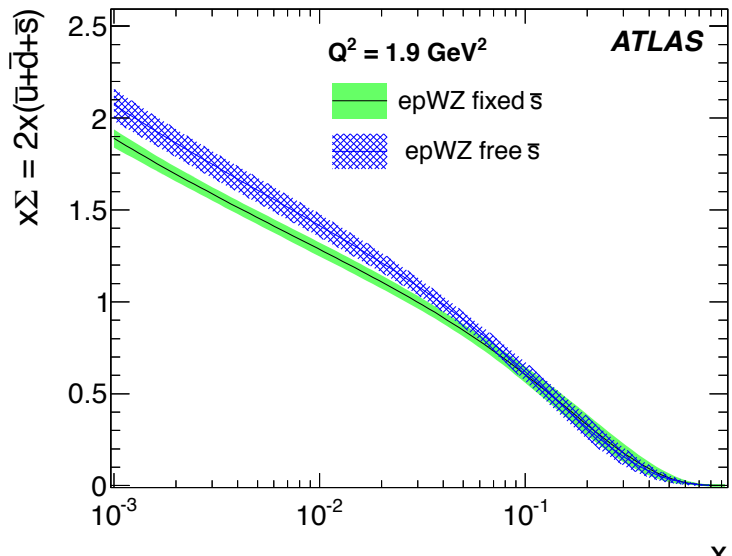
LHeC is unique in various areas, e.g.:
Low x and saturation physics
Strong coupling constant to 0.1% level

LHC and LHeC - Strange Quark Distribution

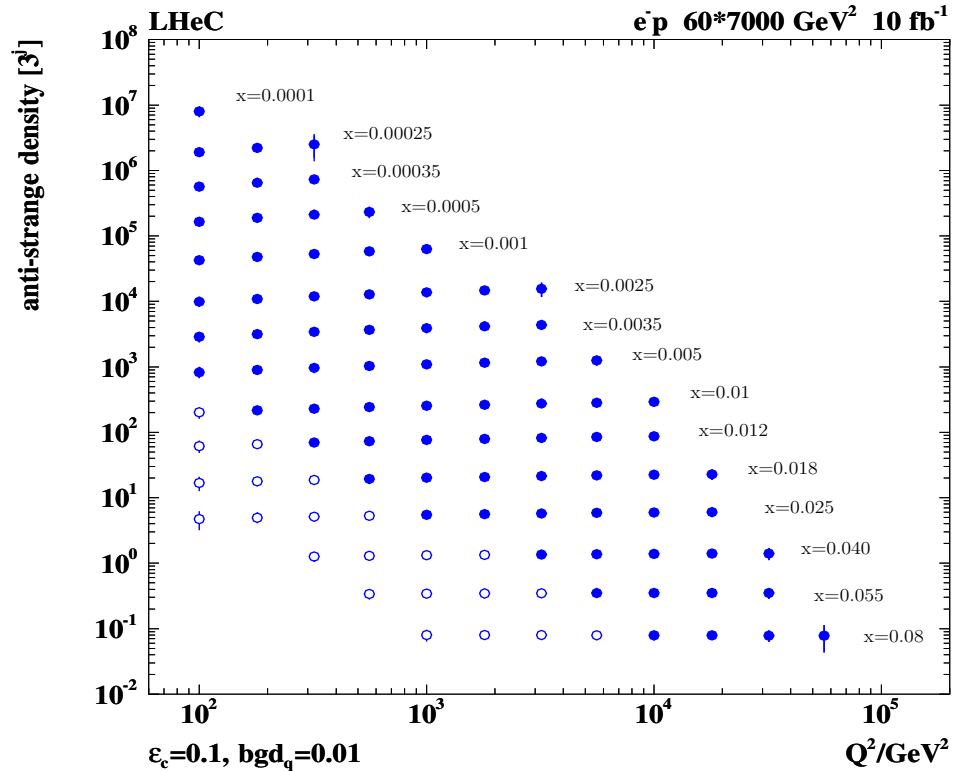
ATLAS → PRL



Trend confirmed in NNPDF collider only fit

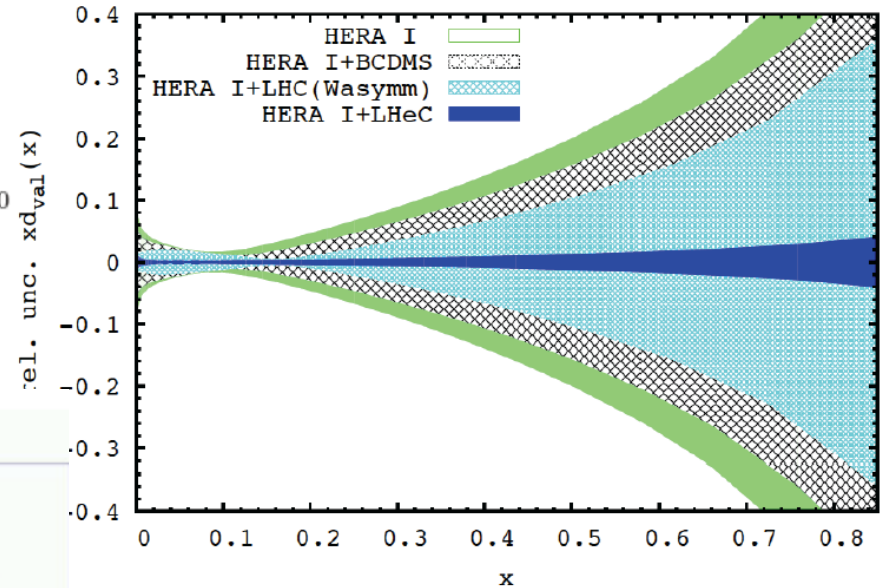
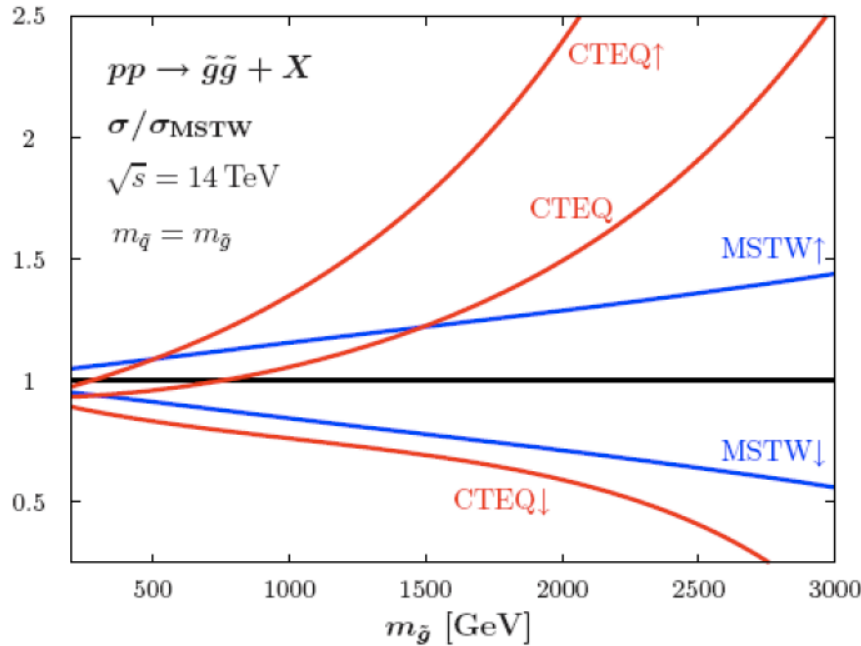


Change of strange affects sea - UHE ν

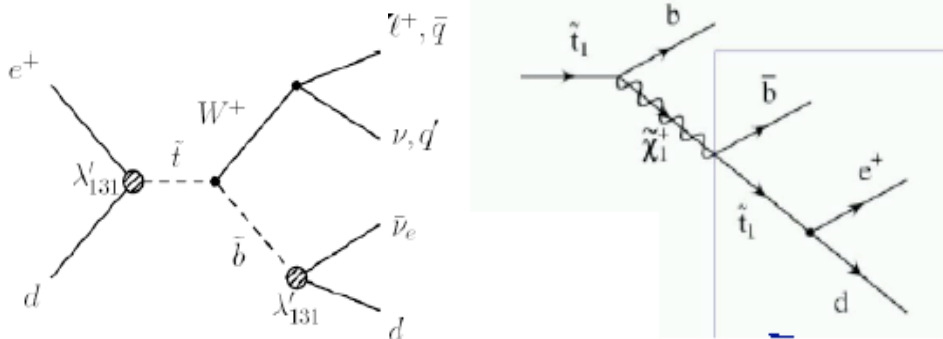


SUSY

HL-LHC will explore highest mass range. This requires to control very high Bj x, where LHeC pins down partons such that resummation and factorisation effects can be controlled.



RPV SUSY in 3rd generation?

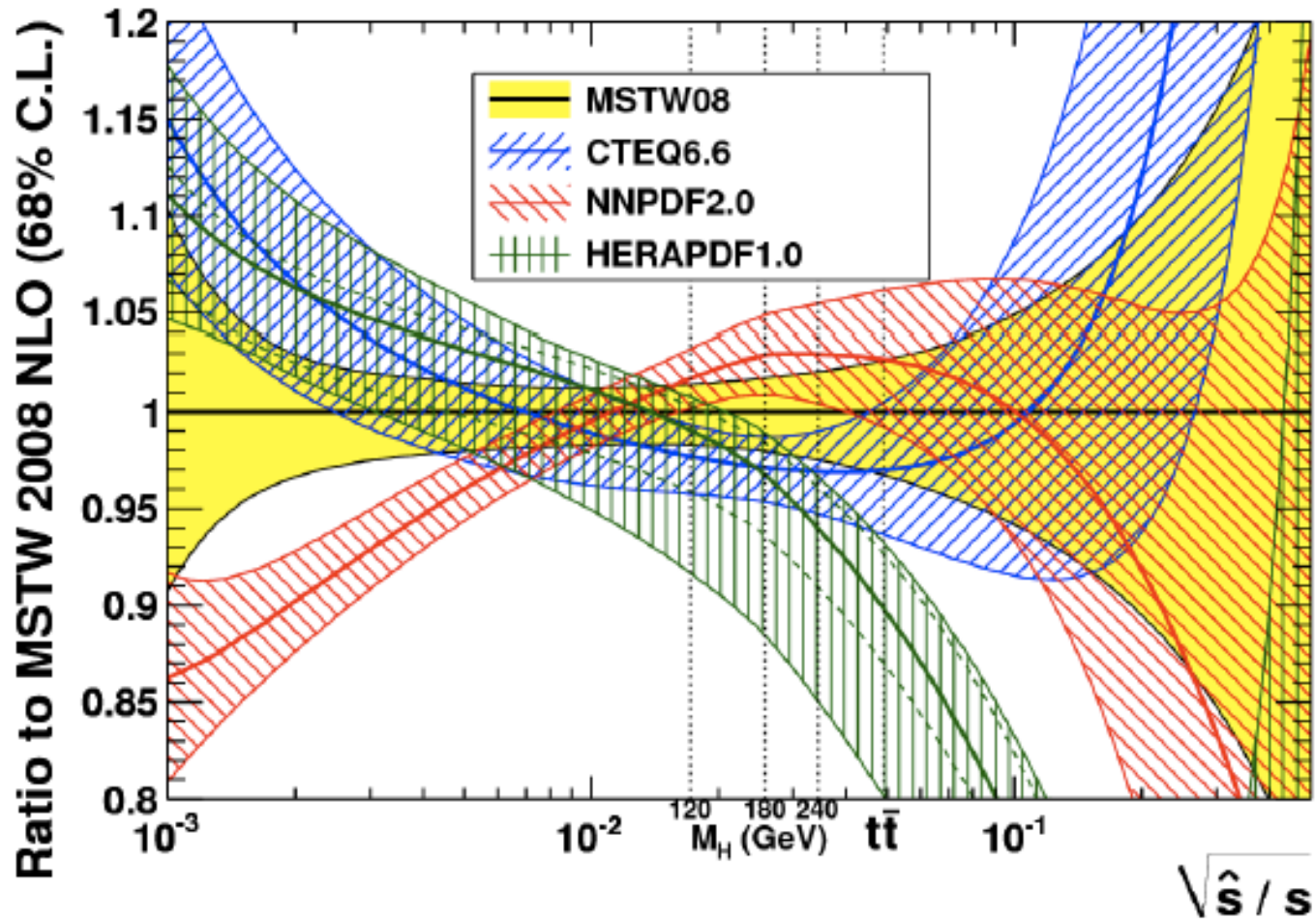


$$W_R = \frac{1}{2} \lambda_{ijk} L_i L_j \bar{E}_k + \lambda'_{ijk} L_i Q_j \bar{D}_k + \frac{1}{2} \lambda''_{ijk} \bar{U}_i \bar{D}_j \bar{D}_k$$

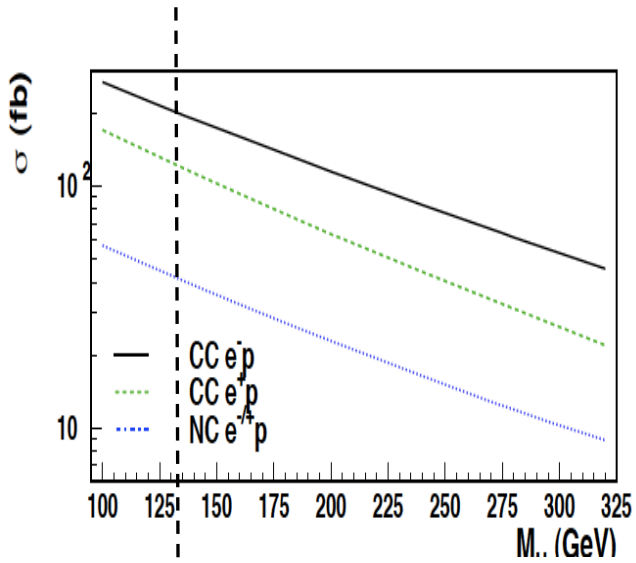
L: LH (s)leptons, **Q**: LH (s)quarks, **D**: RH down-type (s)quarks
 i, j, k generation indices (27 couplings)

gg luminosity at LHC ($\sqrt{s} = 7$ TeV)

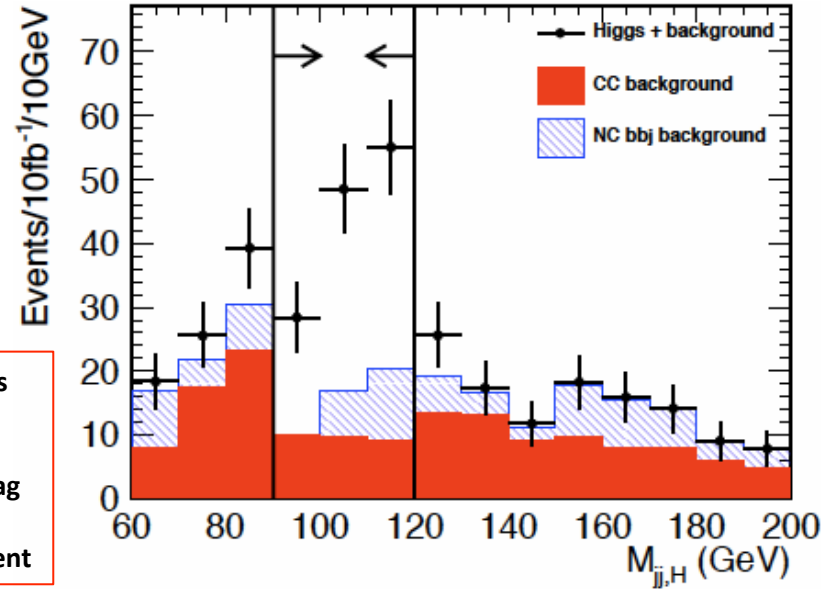
G. Watt



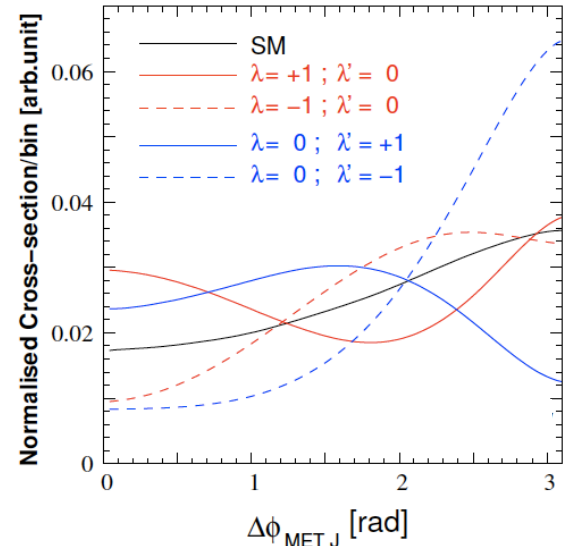
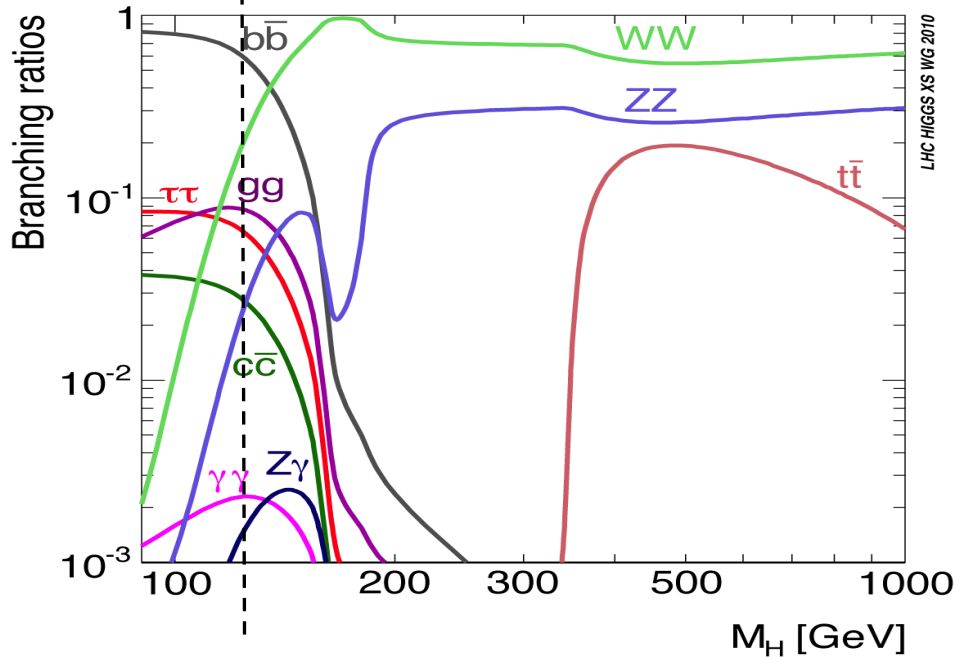
Higgs



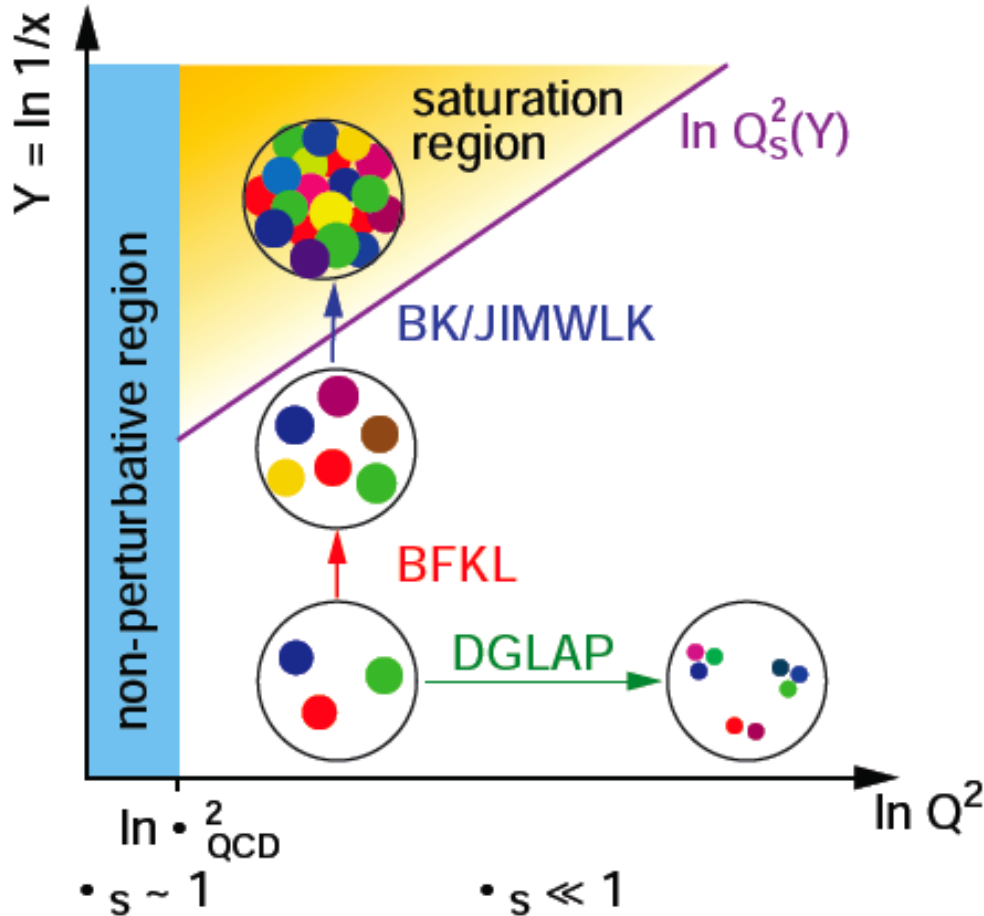
Process determines much of detector acceptance and calibration and b tag (also single top) and L/E_e requirement



Higgs is light (or absent), CC: $WW \rightarrow H \rightarrow bb$
 CP even: SM, CP odd: nonSM, mixture?



High Parton Densities

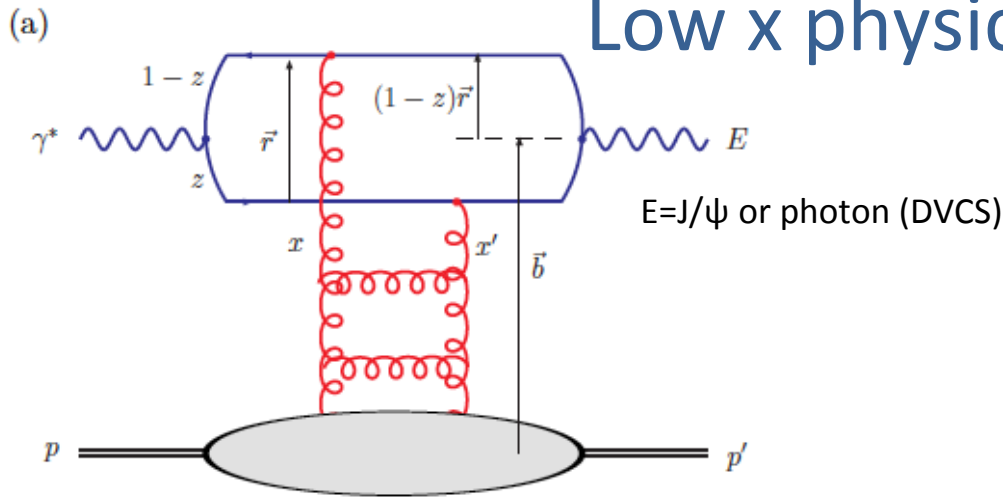


Should lead to non-linear evolution theory and eventually discover saturation of rise of gluon density (unitarity limit?)

Needs highest energy to be studied in both ep and eA.

CDR $L_{eN} \cong 3-10 * 10^{31} \text{ cm}^{-2}\text{s}^{-1}$ for D,A - not optimised

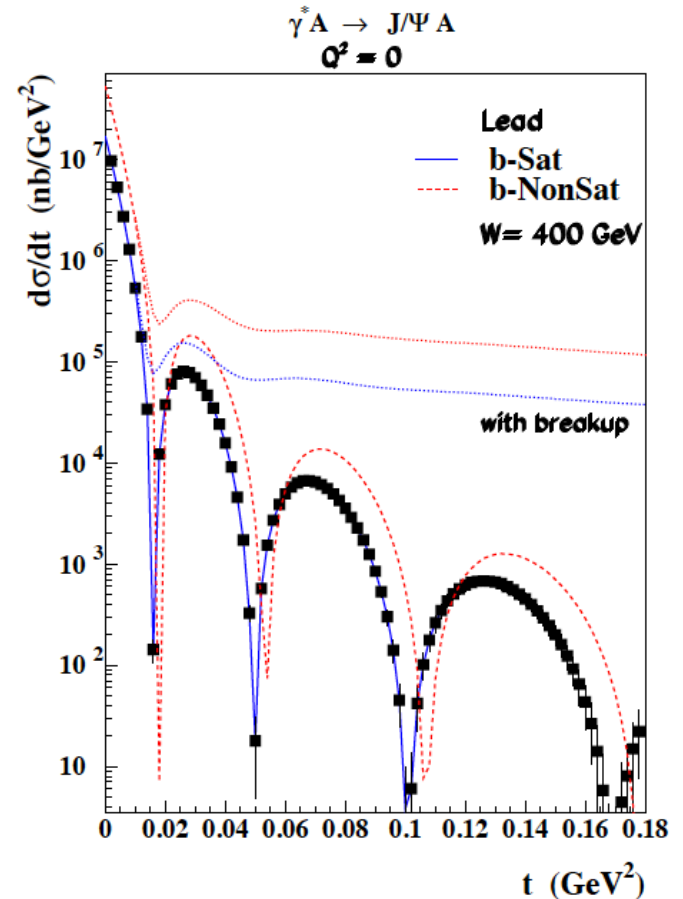
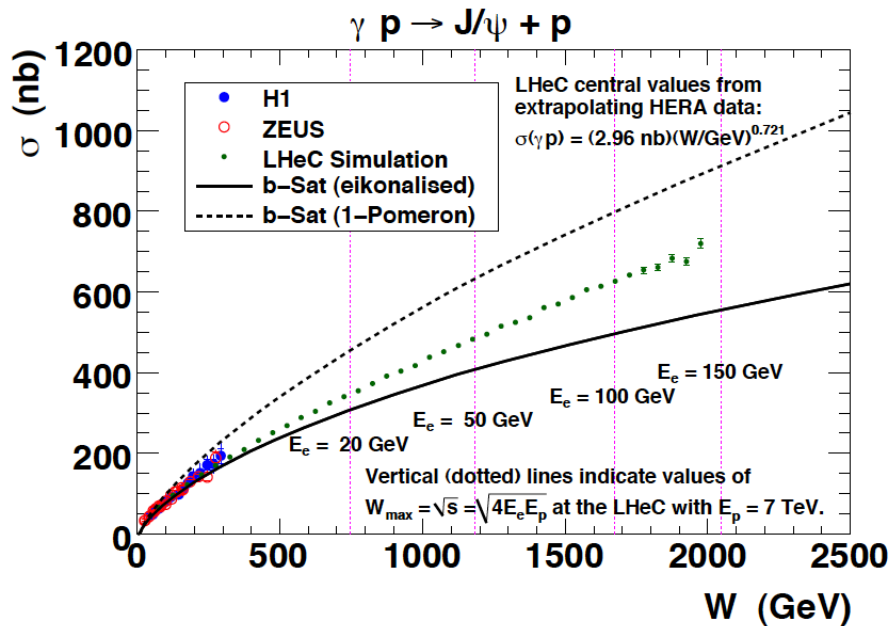
Low x physics - J/ψ in γ* p/A



Test of saturation

$$\sigma_{T,L}^{\gamma^* p}(x, Q) = \text{Im} A_{T,L}^{\gamma^* p \rightarrow \gamma^* p}(x, Q, \Delta = 0) = \sum_f \int d^2 r \int_0^1 \frac{dz}{4\pi} (\Psi^* \Psi)_{T,L}^f \int d^2 b \frac{d\sigma_{qq}}{d^2 b}$$

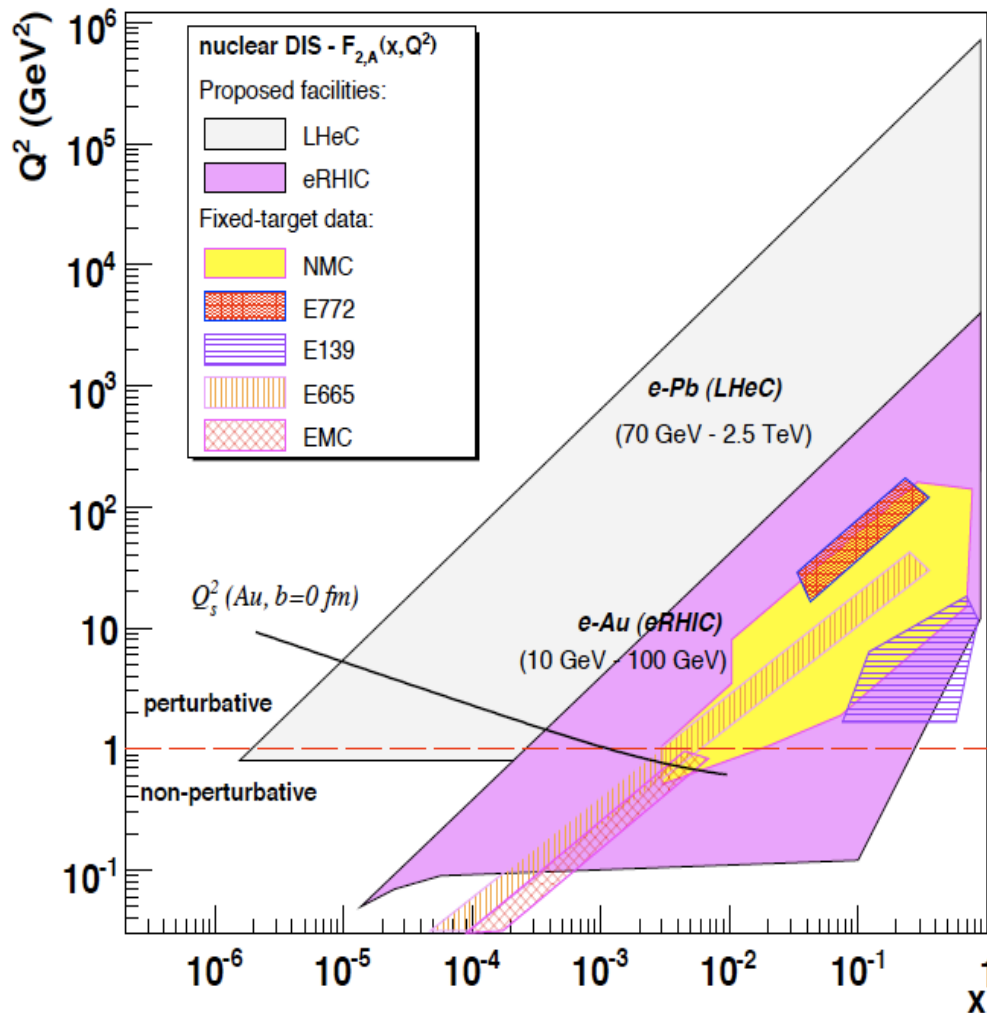
Optical theorem relates J/ψ to $F_T = F_2 - F_L$



Coherent production in $\gamma^* A$

Probing of nuclear matter

Electron-Ion Scattering



EIC programme:
see recent workshop arXiv:1108.1713 [nucl-th]

Dipole models predict **saturation** which resummation in pQCD moves to lower x ..
It requires highest energy, low x , $Q^2 > M_p^2$

Saturation at the LHeC is predicted to be observed both in ep AND in eA.
This combination is crucial to disentangle nuclear from unitarity effects.

Expect **qualitative changes of behaviour**

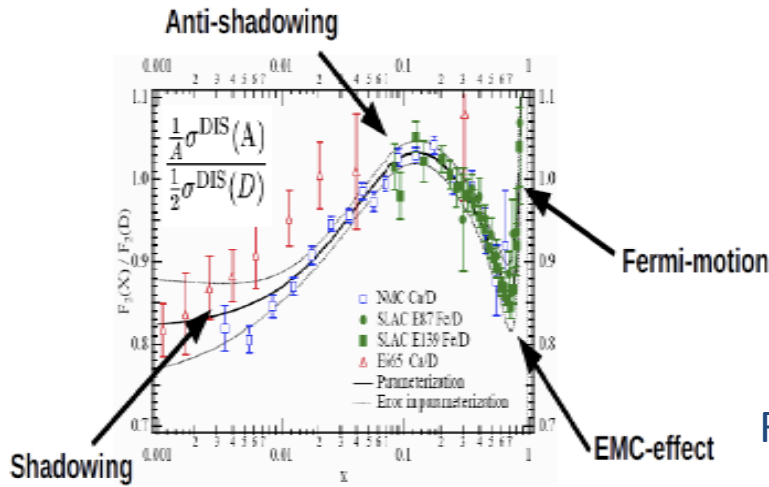
- Black body limit of F_2
- Saturation amplified with $A^{1/3}$
- Rise of diffraction to 50%? ...

Below $x \sim 10^{-2}$: DIS data end. NO flavour separation yet. However indications are that e.g. shadowing is flavour dependent.

Deuterons: tag spectator,
relate shadowing-diffraction (Gribov)!
stabilise QCD evolution (singlet!)

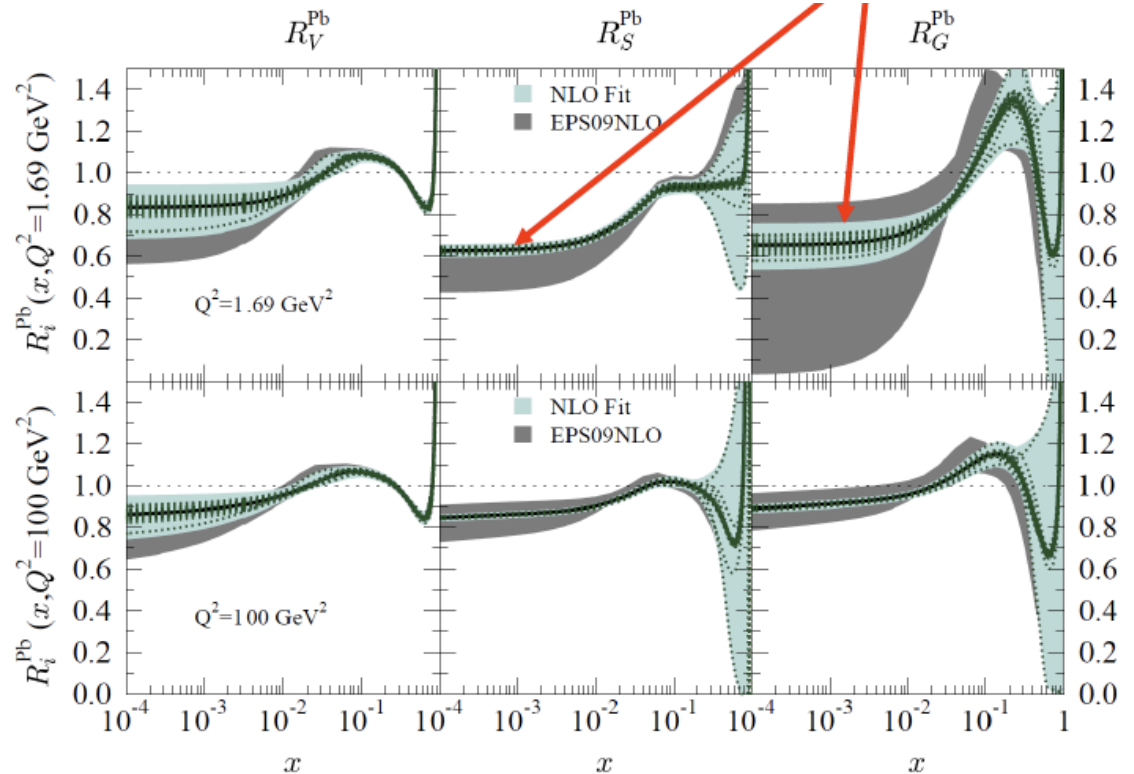
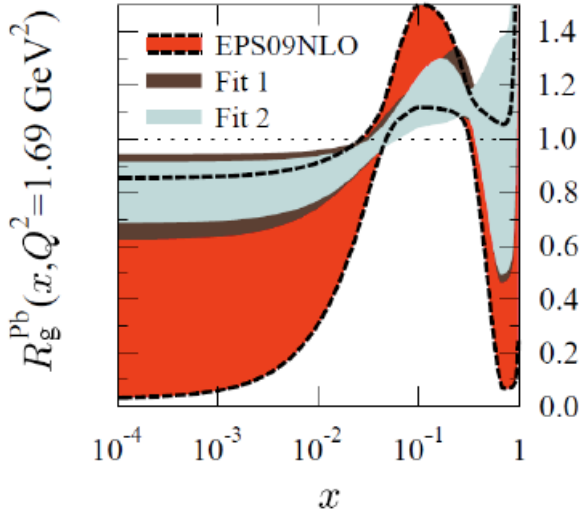
Neutron (light sea, UHE neutrinos, QPM)

Nuclear Parton Distributions



$$R = q^{\text{Pb}}/q^{\text{p}}$$

Study using eA LHeC pseudodata



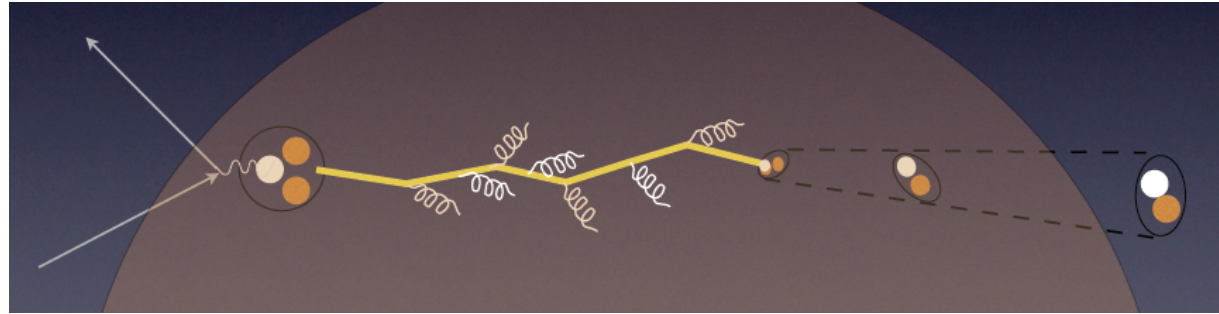
→ A complete determination of nPDFs in grossly extended range, into nonlinear regime
 nPDFs - certainly more diverse than in V,S,G terms and cleaner than pA at the LHC

In-medium Hadronisation

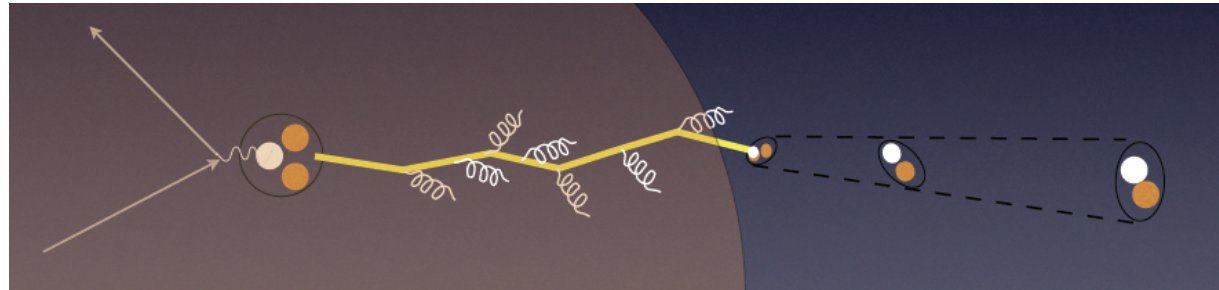
The study of particle production in eA (fragmentation functions and hadrochemistry) allows the study of the space-time picture of hadronisation (the final phase of QGP).

Low energy (ν): need of hadronization inside.

Parton propagation: pt broadening
Hadron formation: attenuation



High energy (ν): partonic evolution altered in the nuclear medium.

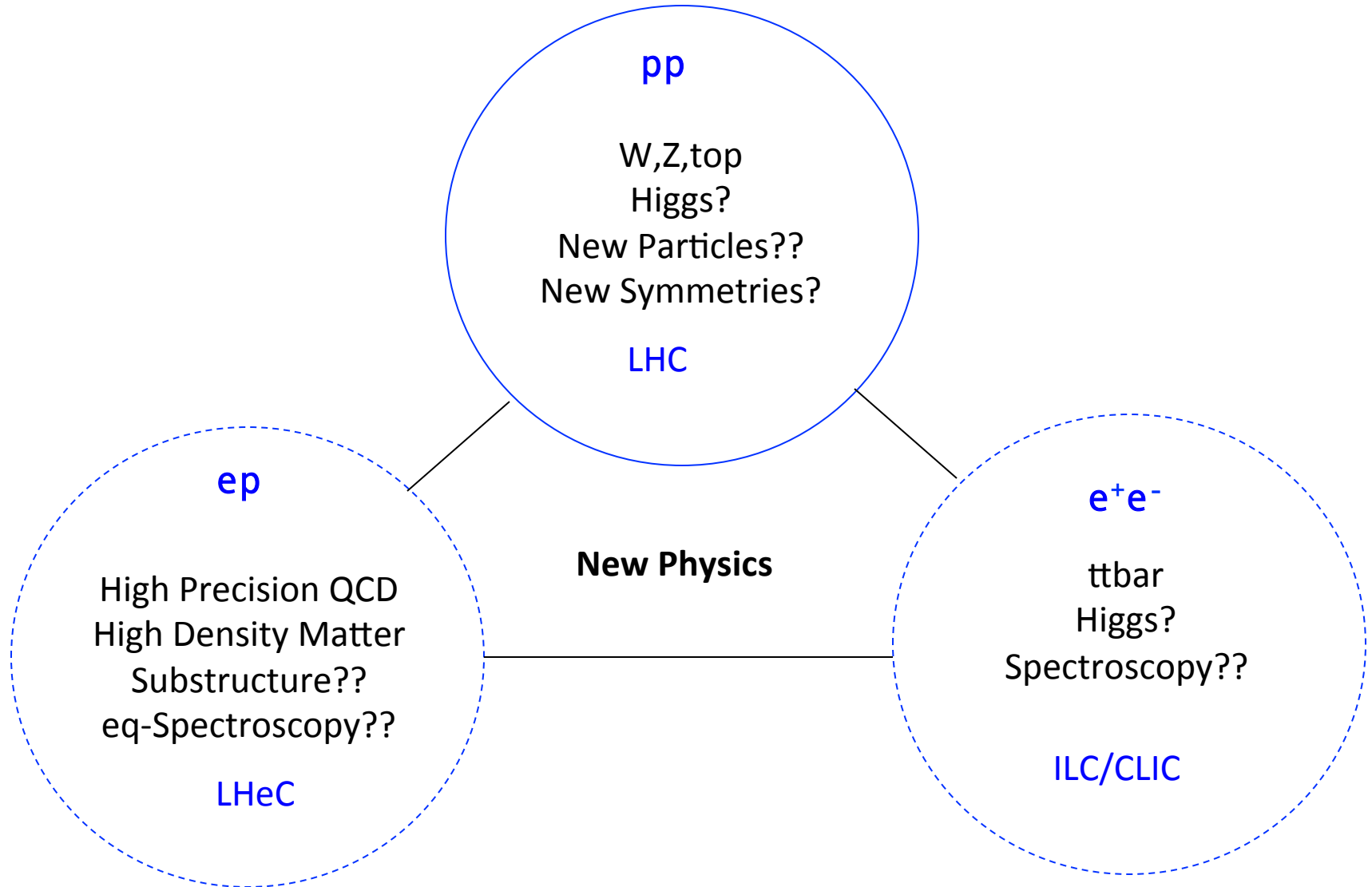


W.Brooks, Divonne09

LHeC :

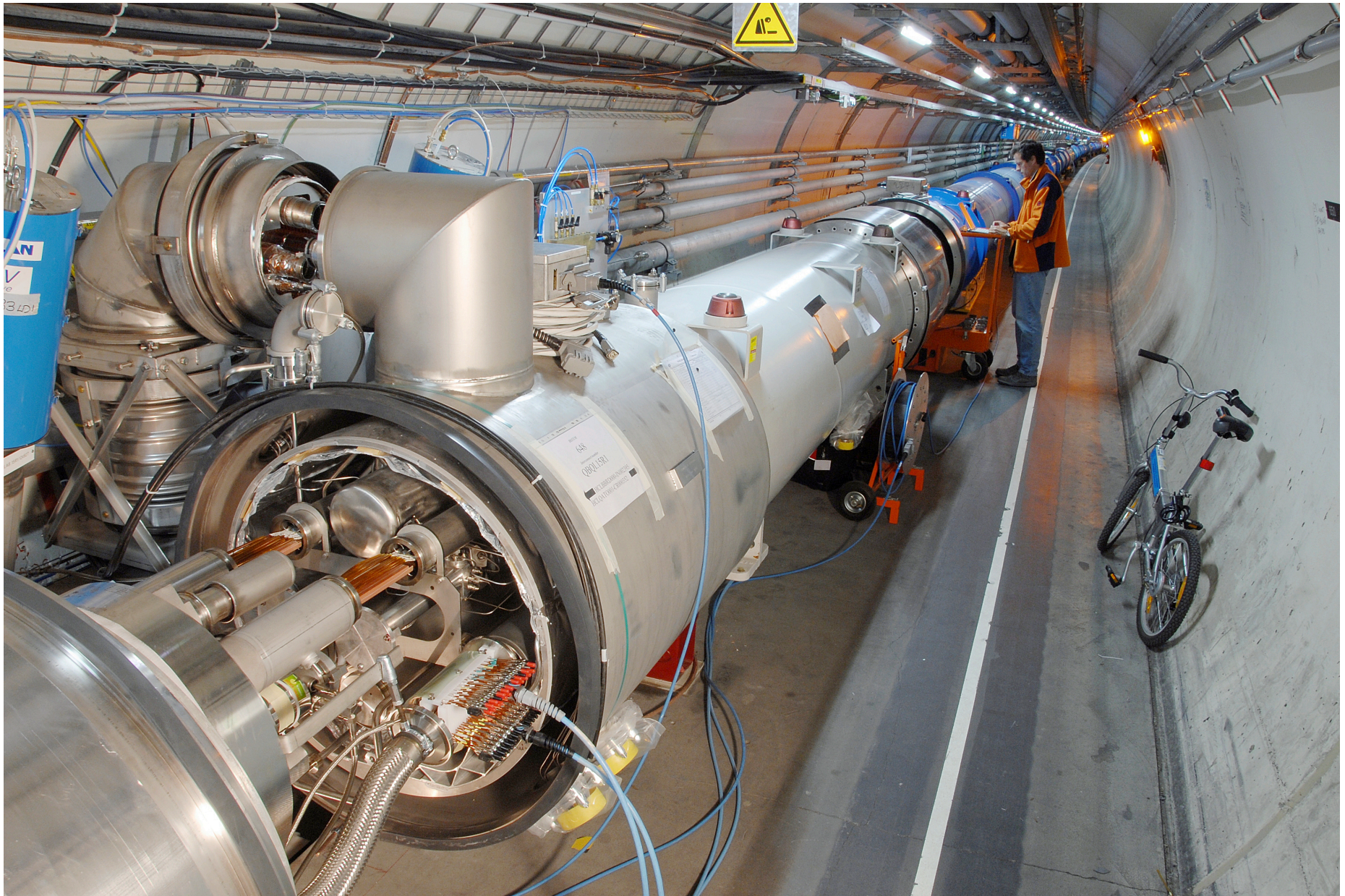
- + study the transition from small to high energies in hugely extended range wrt. fixed target data
- + test of the energy loss mechanism crucial for understanding of the medium produced in HIC
- + detailed study of heavy quark hadronisation ...

The TeV Scale [2010-2035..]



Accelerator and Detector

How can we use the LHC for ep/A?



e Ring- p/A Ring – “RR”

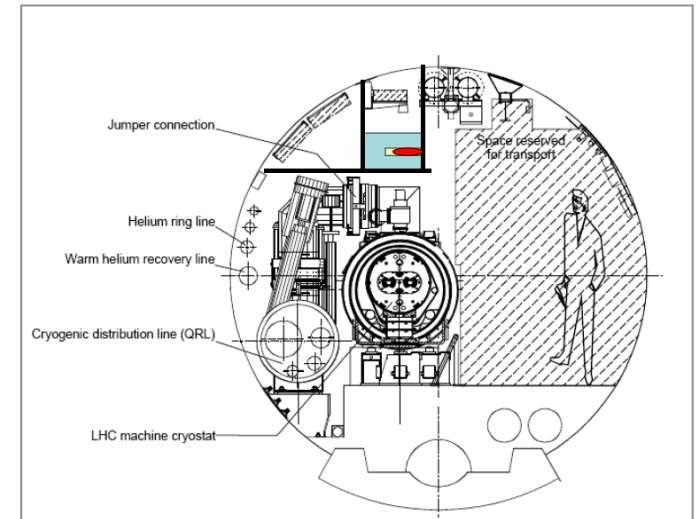
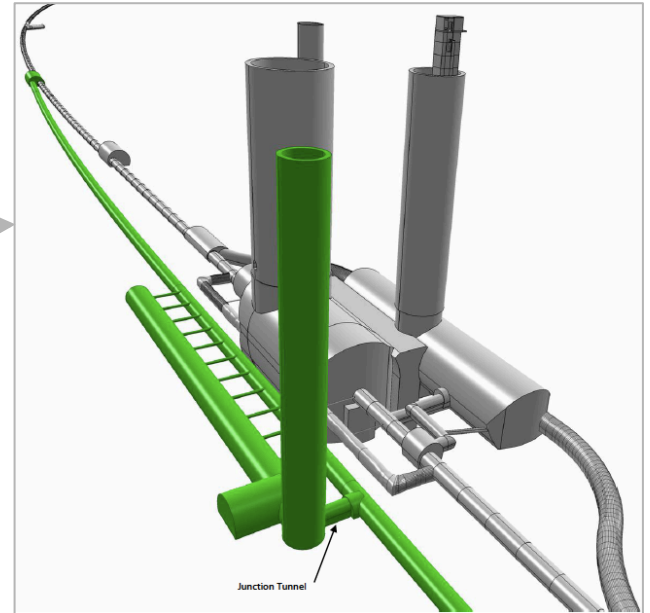
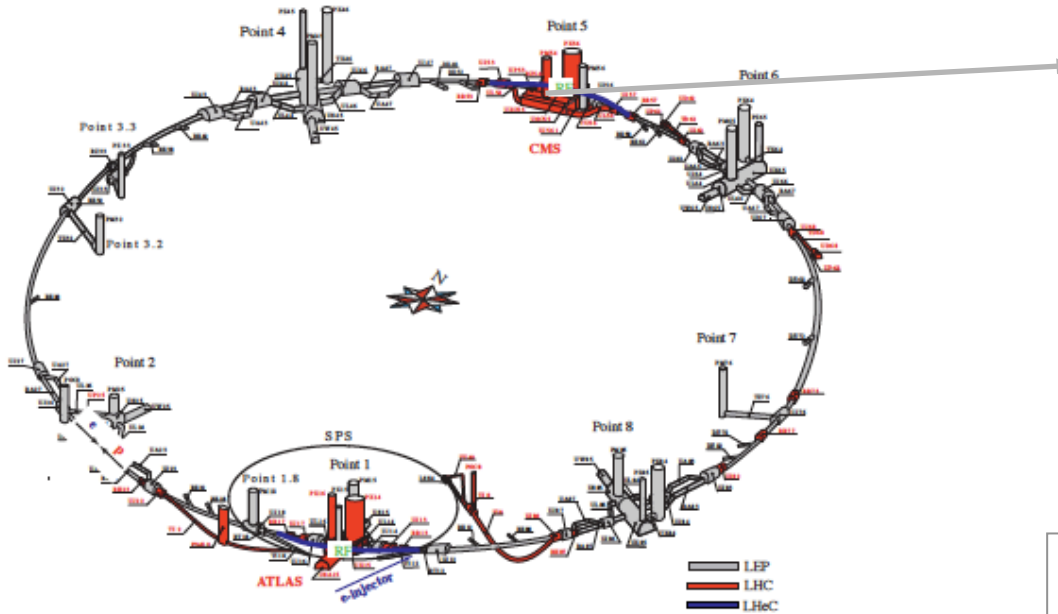
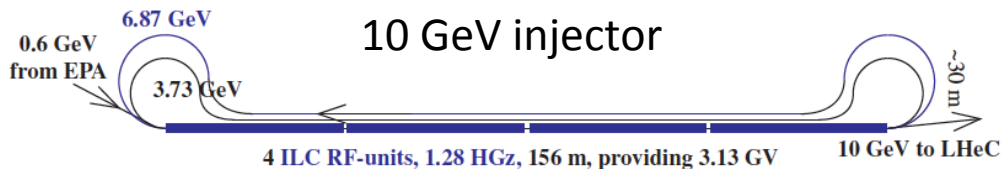


Figure 1: Schematic Layout of the LHC (grey/red) with the bypasses of CMS and ATLAS for the ring electron beam (blue) in the RR version. The e injector is a 10 GeV superconducting linac in triple racetrack configuration which is considered to reach the ring via the bypass around ATLAS.



10 GeV injection: dipoles with low field and 10^{-4} reproducibility

Magnets

9 System Design

- 9.1 Magnets for the Interaction Region
 - 9.1.1 Introduction
 - 9.1.2 Magnets for the ring-ring option
 - 9.1.3 Magnets for the linac-ring option
- 9.2 Accelerator Magnets
 - 9.2.1 Dipole Magnets
 - 9.2.2 BINP Model
 - 9.2.3 CERN Model
 - 9.2.4 Quadrupole and Corrector Magnets
- 9.3 Ring-Ring RF Design
 - 9.3.1 Design Parameters
 - 9.3.2 Cavities and klystrons
- 9.4 Linac-Ring RF Design
 - 9.4.1 Design Parameters
 - 9.4.2 Layout and RF powering
 - 9.4.3 Arc RF systems
- 9.5 Crab crossing for the LHeC
 - 9.5.1 Luminosity Reduction
 - 9.5.2 Crossing Schemes
 - 9.5.3 RF Technology
- 9.6 Vacuum
 - 9.6.1 Vacuum requirements
 - 9.6.2 Synchrotron radiation
 - 9.6.3 Vacuum engineering issues
- 9.7 Beam Pipe Design
 - 9.7.1 Requirements
 - 9.7.2 Choice of Materials for beampipes
 - 9.7.3 Beampipe Geometries
 - 9.7.4 Vacuum Instrumentation
 - 9.7.5 Synchrotron Radiation Masks
 - 9.7.6 Installation and Integration
- 9.8 Cryogenics
 - 9.8.1 Ring-Ring Cryogenics Design
 - 9.8.2 Linac-Ring Cryogenics Design
 - 9.8.3 General Conclusions Cryogenics for LHeC
- 9.9 Beam Dumps and Injection Regions
 - 9.9.1 Injection Region Design for Ring-Ring Option
 - 9.9.2 Injection transfer line for the Ring-Ring Option
 - 9.9.3 60 GeV internal dump for Ring-Ring Option
 - 9.9.4 Post collision line for 140 GeV Linac-Ring option
 - 9.9.5 Absorber for 140 GeV Linac-Ring option
 - 9.9.6 Energy deposition studies for the Linac-Ring option
 - 9.9.7 Beam line dump for ERL Linac-Ring option
 - 9.9.8 Absorber for ERL Linac-Ring option

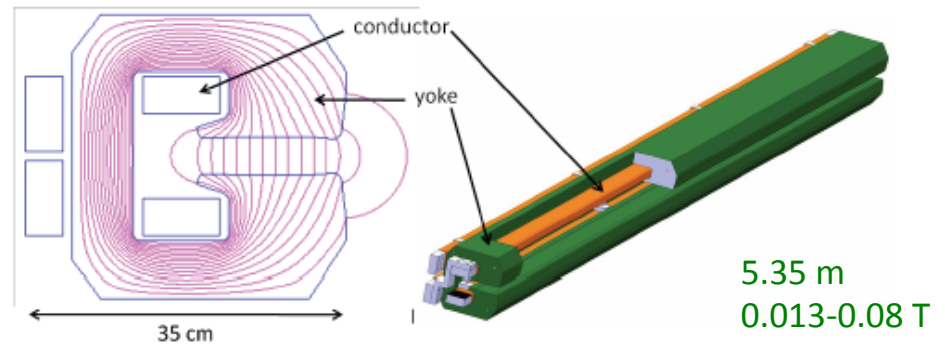


Fig. 2. Field lines and artistic view of a LHeC arc dipole.

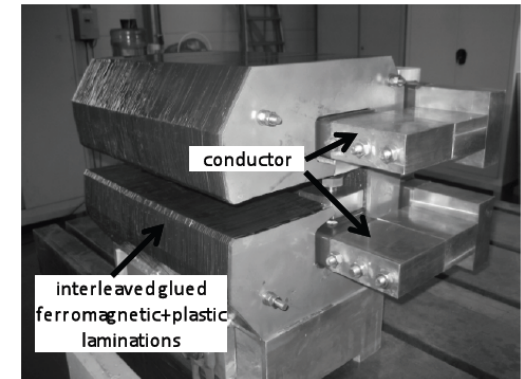
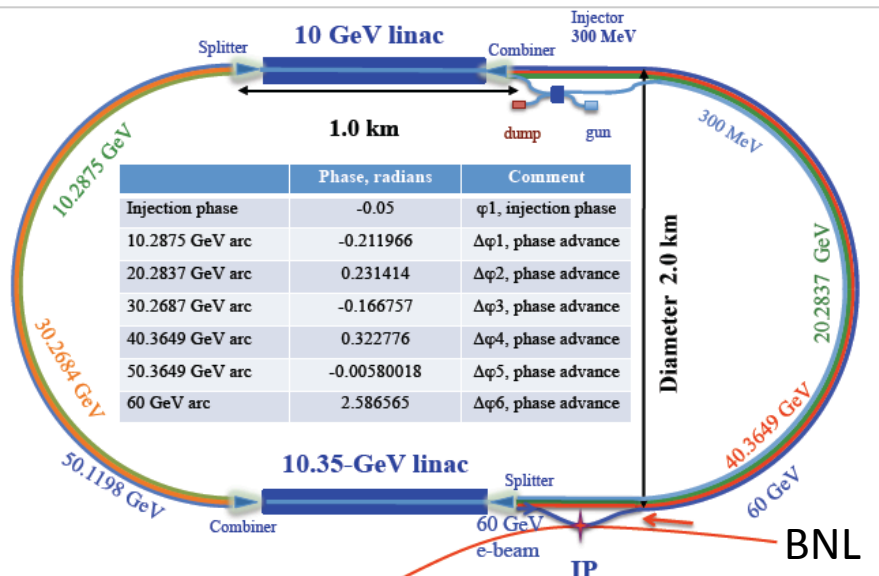
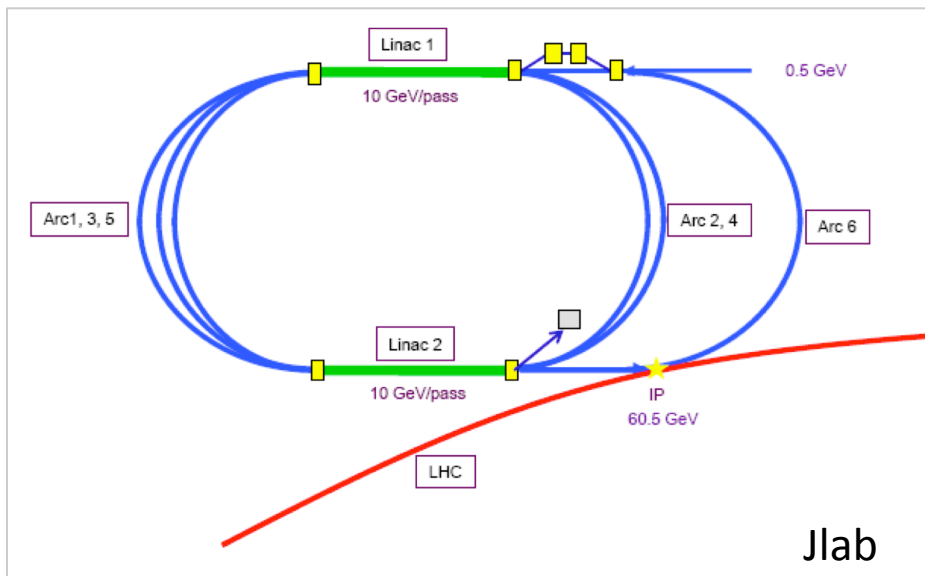
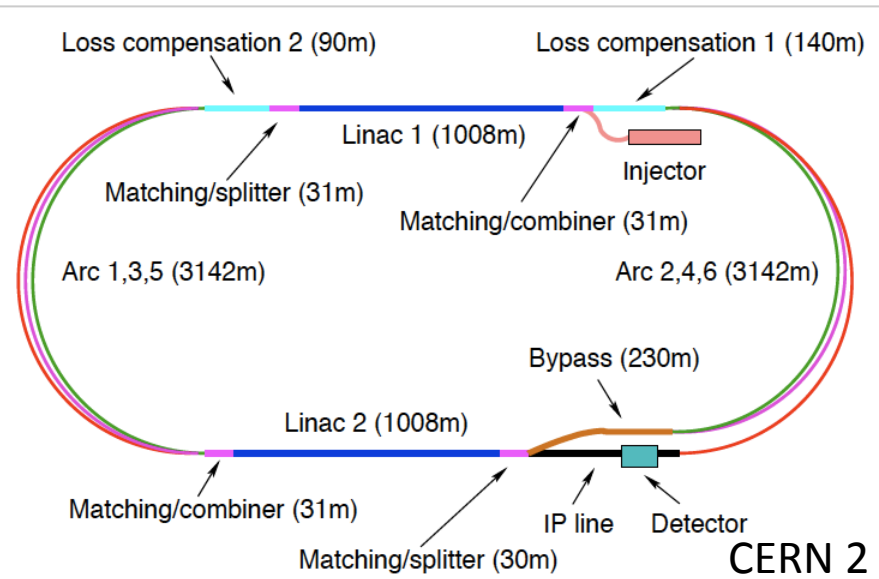
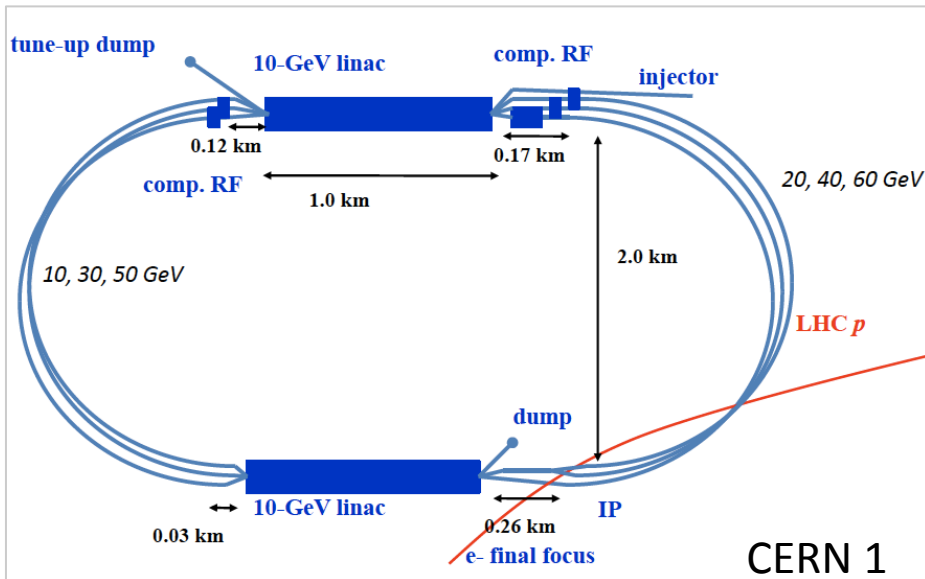


TABLE II REPRODUCIBILITY OF MAGNETIC FIELD OVER 8 CYCLES

Model	Low field	High fields
Maximum Relative Deviation from Average		
Model 1 (NiFe steel)	$5 \cdot 10^{-5}$	$4 \cdot 10^{-5}$
Model 2 (Low carbon steel)	$6 \cdot 10^{-5}$	$6 \cdot 10^{-5}$
Model 3 (Grain oriented 3.5% Si steel)	$4 \cdot 10^{-5}$	$6 \cdot 10^{-5}$
Standard Deviation from Average		
Model 1 (NiFe steel)	$3 \cdot 10^{-5}$	$3 \cdot 10^{-5}$
Model 2 (Low carbon steel)	$4 \cdot 10^{-5}$	$5 \cdot 10^{-5}$
Model 3 (Grain oriented 3.5% Si steel)	$2 \cdot 10^{-5}$	$4 \cdot 10^{-5}$

Prototypes from BINP and CERN: function to spec's

60 GeV Energy Recovery Linac



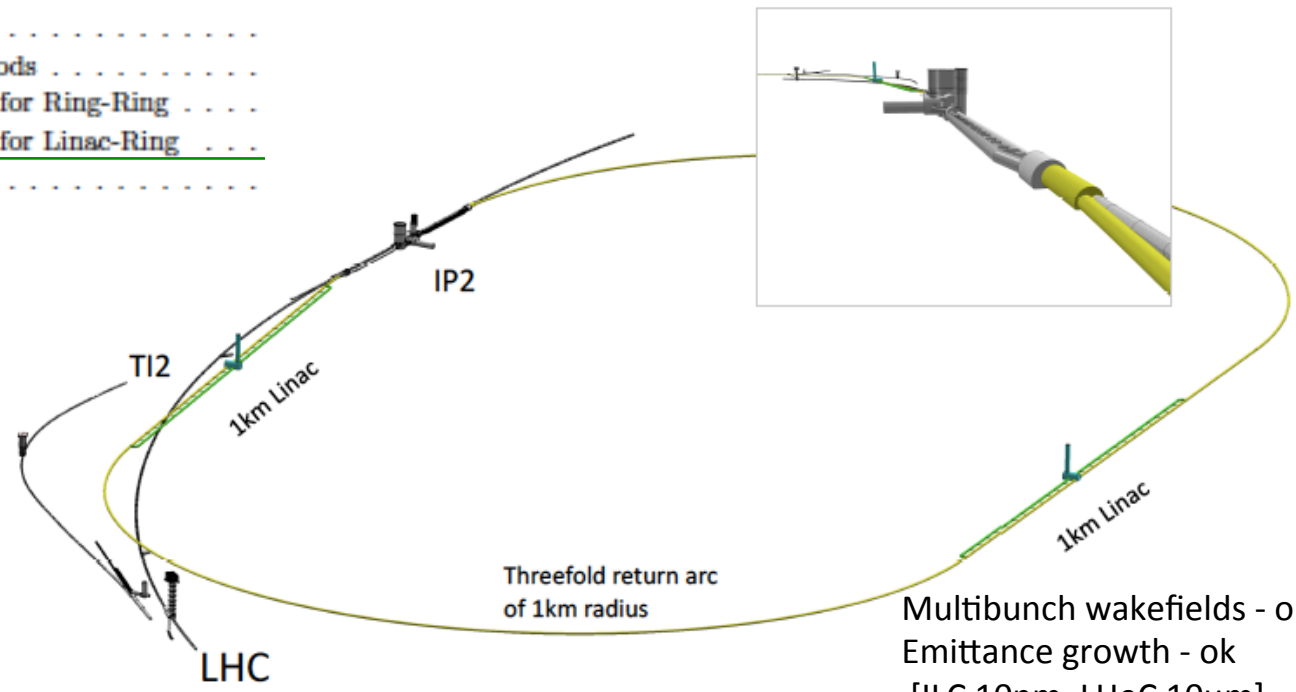
Two 10 GeV energy recovery Linacs, 3 returns, 720 MHz cavities

Linac Infrastructure

10 Civil Engineering and Services

- 10.1 Overview
- 10.2 Location, Geology and Construction Methods
 - 10.2.1 Location
 - 10.2.2 Land Features
 - 10.2.3 Geology
 - 10.2.4 Site Development
 - 10.2.5 Construction Methods
- 10.3 Civil Engineering Layouts for Ring-Ring
- 10.4 Civil Engineering Layouts for Linac-Ring
- 10.5 Summary

$$U_{LHeC} = U_{LHC} / 3 : 1.5 \times \text{HERA}$$



944 cavities
 59 cryo modules per linac
 721 MHz
 20 MV/m CW

Multibunch wakefields - ok
 Emittance growth - ok
 [ILC 10nm, LHeC 10μm]
 36σ separation at 3.5m - ok
 Fast ion instability - probably ok
 with clearing gap (1/3)

Figure 10.11: View on the ERL placed inside the LHC ring and tangential to IP2. TI2 is the injection line into the LHC. The insert shows the view towards IP2, which currently houses the ALICE experiment, from the direction of the protons colliding with the electron beam incoming from behind.

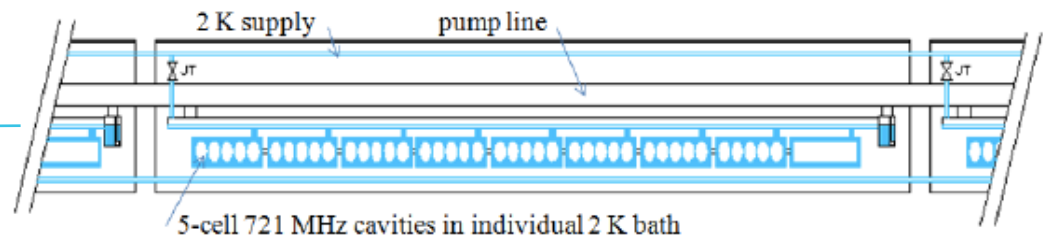
Cryogenics

9 System Design

- 9.1 Magnets for the Interaction Region
 - 9.1.1 Introduction
 - 9.1.2 Magnets for the ring-ring option
 - 9.1.3 Magnets for the linac-ring option
- 9.2 Accelerator Magnets
 - 9.2.1 Dipole Magnets
 - 9.2.2 BINP Model
 - 9.2.3 CERN Model
 - 9.2.4 Quadrupole and Corrector Magnets
- 9.3 Ring-Ring RF Design
 - 9.3.1 Design Parameters
 - 9.3.2 Cavities and klystrons
- 9.4 Linac-Ring RF Design
 - 9.4.1 Design Parameters
 - 9.4.2 Layout and RF powering
 - 9.4.3 Arc RF systems
- 9.5 Crab crossing for the LHeC
 - 9.5.1 Luminosity Reduction
 - 9.5.2 Crossing Schemes
 - 9.5.3 RF Technology
- 9.6 Vacuum
 - 9.6.1 Vacuum requirements
 - 9.6.2 Synchrotron radiation
 - 9.6.3 Vacuum engineering issues
- 9.7 Beam Pipe Design
 - 9.7.1 Requirements
 - 9.7.2 Choice of Materials for beampipes
 - 9.7.3 Beampipe Geometries
 - 9.7.4 Vacuum Instrumentation
 - 9.7.5 Synchrotron Radiation Masks
 - 9.7.6 Installation and Integration
- 9.8 Cryogenics
 - 9.8.1 Ring-Ring Cryogenics Design
 - 9.8.2 Linac-Ring Cryogenics Design
 - 9.8.3 General Conclusions Cryogenics for LHeC
- 9.9 Beam Dumps and Injection Regions
 - 9.9.1 Injection Region Design for Ring-Ring Option
 - 9.9.2 Injection transfer line for the Ring-Ring Option
 - 9.9.3 60 GeV internal dump for Ring-Ring Option
 - 9.9.4 Post collision line for 140 GeV Linac-Ring option
 - 9.9.5 Absorber for 140 GeV Linac-Ring option
 - 9.9.6 Energy deposition studies for the Linac-Ring option
 - 9.9.7 Beam line dump for ERL Linac-Ring option
 - 9.9.8 Absorber for ERL Linac-Ring option

Table 2: Components of the Electron Accelerators

	Ring	Linac
magnets		
beam energy	60 GeV	
number of dipoles	3080	3600
dipole field [T]	0.013 – 0.076	0.046 – 0.264
total nr of quads	866	1588
RF and cryogenics		
number of cavities	112	944
gradient [MV/m]	11.9	20
RF power [MW]	49	39
cavity voltage [MV]	5	21.2
cavity R/Q [Ω]	114	285
cavity Q_0	–	$2.5 \cdot 10^{10}$
cooling power [kW]	5.4@4.2 K	30@2 K



systems will consist of a complex task. Further cavities and cryomodules will require a limited R&D program. From this we expect improved quality factors with respect to today's state of the art. The cryogenics of the L-R version consists of a formidable engineering challenge, however, it is feasible and, CERN disposes of the respective know-how.

Table 1: Parameters of the RR and RL configurations.

	Ring	Linac	
electron beam			
beam energy E_e	60 GeV		
e^- (e^+) per bunch N_e [10^9]	20 (20)	1 (0.1)	
e^- (e^+) polarisation [%]	40 (40)	90 (0)	
bunch length [mm]	10	0.6	
tr. emittance at IP $\gamma\epsilon_{x,y}^e$ [mm]	0.58, 0.29	0.05	
IP β function $\beta_{x,y}^*$ [m]	0.4, 0.2	0.12	
beam current [mA]	131	6.6	
energy recovery intensity gain	—	17	Linac has real γ beam option
total wall plug power	100 MW		
syn rad power [kW]	51	49	
critical energy [keV]	163	718	
proton beam			
beam energy E_p	7 TeV		Proton beam parameters: E_p perhaps 6.5 TeV N_p almost achieved ϵ_p already lower in 2011
protons per bunch N_p	$1.7 \cdot 10^{11}$		
transverse emittance $\gamma\epsilon_{x,y}^p$	$3.75 \mu\text{m}$		
collider			
Lum e^-p (e^+p) [$10^{32}\text{cm}^{-2}\text{s}^{-1}$]	9 (9)	10 (1)	
bunch spacing	25 ns		Both the ring and the linac are feasible and both come very close to the desired performance. The decision is essentially taken for the linac.
rms beam spot size $\sigma_{x,y}$ [μm]	30, 16	7	
crossing angle θ [mrad]	1	0	
$L_{eN} = A L_{eA}$ [$10^{32}\text{cm}^{-2}\text{s}^{-1}$]	0.3	1	

LHeC Accelerator Design: Participating Institutes



12 Detector Requirements

12.1 Requirements on the LHeC Detector

12.1.1 Installation and Magnets

12.1.2 Kinematic reconstruction

12.1.3 Acceptance regions - scattered electron

12.1.4 Acceptance regions - hadronic final state

12.1.5 Acceptance at the High Energy LHC

12.1.6 Energy Resolution and Calibration

12.1.7 Tracking Requirements

12.1.8 Particle Identification Requirements

12.1.9 Summary of the Requirements on the LHeC Detector

13 Central Detector

13.1 Basic Detector Description

13.1.1 Baseline Detector Layout

13.1.2 An Alternative Solenoid Placement - Option B

13.2 Magnet Design

13.2.1 Magnets configuration

13.2.2 Detector Solenoid

13.2.3 Detector integrated e-beam bending dipoles

13.2.4 Cryogenics for magnets and calorimeter

13.2.5 Twin Solenoid System

13.3 Tracking Detector

13.3.1 Tracking Detector - Baseline Layout

13.3.2 Performance

13.3.3 Tracking detector design criteria and possible solutions

13.4 Calorimetry

13.4.1 The Barrel Electromagnetic Calorimeter

13.4.2 The Hadronic Barrel Calorimeter

13.4.3 Endcap Calorimeters

13.5 Calorimeter Simulation

13.5.1 The Barrel LAr Calorimeter Simulation

13.5.2 The Barrel Tile Calorimeter Simulation

13.5.3 Combined Liquid Argon and Tile Calorimeter Simulation

13.5.4 Lead-Scintillator Electromagnetic Option

13.5.5 Forward and Backward Inserts Calorimeter Simulation

13.6 Calorimeter Summary

13.7 Muon Detector

13.7.1 Muon detector design

13.7.2 The LHeC muon detector options

13.7.3 Forward Muon Extensions

13.7.4 Muon Detector Summary

13.8 Event and Detector Simulations

13.8.1 Pythia6

13.8.2 1 MeV Neutron Equivalent

13.8.3 Nearest Neighbor

13.8.4 Cross Checking

13.8.5 Future Goals

14 Forward and Backward Detectors

14.1 Luminosity Measurement and Electron Tagging

14.1.1 Options

14.1.2 Use of the Main LHeC Detector

14.1.3 Dedicated Luminosity Detectors in the tunnel

14.1.4 Small angle Electron Tagger

14.1.5 Summary and Open Questions

14.2 Polarimeter

14.2.1 Polarisation from the scattered photons

14.2.2 Polarisation from the scattered electrons

14.3 Zero Degree Calorimeter

14.3.1 ZDC detector design

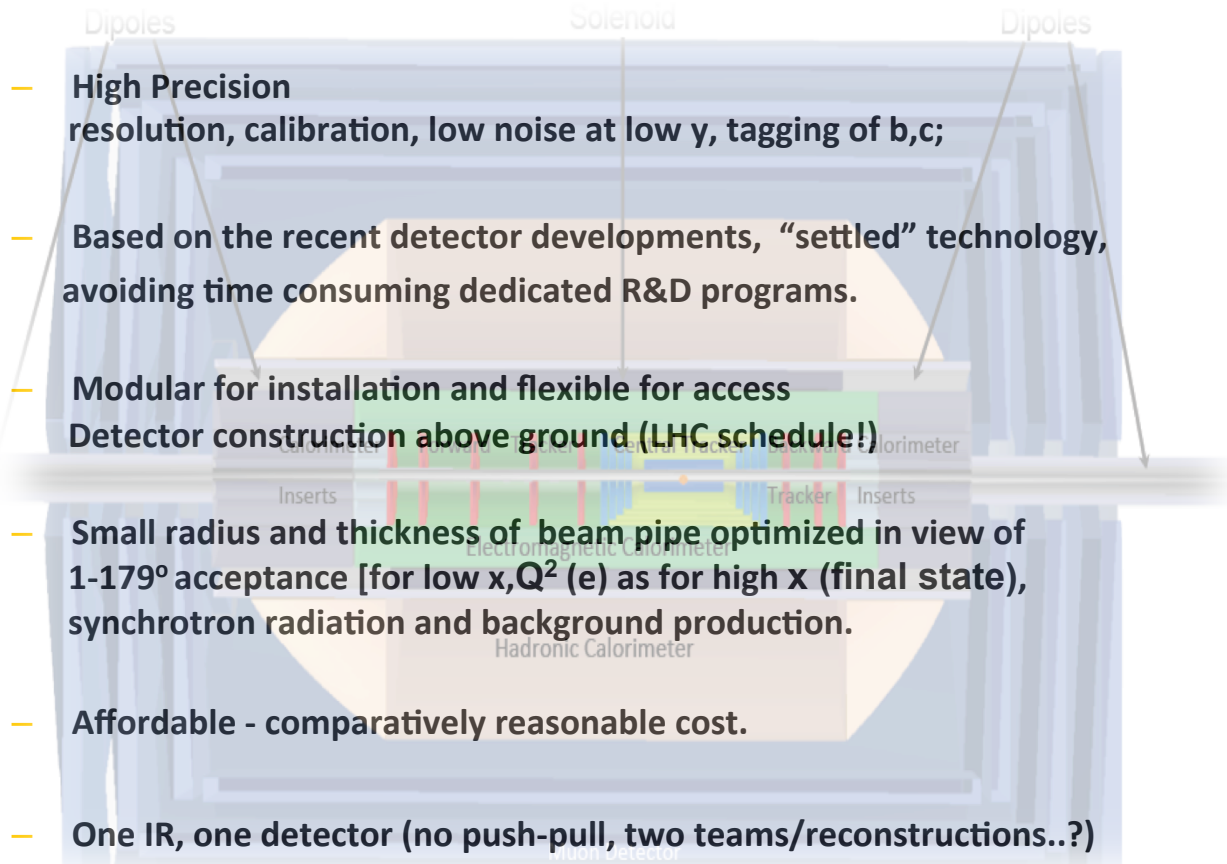
14.3.2 Neutron Calorimeter

14.3.3 Proton Calorimeter

14.3.4 Calibration and monitoring

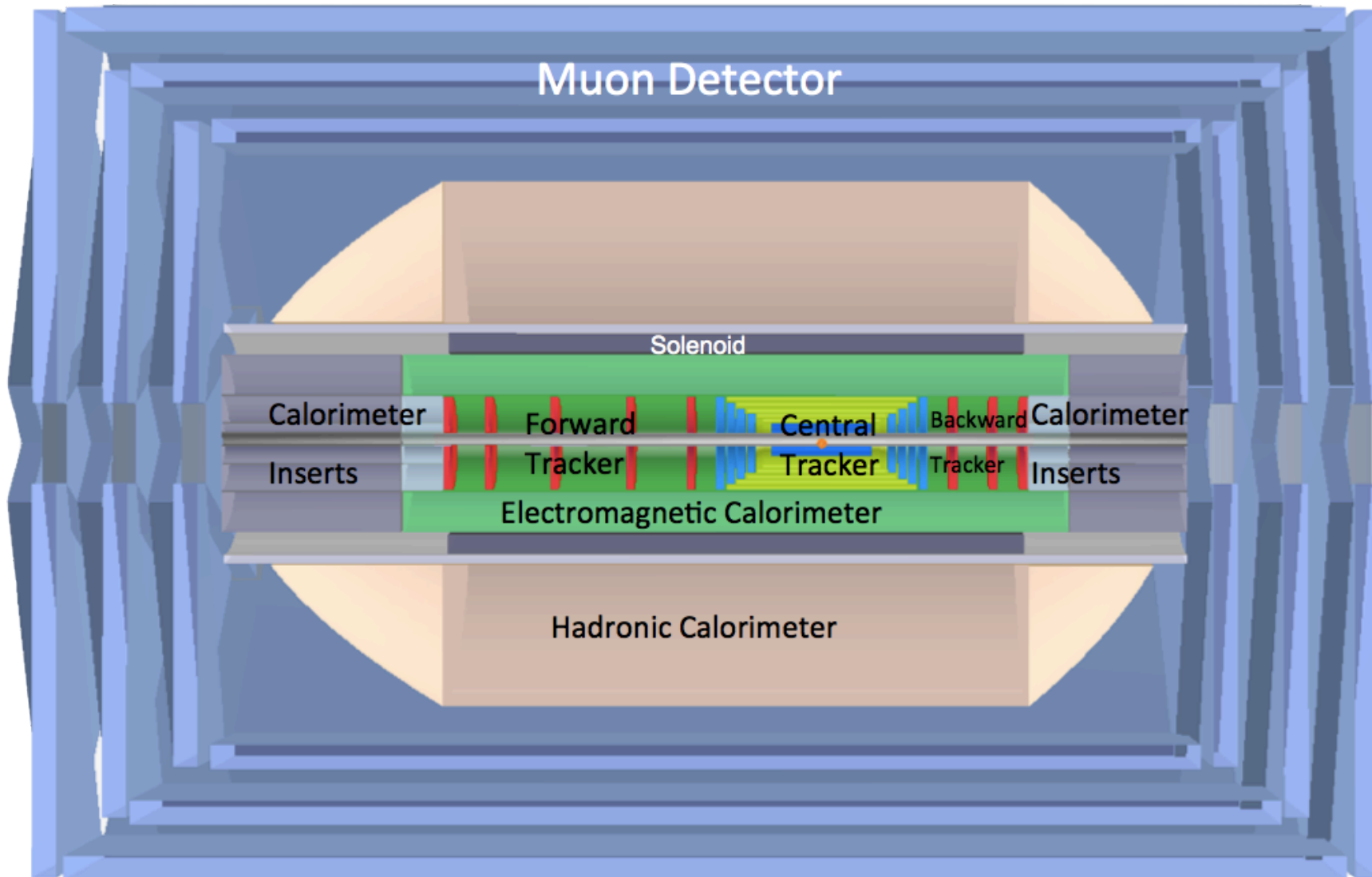
14.4 Forward Proton Detection

Detector Requirements



- **High Precision**
resolution, calibration, low noise at low y , tagging of b,c;
- **Based on the recent detector developments, “settled” technology,**
avoiding time consuming dedicated R&D programs.
- **Modular for installation and flexible for access**
Detector construction above ground (LHC schedule!)
- **Small radius and thickness of beam pipe optimized in view of**
1-179° acceptance [for low x, Q^2 (e) as for high x (final state),
synchrotron radiation and background production.
- **Affordable - comparatively reasonable cost.**
- **One IR, one detector (no push-pull, two teams/reconstructions..?)**

LHeC Detector Overview



Detector option 1 for LR and full acceptance coverage

Forward/backward asymmetry in energy deposited and thus in geometry and technology

Present dimensions: $L \times D = 14 \times 9 \text{ m}^2$ [CMS $21 \times 15 \text{ m}^2$, ATLAS $45 \times 25 \text{ m}^2$]

Taggers at -62m (e), 100m (γ ,LR), -22.4m (γ ,RR), +100m (n), +420m (p)

Silicon Tracker and EM Calorimeter

Transverse momentum
 $\Delta p_t / p_t^2 \rightarrow 6 \cdot 10^{-4} \text{ GeV}^{-1}$
 transverse
 impact parameter
 $\rightarrow 10 \mu\text{m}$

Central Pixel Tracker

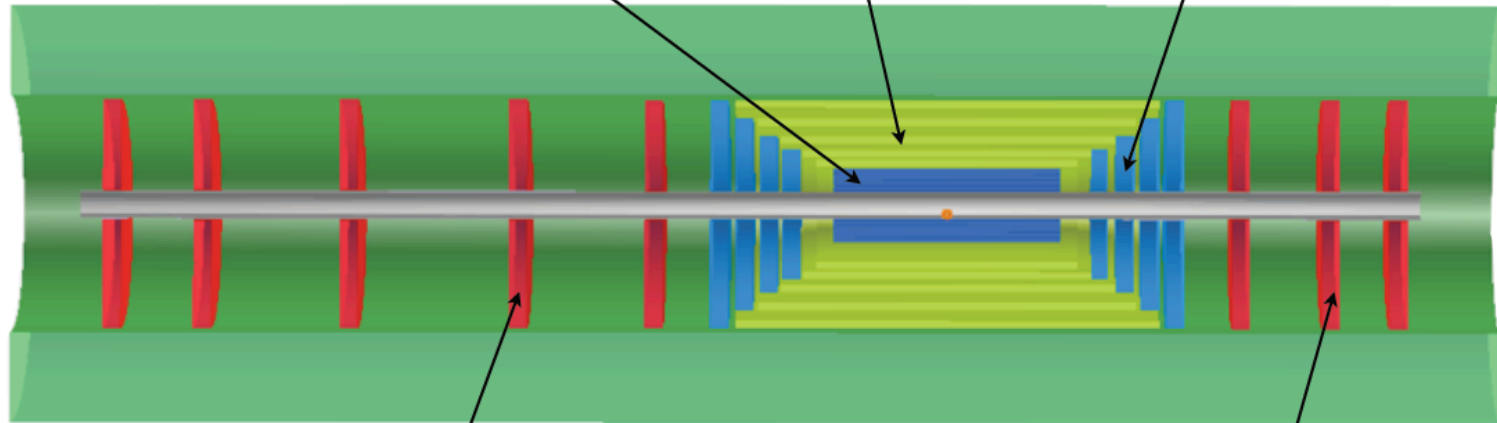
4 layer **CPT**:
 min-inner-R = 3.1 cm
 max-inner-R = 10.9 cm
 $\Delta R = 15. \text{ cm}$

Central Si Tracker

CST - ΔR 3.5cm each
 1. layer: inner R = 21.2 cm
 2. layer: = 25.6 cm
 3. layer: = 31.2 cm
 4. layer: = 36.7 cm
 5. layer: = 42.7 cm

Central Forward/Backward Tracker

4 **CFT/CBT**
 min-inner-R = 3.1 cm, max-inner-R = 10.9 cm



Forward Si Tracker

FST - $\Delta Z = 8. \text{ cm}$
 min-inner-R = 3.1 cm; max-inner-R = 10.9 cm
 outer R = 46.2 cm
 Planes 1-5:
 $z_{s-1} = 370. / 330. / 265. / 190. / 130. \text{ cm}$

Backward Si Tracker

BST - $\Delta Z = 8. \text{ cm}$
 min-inner-R = 3.1 cm; max-inner-R = 10.9 cm
 outer R = 46.2 cm
 Planes 1-3:
 $z_{l-3} = -130. / -170. / -200. \text{ cm}$

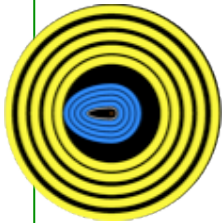
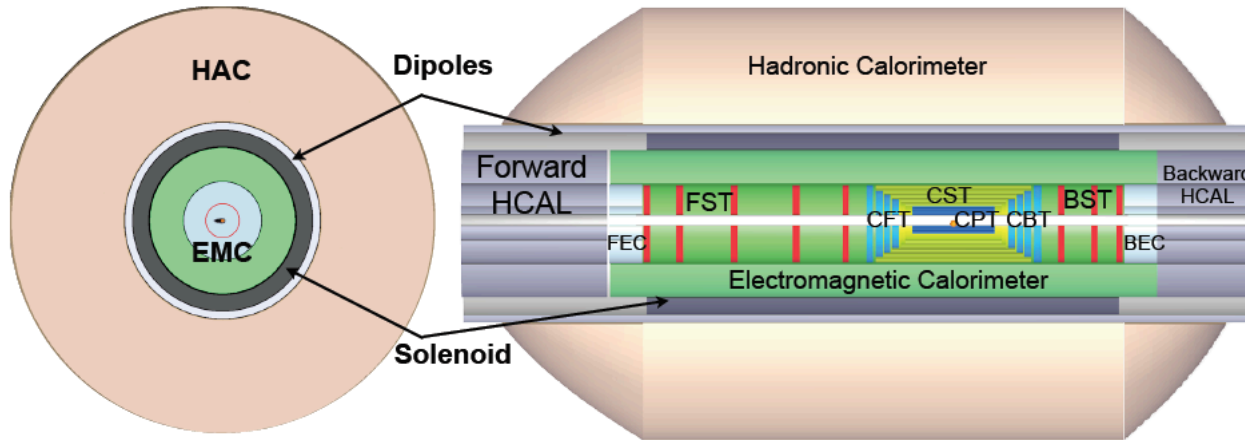


Figure 13.18: Tracker and barrel Electromagnetic-Calorimeter rz view of the baseline detector (Linac-Ring case).

Liquid Argon Electromagnetic Calorimeter



Inside Coil
H1, ATLAS
experience.

Barrel: Pb, 20 X_0 , 11m³

fwd/bwd inserts:

FEC: Si -W, 30 X_0 , 0.3m³

BEC: Si -Pb, 25 X_0 , 0.3m³

Figure 13.30: *x-y* and *r-z* view of the LHeC Barrel EM calorimeter (green).

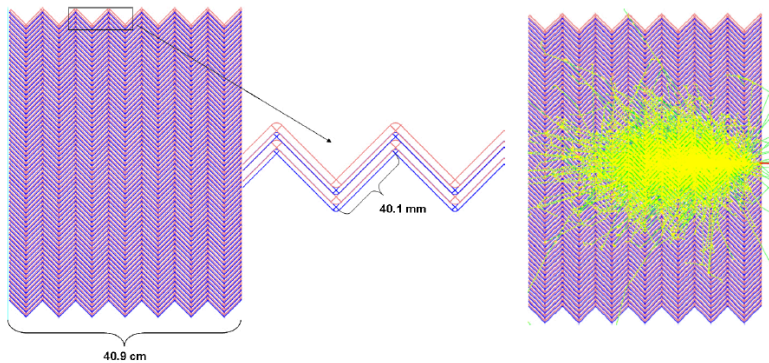


Figure 13.35: View of the parallel geometry accordion calorimeter (left) and simulation of a single electron shower with initial energy of 20 GeV (right).

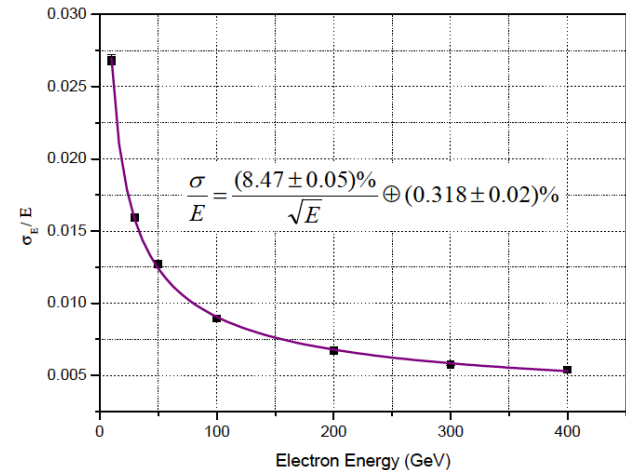


Figure 13.36: LAr accordion calorimeter energy resolution for electrons between 10 and 400 GeV.

GEANT4 Simulation

Hadronic Tile Calorimeter

E-Calo Parts	FEC1	FEC2		EMC		BEC2	BEC1
Min. Inner radius R [cm]	3.1	21		48		21	3.1
Min. polar angle θ [°]	0.48	3.2		6.6/168.9		174.2	179.1
Max. pseudorapidity η	5.5	3.6		2.8/-2.3		-3.	-4.8
Outer radius [cm]	20	46		88		46	20
z -length [cm]	40	40		660		40	40
Volume [m ³]	0.3			11.3		0.3	

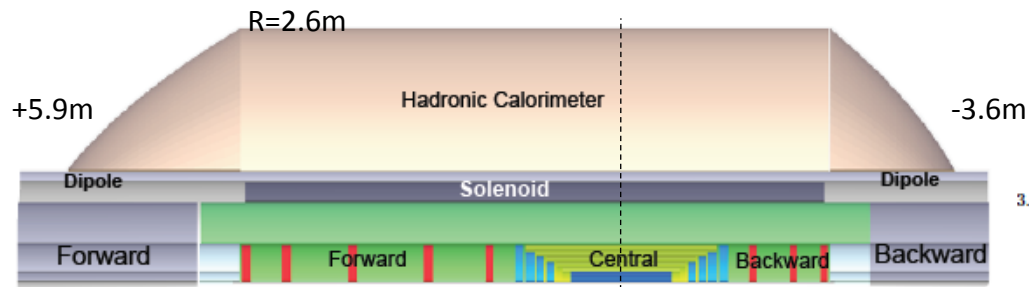
H-Calo Parts barrel			FHC4	HAC	BHC4		
Inner radius [cm]			120	120	120		
Outer radius [cm]			260	260	260		
z -length [cm]			217	580	157		
Volume [m ³]			121.2				

H-Calo Parts Inserts	FHC1	FHC2	FHC3		BHC3	BHC2	BHC1
Min. inner radius R [cm]	11	21	48		48	21	11
Min. polar angle θ [°]	0.43	2.9	6.6		169.	175.2	179.3
Max/min pseudorapidity η	5.6	3.7	2.9		-2.4	-3.2	-5.
Outer radius [cm]	20	46	88		88	46	20
z -length [cm]	177	177	177		117	117	117
Volume [m ³]	4.2				2.8		

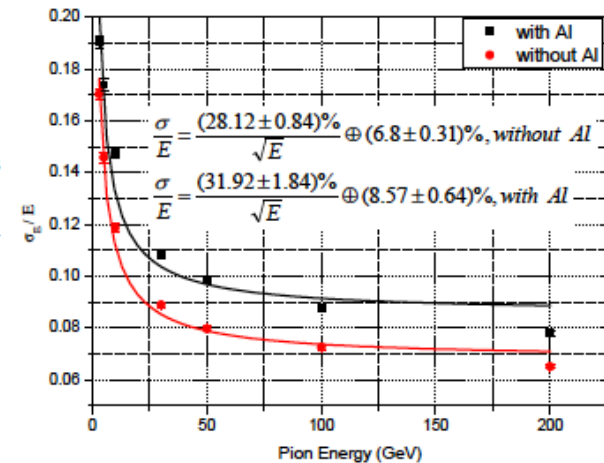
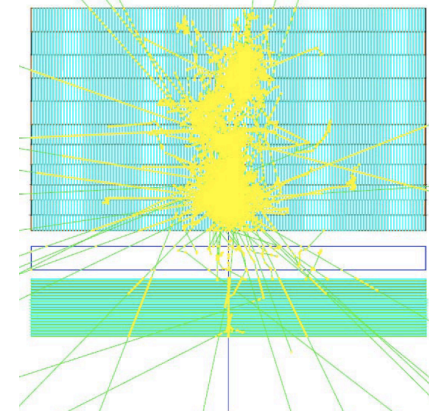
Table 13.6: Summary of calorimeter dimensions.

The electromagnetic barrel calorimeter is currently represented by the barrel part EMC (LAR-Pb module); the setup reaches $X_0 \approx 25$ radiation length) and the movable inserts forward FEC1, FEC2 (Si-W modules ($X_0 \approx 30$) and the backward BEC1, BEC2 (Si-Pb modules; $X_0 \approx 25$).

The hadronic barrel parts are represented by FHC4, HAC, BHC4 (forward, central and backward - Scintillator-Fe Tile modules; $\lambda_I \approx 8$ interaction length) and the movable inserts FHC1, FHC2, FHC3 (Si-W modules; $\lambda_I \approx 10$), BHC1, BHC2, BHC3 (Si-Cu modules, $\lambda_I \approx 8$) see Fig. 13.9.



Outside Coil: flux return Modular. ATLAS experience.

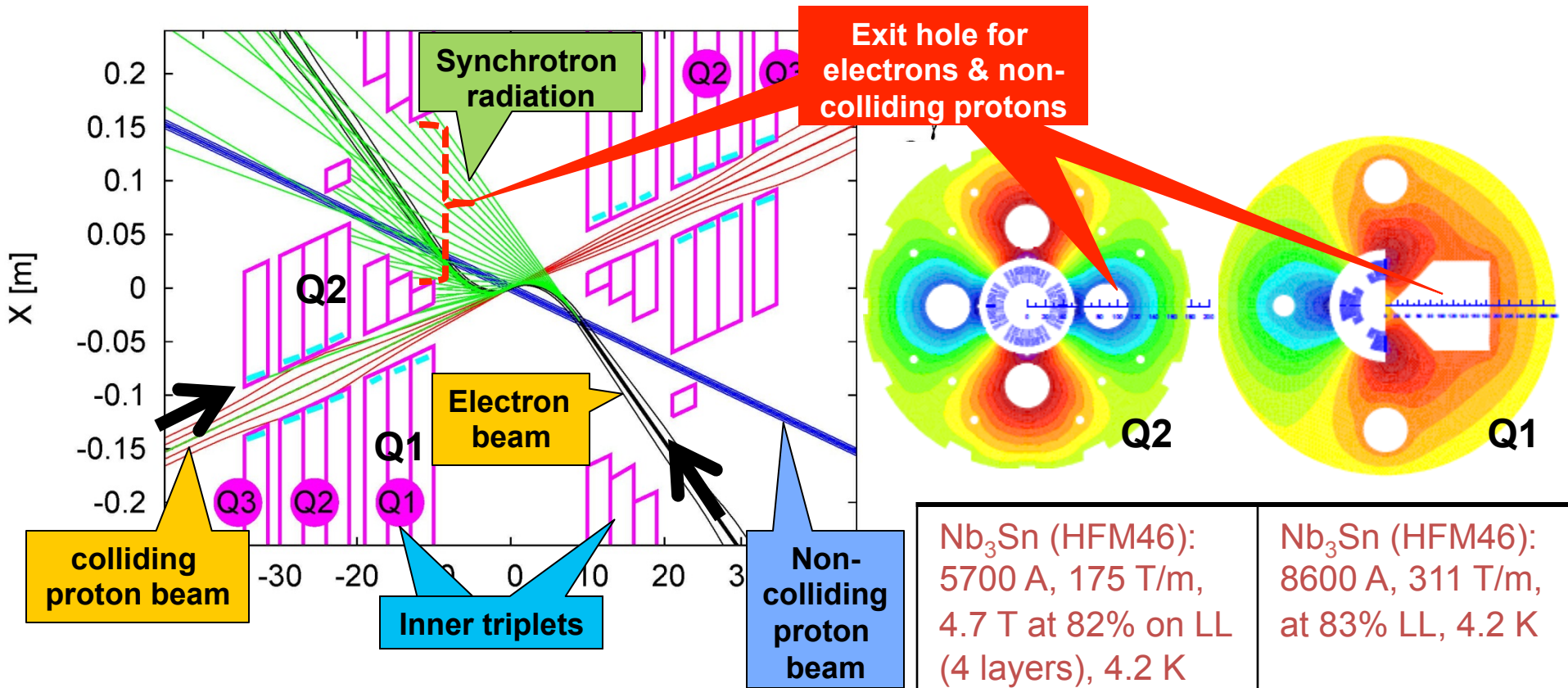


3.37: Accordion and Tile Calorimeter energy resolution for pions with and without 14cm Al block.

Combined GEANT4 Calorimeter Simulation

Some current+next steps

LR LHeC IR layout & SC IR quadrupoles



Nb ₃ Sn (HFM46): 5700 A, 175 T/m, 4.7 T at 82% on LL (4 layers), 4.2 K	Nb ₃ Sn (HFM46): 8600 A, 311 T/m, at 83% LL, 4.2 K
46 mm (half) ap., 63 mm beam sep.	23 mm ap.. 87 mm beam sep.
0.5 T, 25 T/m	0.09 T, 9 T/m

High-gradient SC IR quadrupoles based on Nb₃Sn for colliding proton beam with common low-field

L.Bottura
Chamonix 2/12

Magnet Development at CERN

on Magnet R+D
for LHeC + HE-LHC

LHeC

		LHeC RR dipole prototype	CRISP and fast cycled SC magnets	MQXC R&D	EuCARD FReSCa-II	DS 11 T MB program	US-LARP IR quadrupole program	EuCARD HTS insert	EuCARD2 HTS model	activated SC magnets handling for	Comments
Low field resistive magnets	field quality and reproducibility	X									demonstrated
	operating cost		X								tests planned in 2012
	integration in the LHC tunnel									X	study launched in 2012 (LS1)
IR magnets	large aperture			X			X				results in 2012...2014
	large gradient						X				
	heat removal		X	X							results in 2012
co-activities and tunnel works										X	integration study and models (BINP); schedule revision

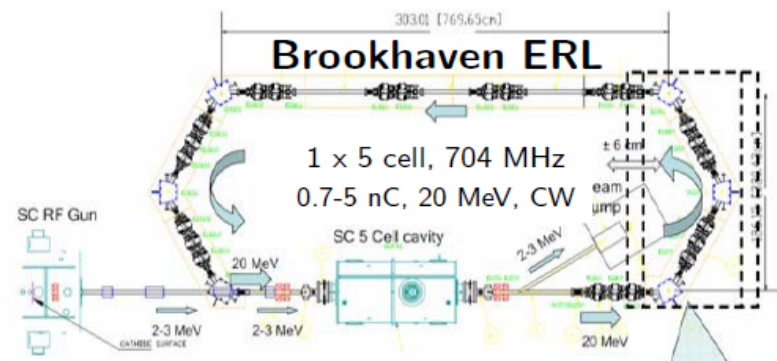
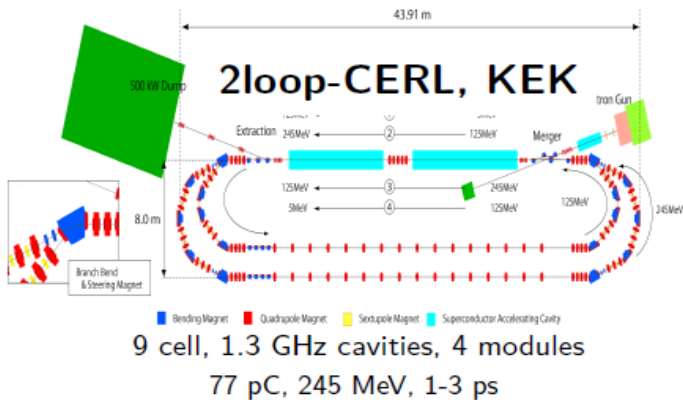
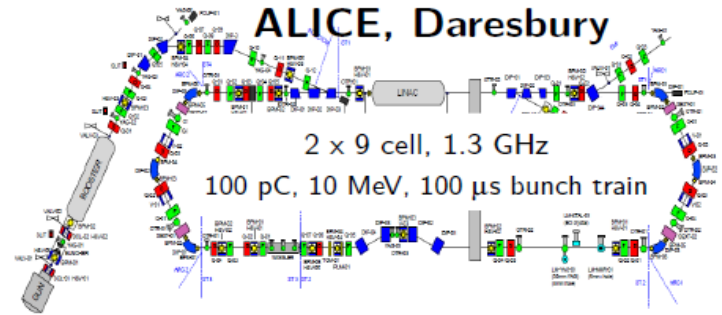
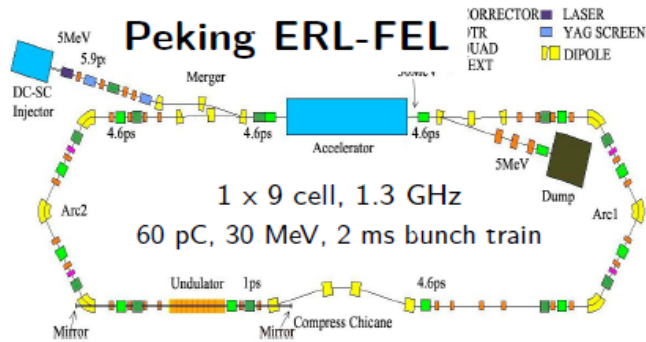
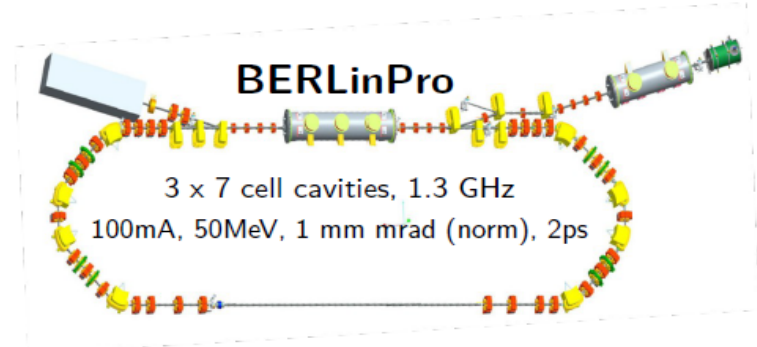
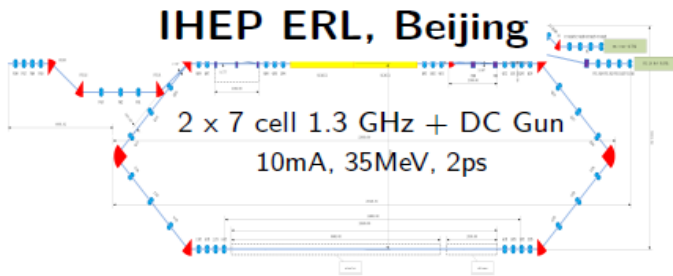
HE-LHC

Very high field magnets	15 T dipole outsert				X						deliverable Q1 2014
	5 T dipole insert							X	X		EuCARD2 proposal
	high gradient quadrupoles						X				US-LARP technology demonstration by 2014
	magnet protection				X	X	X				
	heat loads and removal			X	X						dedicated model tests
	field quality					X	X		X		
Pulsed SC magnets	quench performance and margin		X								
	low-loss cables		X								
Transfer lines											options reviewed at HE-LHC workshop in Malta, 2010
Material availability and cost					X	X	X	X	X		
Installation in 2030										X	study launched in 2012 (LS1)

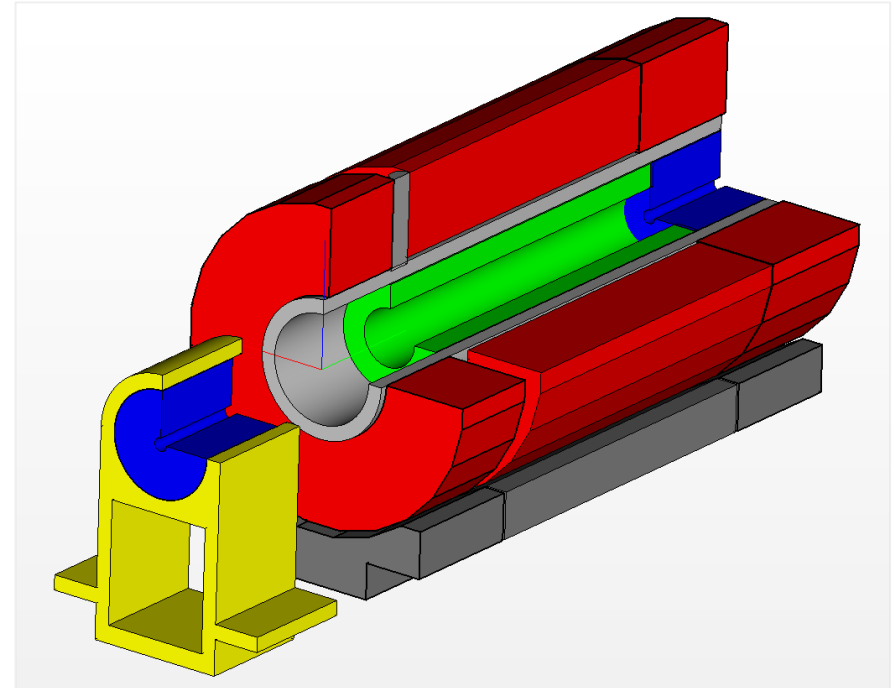
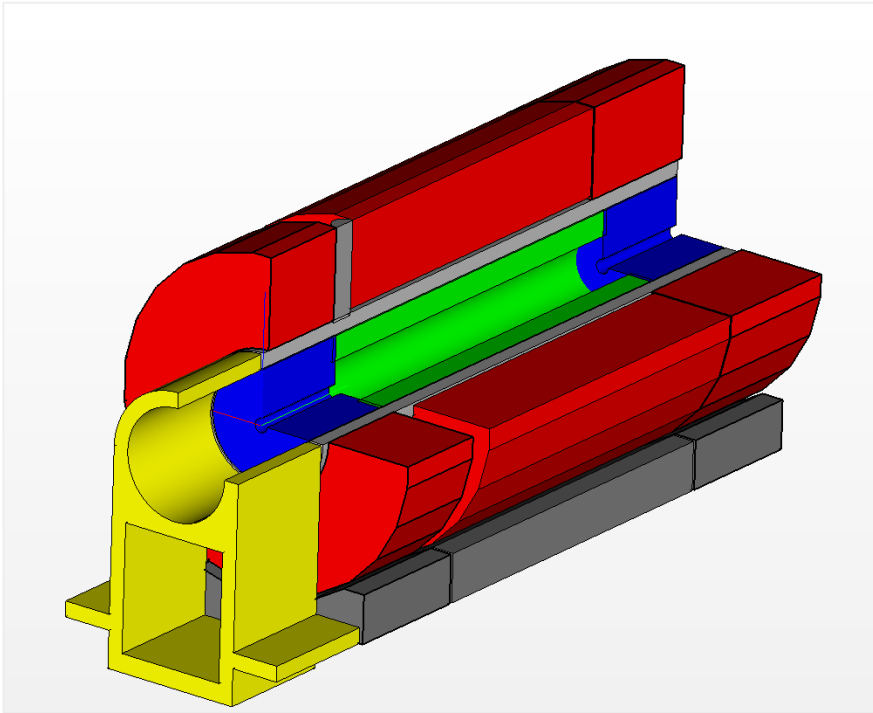
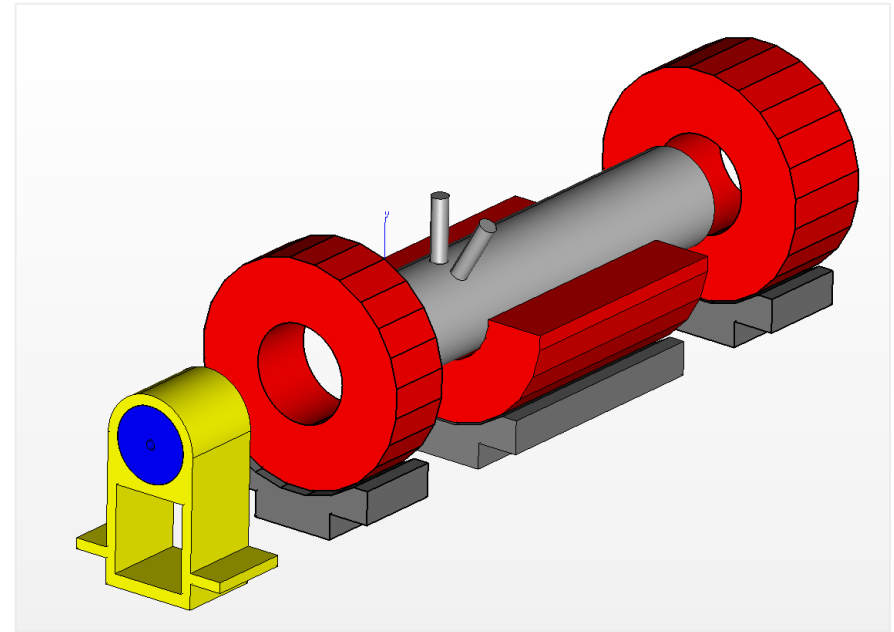
ERL Choice of frequency (Erk Jensen - Chamomix12)

- The frequency has to be a harmonic of 20.04 MHz!
- LHeC baseline: 721.42 MHz, alternative 1322.6 MHz.
- **Advantages of lower frequency:**
 - Less cryo-power
 - High-power couplers easier
 - Less cells per cavity – less trapped modes
 - Less beam loading and transverse wake – better beam stability
 - Less HOM power
 - Synergy with SPL, e-RHIC and ESS.
- **Advantages of higher frequency:**
 - Larger $R/Q \rightarrow$ with same Q_{ext} less RF power (but Q_{ext} must be reduced!)
 - Synergy with ILC/X-FEL

Collaboration on ERL



Detector has to be pre-mounted on top of IP2, the hall be emptied, the detector lowered and to be mounted inside the L3 magnet barrel during the 2-3 years shutdown LS3



Concluding Remarks

The physics of deep inelastic scattering has been an essential part of HEP.

Major breakthroughs in (particle) physics are difficult to plan, despite certain “overconfidence of theorists” [Ledermann ICHEP 1980] in the past.

The LHeC has passed a major milestone with a refereed CDR, supported and monitored by CERN, ECFA and NuPECC, soon to be published.

The time schedule of the LHC is such that there is not more time than a decade+ for realising the LHeC. This requires to continue to be realistic.

Collaborations are soon to be built for further design, of the machine and the detector. The experimental prospect challenges theory and requires to continue our intimate interaction with our thy colleagues.

A programme of technical and physics developments and a corresponding project structure are being developed, with the goal to enable a project decision by 2015 based on a technical design.

You are invited to join the workshop and so you wish the project too.



Next Workshop - Chavannes 14/15.6.2012

Page 1 of 1

13-11-2010

Societe / Salle

Horaires

LHeC

Odyssee



09:00
- 12:00

BOIRAUD MINGUET

Venus - 2. floor



09:00
- 18:00

PATTES TENDUES

Mars



08:00
- 18:00

backup

Legend:

- CERN existing LHC
- CLIC 500 GeV
- CLIC 3 TeV
- ILC 500 GeV
- LHeC

Potential underground tunnel

Jura Mountains

IP

Lake Geneva

Geneva

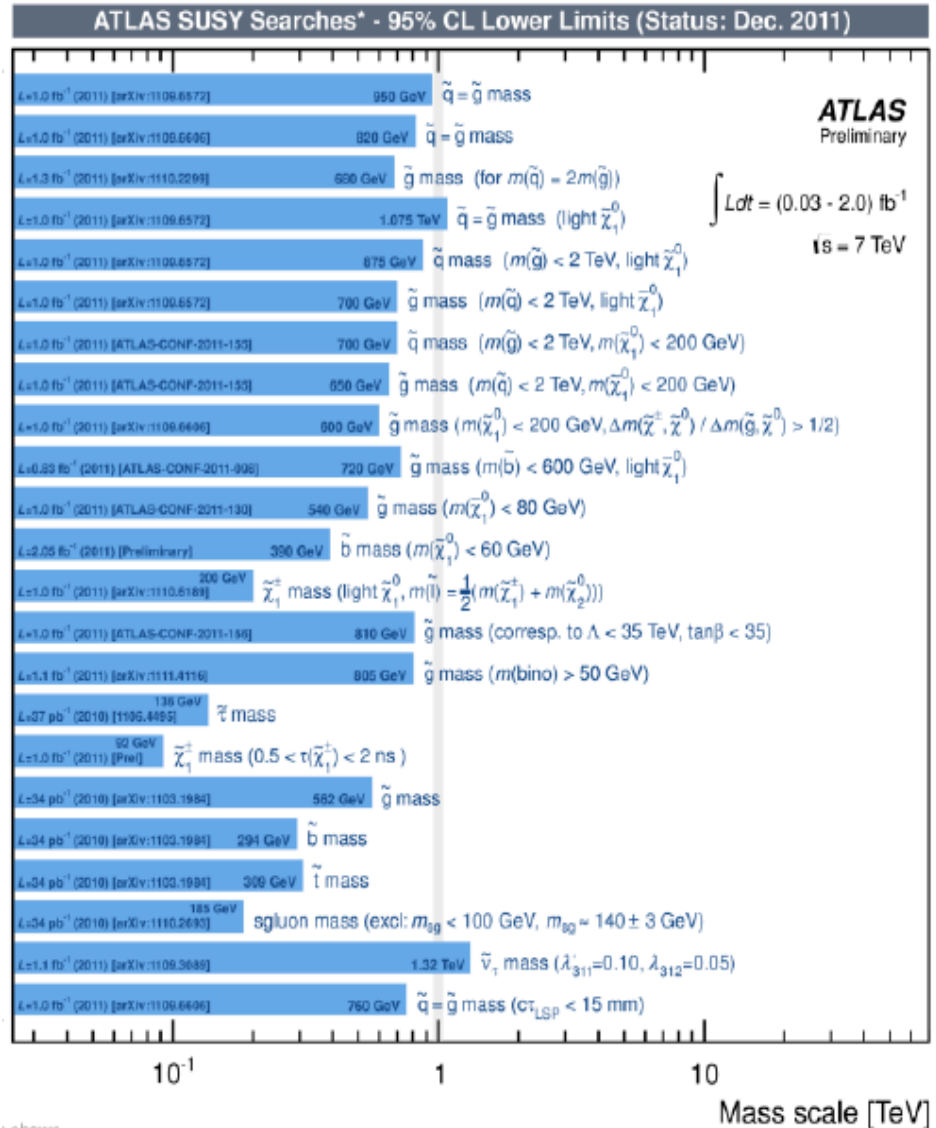
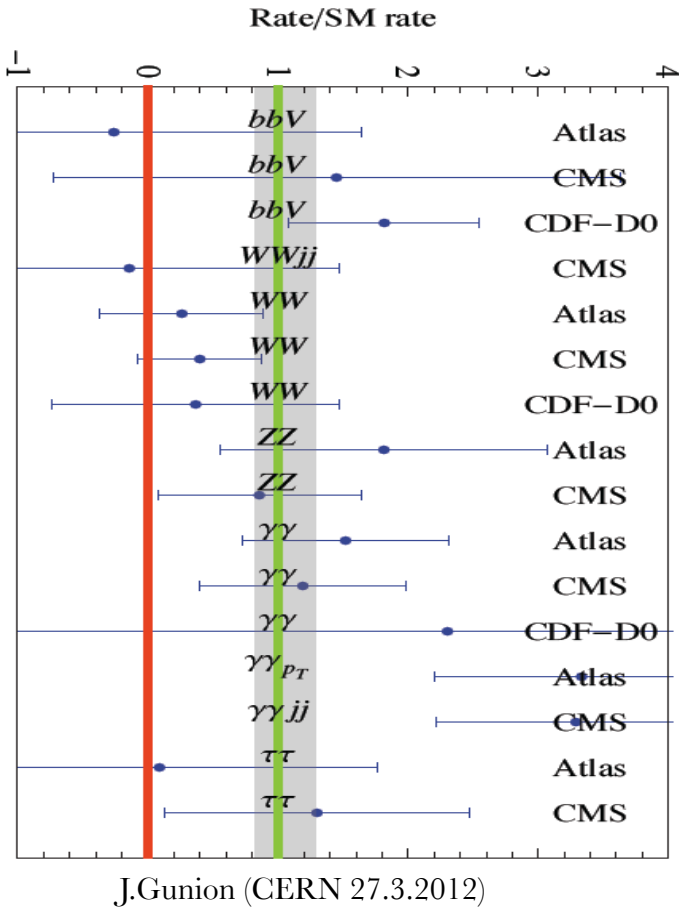
---- sLHC 40 TeV (private guess)

Schematic layouts for several potential future projects are shown on this Google Earth view of the Geneva region around CERN:

- CLIC (Compact Linear Collider) at collision energies of 500GeV and 3 TeV.
- ILC (International Linear Collider) at 500GeV energy
- The Linear-Ring Solution of LHeC (A new electron beam supplied via a 60 GeV

LHC

Selected SUSY Search Results → 3rd generation?



Technicolor ??

“We argue that the existence of fundamental scalar fields constitutes a serious flaw of the Weinberg-Salam theory...”

L.Susskind, Dynamics of Spontaneous Symmetry Breaking in the Weinberg Salam Theory. Phys D20 (1979) 2619-2625
 Dimopoulos, Susskind: Mass Without Scalars NP. B155 (1979) 237

CMS similar results

LHCb: $B_s \rightarrow \mu \mu < 4.5 \cdot 10^{-9} \text{ SM}(3.2 \pm 0.2) \cdot 10^{-9}$

What HERA could not do or has not done

HERA in one box the first ep collider

$$E_p * E_e =$$
$$920 * 27.6 \text{ GeV}^2$$
$$\sqrt{s} = 2\sqrt{E_e E_p} = 320 \text{ GeV}$$

$$L = 1.4 \cdot 10^{31} \text{ cm}^{-2} \text{ s}^{-1}$$

$$\rightarrow \Sigma L = 0.5 \text{ fb}^{-1}$$

1992-2000 & 2003-2007

$$Q^2 = [0.1 \text{ -- } 3 \cdot 10^4] \text{ GeV}^2$$

-4-momentum transfer²

$$x = Q^2 / (s y) \approx 10^{-4} \text{ .. } 0.7$$

Bjorken x

$$y \approx 0.005 \text{ .. } 0.9$$

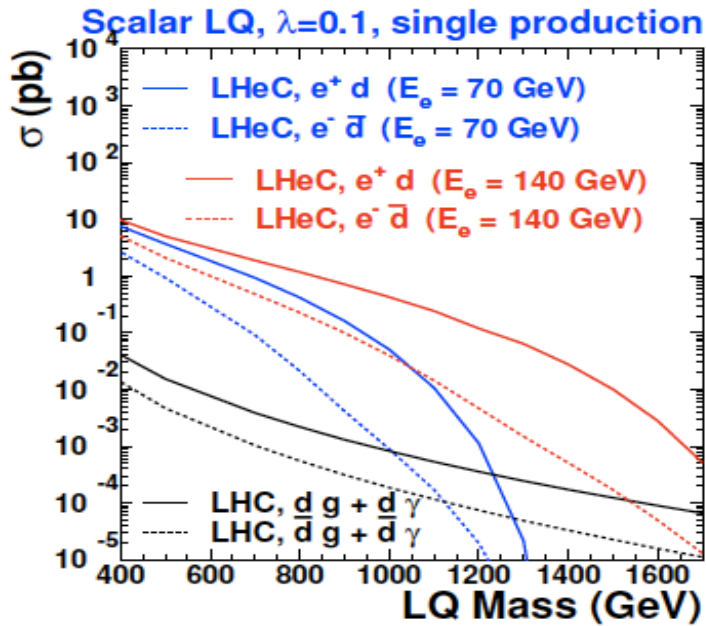
inelasticity

Test of **the isospin symmetry** (u-d) with eD - no deuterons
Investigation of the q-g dynamics in **nuclei** - no time for eA
Verification of **saturation** prediction at low x – too low s
Measurement of the **strange** quark distribution – too low L
Discovery of **Higgs** in WW fusion in CC – too low cross section
Study of **top** quark distribution in the proton – too low s
Precise measurement of F_L – too short running time left
Resolving d/u question at **large Bjorken x** – too low L
Determination of **gluon distribution at hi/lo x** – too small range
High precision measurement of α_s – overall not precise enough
Discovering **instantons, odderons** – don't know why not
Finding **RPV SUSY** and/or leptoquarks – may reside higher up
...

The H1 and ZEUS apparatus were basically well suited
The machine had too low luminosity and running time

HEP needs a TeV energy scale machine with 100 times higher luminosity than HERA to develop DIS physics further and to complement the physics at the LHC. The **Large Hadron Collider p and A beams offer a unique opportunity to build a second ep and first eA collider** at the energy frontier [discussed at DIS since Madison 2005]

Leptoquark Sensitivity



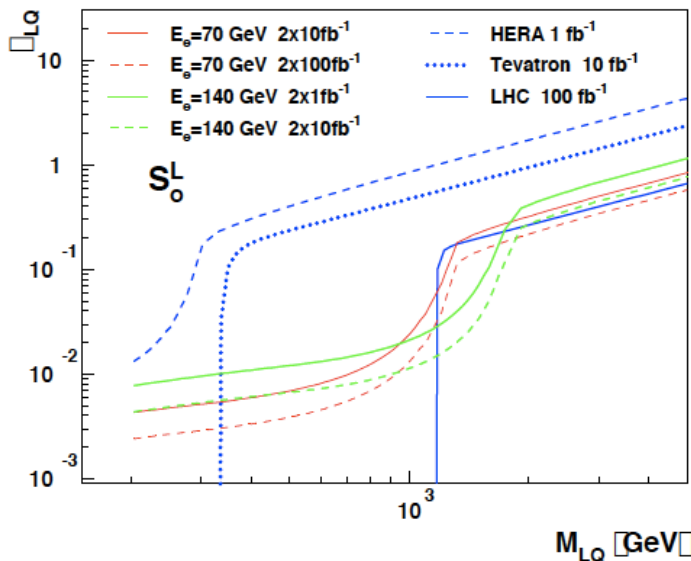
E6 new fields
 TC bound states of technifermions
 PS 4th colour of quarks
 l,q composite models

The cross section in ep is (depending on couplings)
 100 times higher than in pp,
 but LHC is there, has pair production
 and higher energy

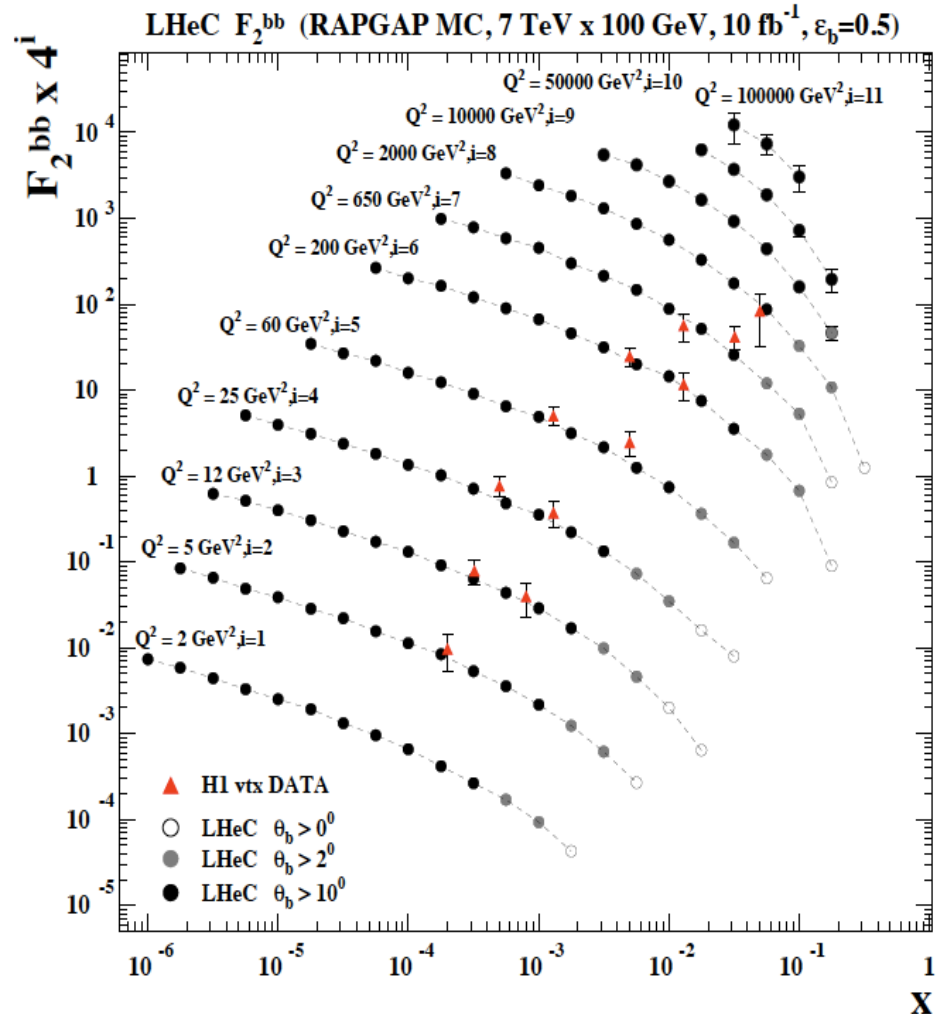
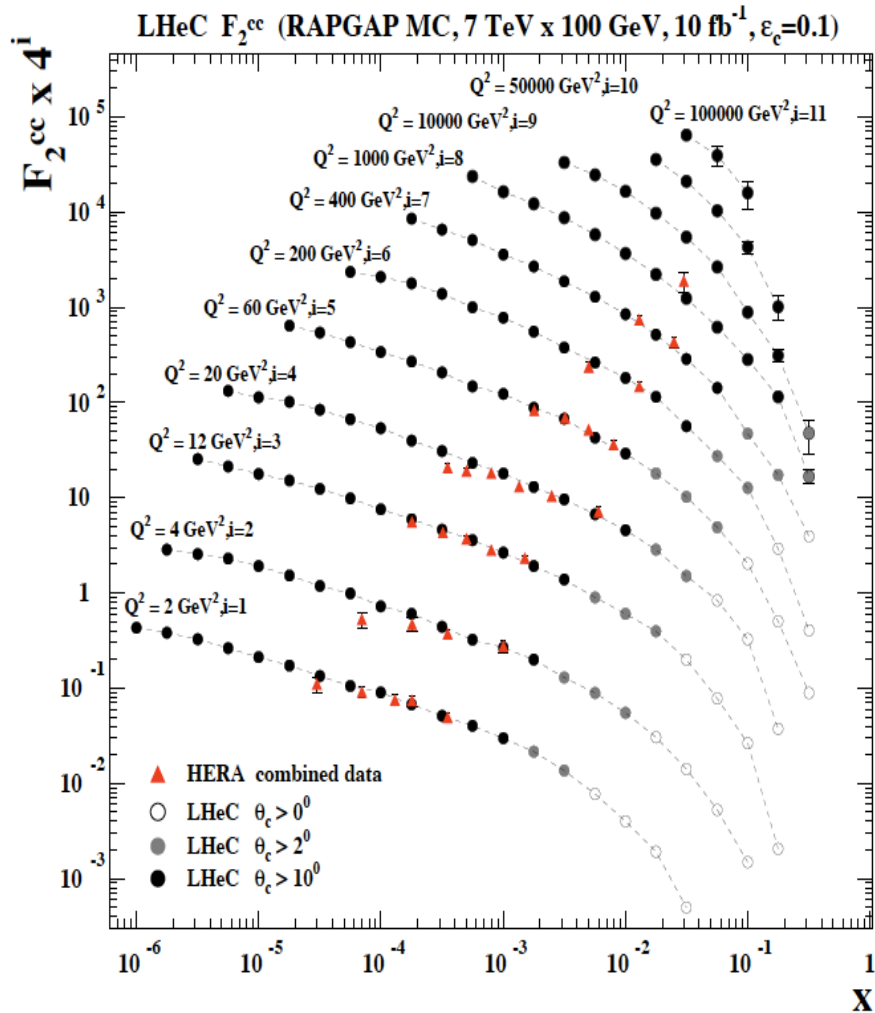
LHeC has mass reach up to about the
 cms energy ($M < \sqrt{s} = 1.3 \dots 2$ TeV
 for 60 .. 140 GeV electron beam energy)

→ IF LQs are discovered at the LHC the
 electron beam energy would possibly
 be adjusted

→ The role of ep would be to determine
 the quantum numbers

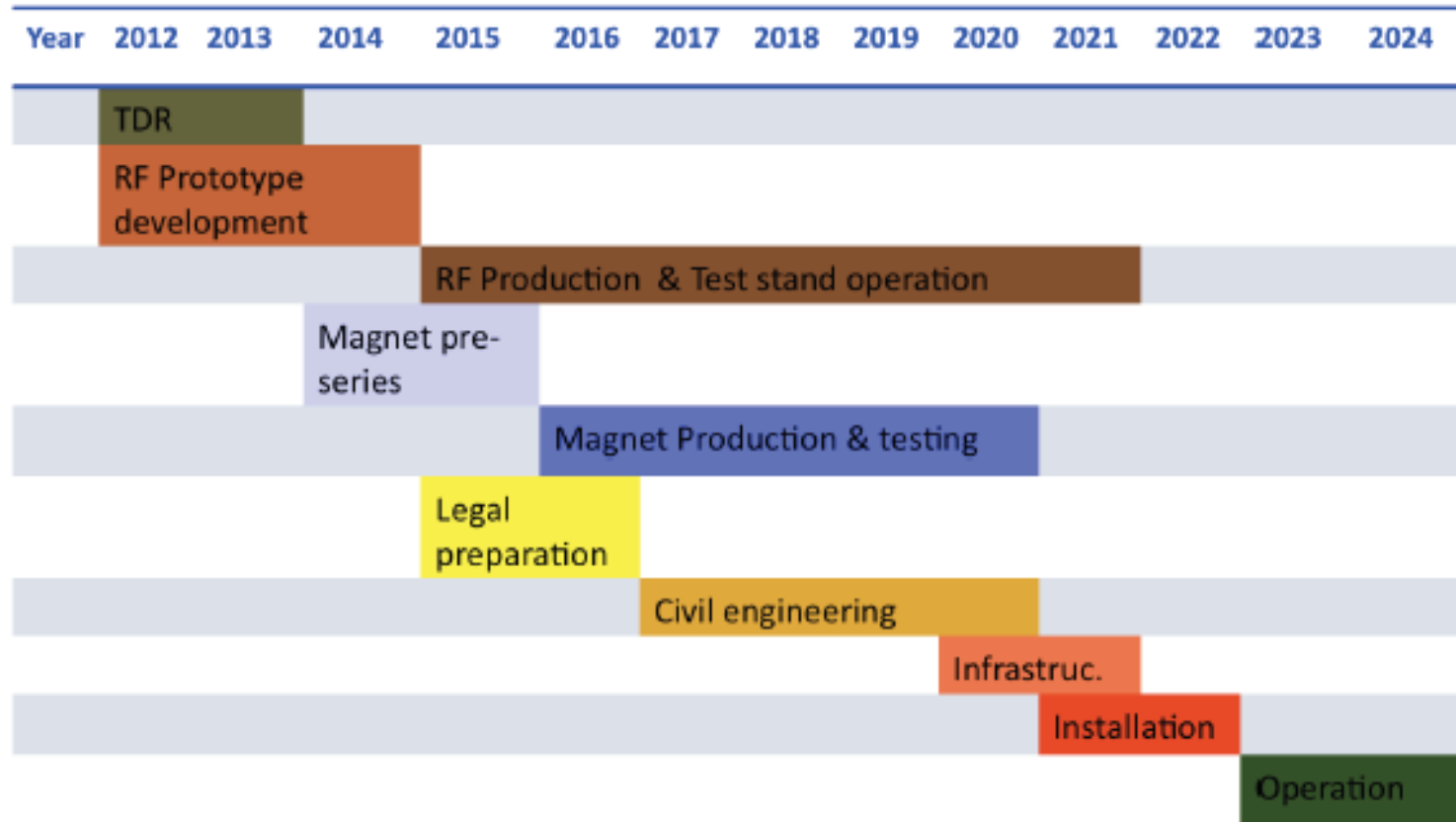


F_2^{charm} and F_2^{beauty} from LHeC



Hugely extended range and much improved precision
will pin down heavy quark behaviour at and away from thresholds

Tentative Time Schedule

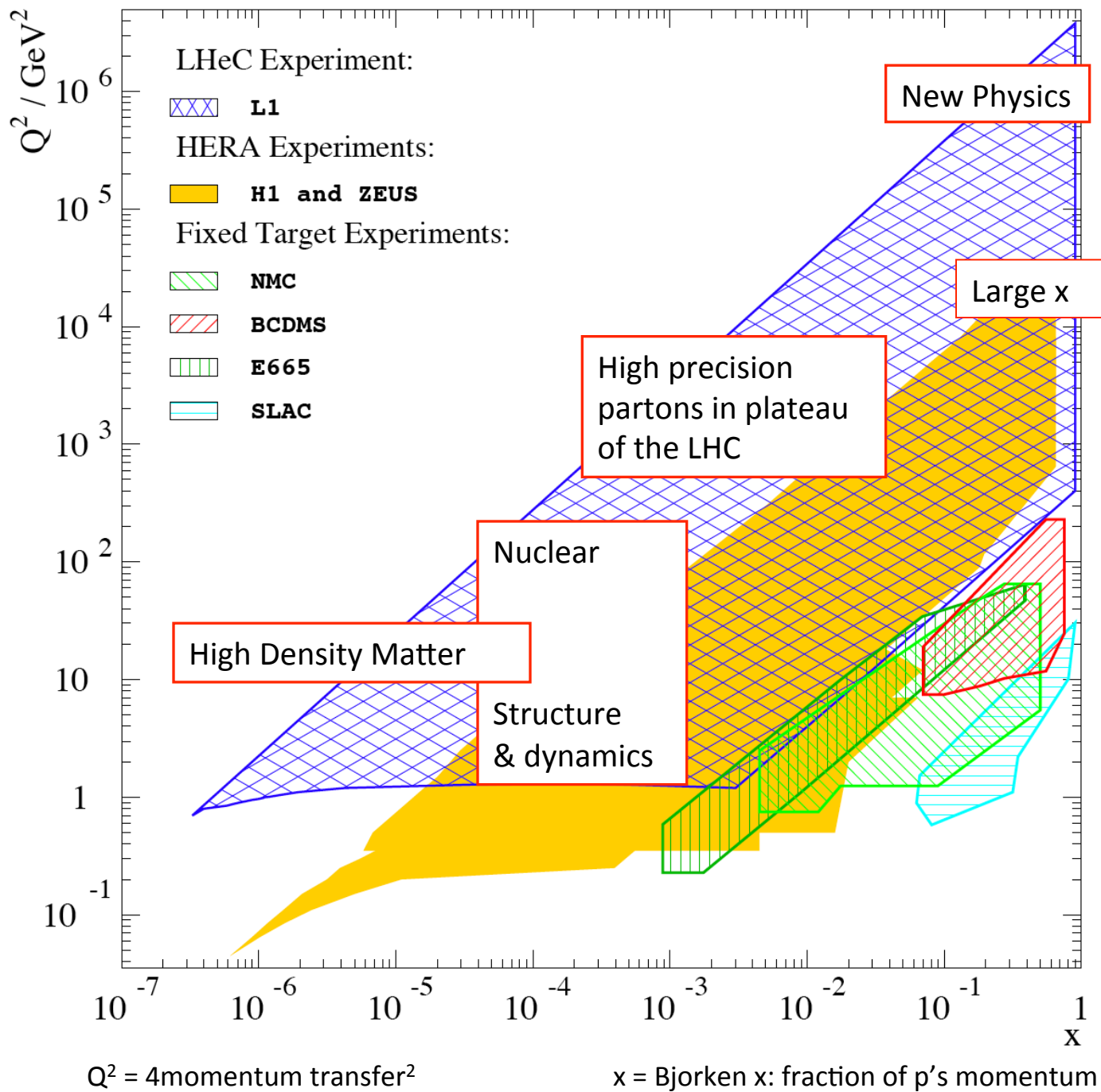


LS3 --- HL LHC



We base our estimates for the project time line on the experience of other projects, such as (LEP, LHC and LINAC4 at CERN and the European XFEL at DESY and the PSI XFEL)

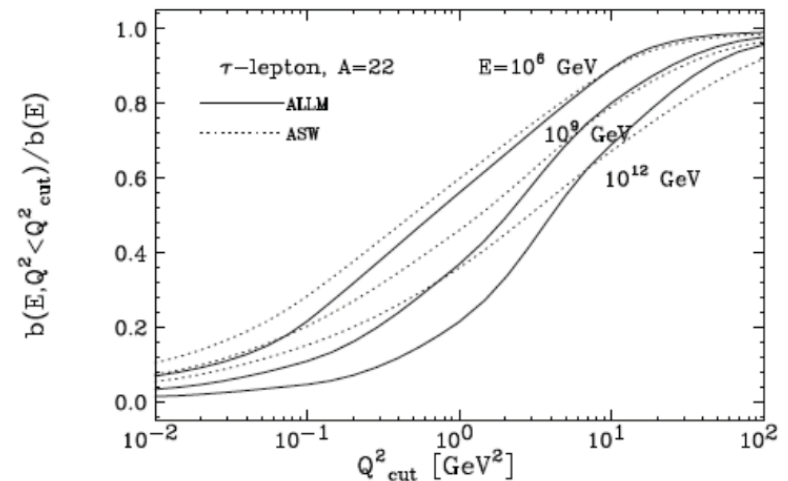
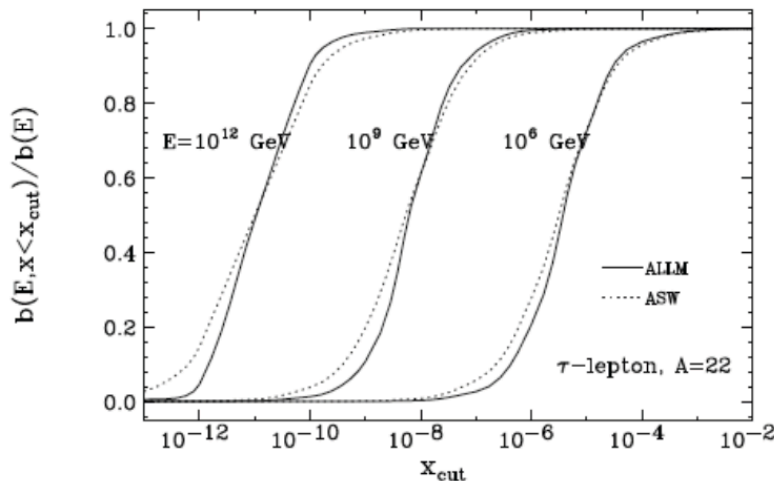
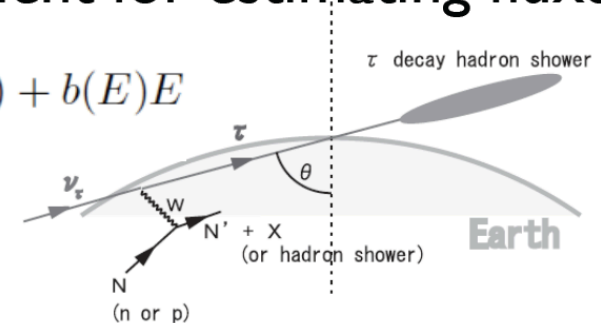
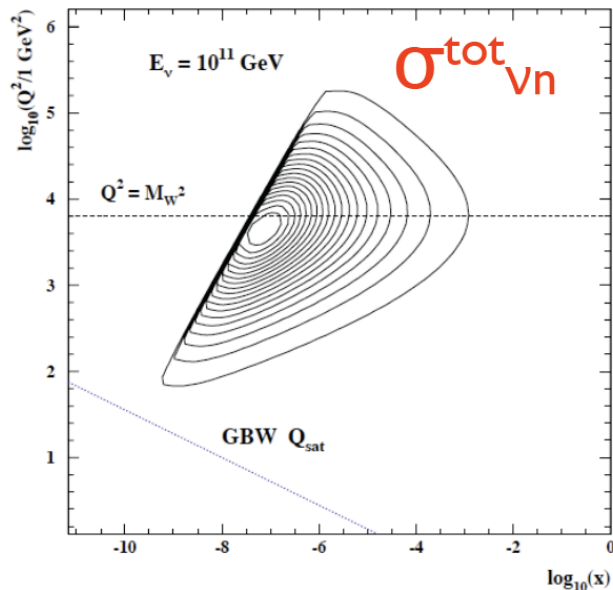
from draft CDR



Neutrino Scattering

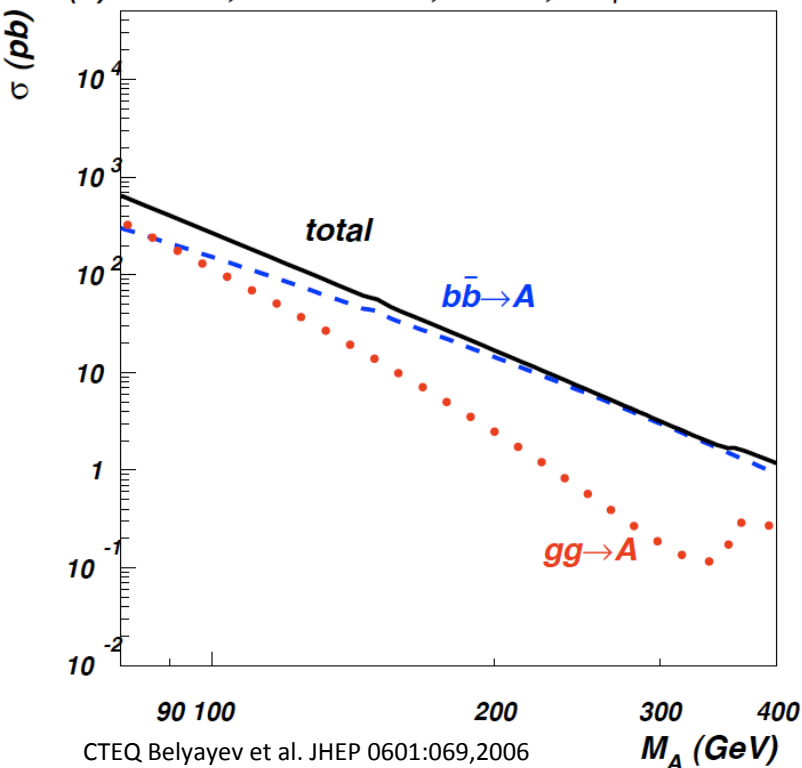
- ν -n/A cross section (τ energy loss) dominated by DIS structure functions (n)pdfs at small-x and large (small) Q^2 .
- Key ingredient for estimating fluxes.

$$-\left\langle \frac{dE}{dX} \right\rangle = a(E) + b(E)E$$



Beauty – MSSM ?? Higgs

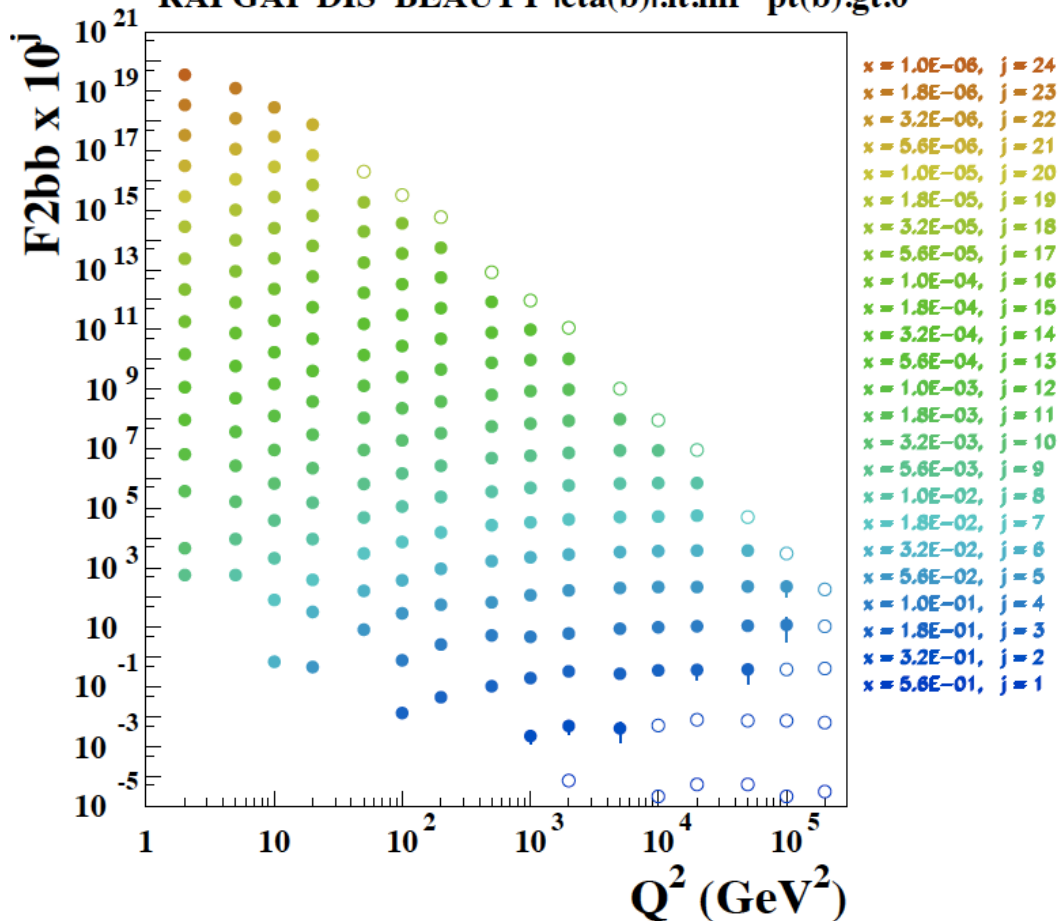
(b) LHC, $\sqrt{s} = 14$ TeV, MSSM, $\tan\beta=10$



In MSSM Higgs production is b dominated

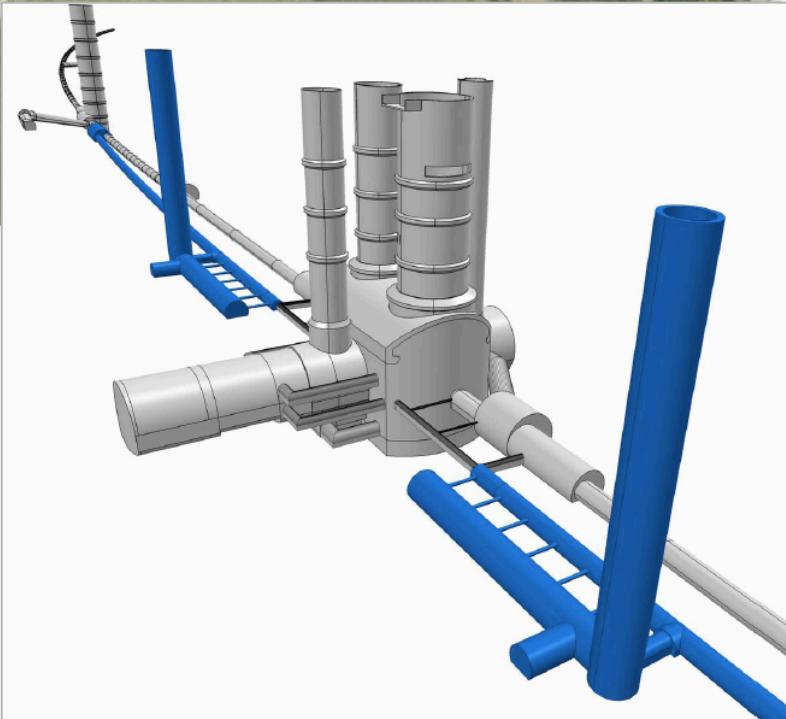
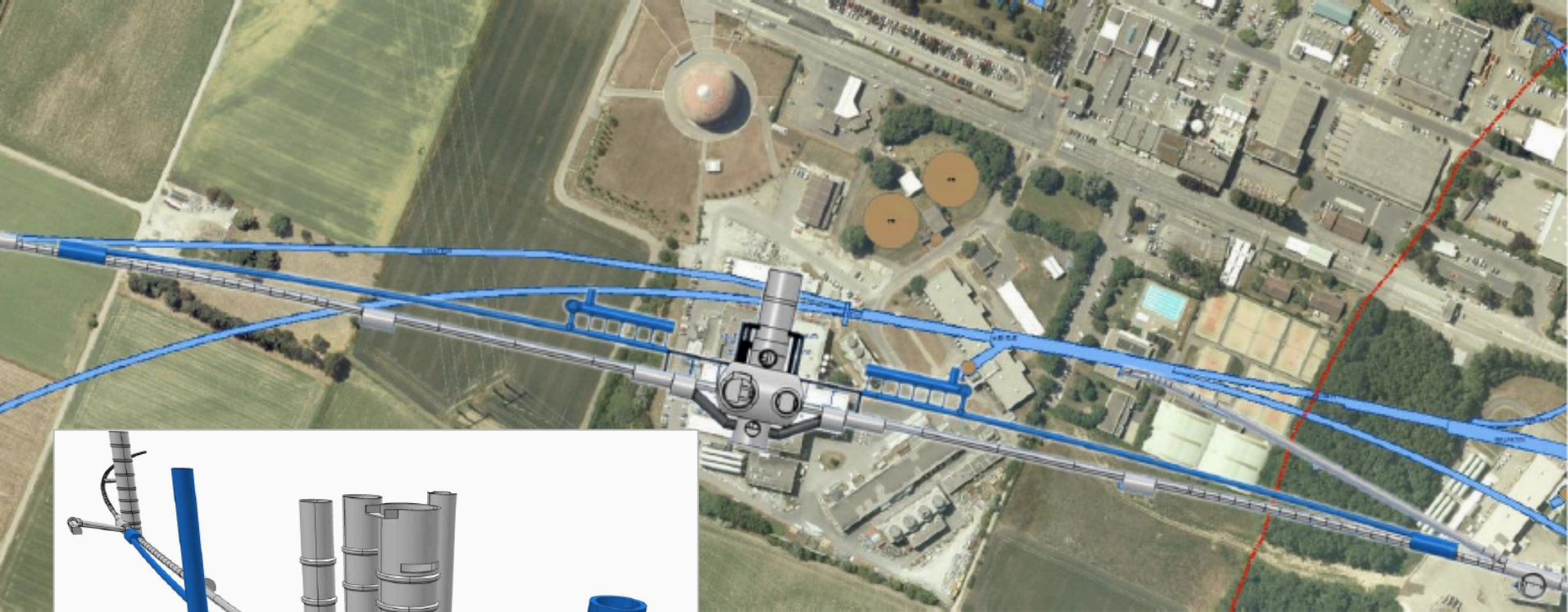
HERA: First measurements of b to ~20%
LHeC: precision measurement of b-df

LHeC 7000x100, 10 fb^{-1} , b -tag-eff. 0.1
 RAPGAP DIS BEAUTY $\text{I}(\text{b}) \cdot \text{I}(\text{t}) \cdot \text{inf} \text{ pt}(\text{b}) \cdot \text{gt.} 0$



LHeC: higher fraction of b, larger range,
 smaller beam spot, better Si detectors

Bypassing ATLAS



For the CDR the bypass concepts were decided to be confined to ATLAS and CMS

Detector Magnets

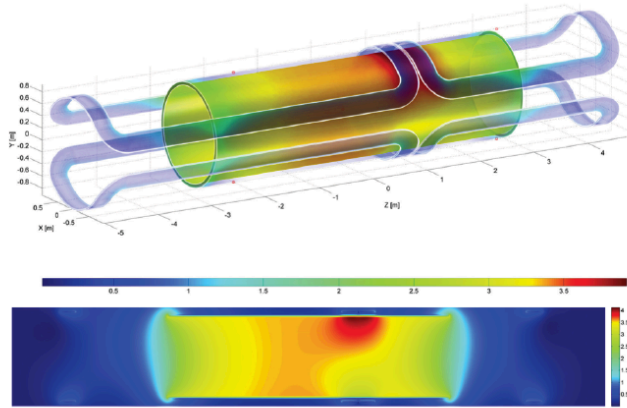


Figure 13.13: Magnetic field of the magnet system of solenoid and the two internal superconducting dipoles at nominal currents (effect of iron ignored). The position of the peak magnetic field of 3.9 T is local due to the adjacent current return heads on top of the solenoid where all magnetic fields add up.

Dipole (for head on LR) and solenoid in common cryostat, perhaps with electromagnetic LAr

3.5T field at ~1m radius to house a Silicon tracker

Based on ATLAS+CMS experience

Property	Parameter	value	unit
Dimensions	Cryostat inner radius	0.900	m
	Length	10.000	m
	Outer radius	1.140	m
	Coil windings inner radius	0.960	m
	Length	5.700	m
	Thickness	60.0	mm
	Support cylinder thickness	0.030	m
	Conductor section, Al-stabilized NbTi/Cu + insulation	30.0 × 6.8	mm ²
	Length	10.8	km
	Superconducting cable section, 20 strands	12.4 × 2.4	mm ²
	Superconducting strand diameter Cu/NbTi ratio = 1.25	1.24	mm
	Masses	Conductor windings	5.7
Support cylinder, solenoid section + dipole sections		5.6	t
Total cold mass		12.8	t
Cryostat including thermal shield		11.2	t
Electro-magnetics	Total mass of cryostat, solenoid and small parts	24	t
	Central magnetic field	3.50	T
	Peak magnetic field in windings (dipoles off)	3.53	T
	Peak magnetic field in solenoid windings (dipoles on)	3.9	T
	Nominal current	10.0	kA
	Number of turns, 2 layers	1683	
	Self-inductance	1.7	H
	Stored energy	82	MJ
	E/m, energy-to-mass ratio of windings	14.2	kJ/kg
	E/m, energy-to-mass ratio of cold mass	9.2	kJ/kg
	Charging time	1.0	hour
	Current rate	2.8	A/s
Margins	Inductive charging voltage	2.3	V
	Coil operating point, nominal / critical current	0.3	
	Temperature margin at 4.6 K operating temperature	2.0	K
Mechanics	Cold mass temperature at quench (no extraction)	~ 80	K
	Mean hoop stress	~ 55	MPa
Cryogenics	Peak stress	~ 85	MPa
	Thermal load at 4.6 K, coil with 50% margin	~ 110	W
	Radiation shield load width 50% margin	~ 650	W
	Cooling down time / quench recovery time	4 and 1	day
	Use of liquid helium	~ 1.5	g/s

Table 13.1: Main parameters of the baseline LHeC Solenoid providing 3.5 T in a free bore of 1.8 m.

Summary of Design Parameters

electron beam	RR	LR	LR
e- energy at IP[GeV]	60	60	140
luminosity [$10^{32} \text{ cm}^{-2}\text{s}^{-1}$]	17	10	0.44
polarization [%]	40	90	90
bunch population [10^9]	26	2.0	1.6
e- bunch length [mm]	10	0.3	0.3
bunch interval [ns]	25	50	50
transv. emit. $\gamma\epsilon_{x,y}$ [mm]	0.58, 0.29	0.05	0.1
rms IP beam size $\sigma_{x,y}$ [μm]	30, 16	7	7
e- IP beta funct. $\beta^*_{x,y}$ [m]	0.18, 0.10	0.12	0.14
full crossing angle [mrad]	0.93	0	0
geometric reduction H_{hg}	0.77	0.91	0.94
repetition rate [Hz]	N/A	N/A	10
beam pulse length [ms]	N/A	N/A	5
ER efficiency	N/A	94%	N/A
average current [mA]	131	6.6	5.4
tot. wall plug power[MW]	100	100	100

proton beam	RR	LR
bunch pop. [10^{11}]	1.7	1.7
tr.emit. $\gamma\epsilon_{x,y}$ [μm]	3.75	3.75
spot size $\sigma_{x,y}$ [μm]	30, 16	7
$\beta^*_{x,y}$ [m]	1.8,0.5	0.1
bunch spacing [ns]	25	25

“ultimate p beam”

1.7 probably conservative
and emittance too

CDR has design also for
D and A ($L_{\text{eN}} \cong 3 * 10^{31} \text{ cm}^{-2}\text{s}^{-1}$)

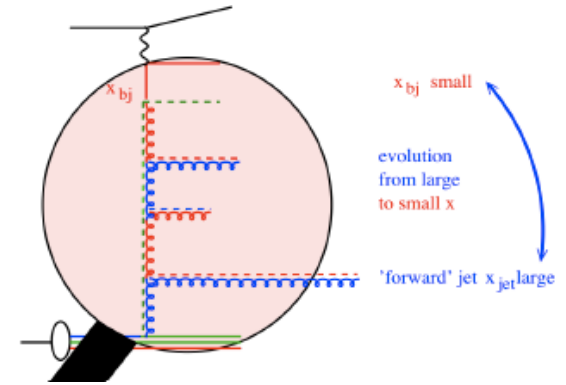
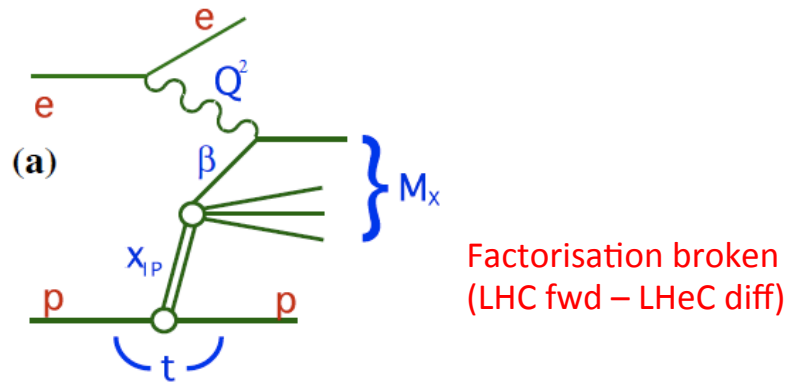
RR= Ring – Ring

LR =Linac –Ring

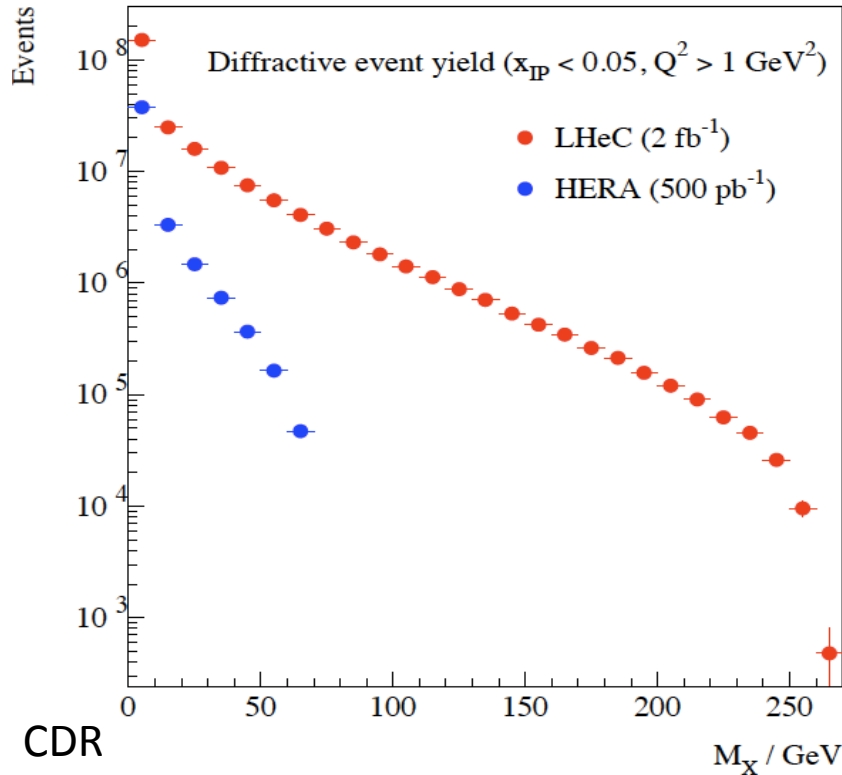
Ring: use 1° as baseline : L/2
Linac: clearing gap: L*2/3

High E_e Linac option (ERL?) if physics demands HE-LHC?

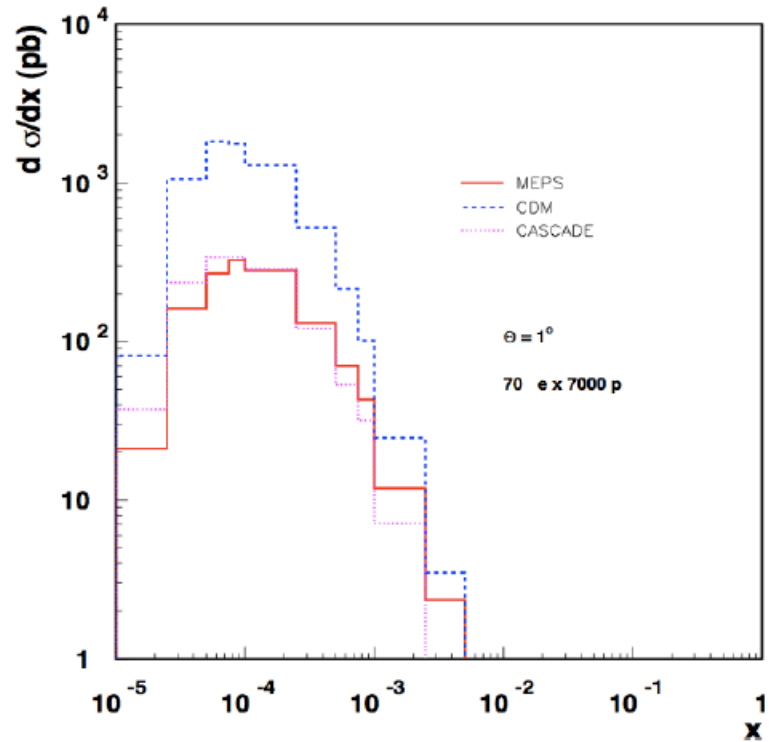
Quark-Gluon Dynamics - Diffraction and HFS (fwd jets)



Production of high mass 1^- states

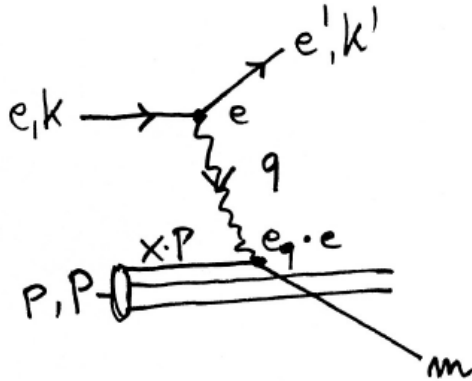


Understand multi-jet emission (unintegr. pdf's), tune MC's



At HERA resolved γ effects mimic non-kt ordered emission

Deep Inelastic Scattering ("DIS")



$$q = (k - k')$$

$$(xP + q)^2 = m^2, P^2 = M_p^2$$

$$Q^2 = -q^2 > 0$$

$$\text{if } : Q^2 \gg x^2 M_p^2, m^2 :$$

$$q^2 + 2xPq = 0 :$$

$$x = \frac{Q^2}{2Pq}$$

"fixed target":

$$P = (M_p, 0, 0, 0)$$

$$2Pq = 2M_p(E - E')$$

$$= 2M_p E \cdot \frac{v}{E} \equiv s \cdot y$$

$$Q^2 = sxy \leq s$$

$$s = 2M_p E$$

$$s = 4E_e E_p$$

- ep collider

$$x = \frac{Q^2}{sy}$$

$$\sigma(ep \rightarrow eX) = \frac{d^2\sigma}{dx dQ^2} \approx \frac{2\pi\alpha^2}{Q^4} (1 + (1-y)^2) \cdot F_2$$

$$F_2(x, Q^2) = x \sum_q e_q^2 (q + \bar{q}),_{q = u, d, s, c, b, t}$$

$$q = q(x, Q^2)$$

In DIS the inclusive cross section depends on two variables, the negative 4-momentum transfer squared (Q^2), which determines the resolving power of the exchanged particle in terms of p substructure, and the variable Bjorken x , which Feynman could relate to the fraction of momentum of the proton carried by a parton [in what he called the 'infinite momentum frame' in which the transverse momenta are neglected].

Deep inelastic scattering resolves the nucleon structure. If s is high: produce new states

Kinematics is determined with scattered electron or with HFS \rightarrow high precision due to redundancy